Philipps-Universität Marburg
Fachbereich Biologie

Active and passive resistance mechanisms of *Bacillus subtilis* against cell envelope targeting antibiotics

Dissertation
zur Erlangung des
Doktorgrads der Naturwissenschaften
(Dr. rer. nat.)

des Fachbereichs Biologie
der Philipps-Universität Marburg

vorgelegt von
Angelika Diehl
aus Frankfurt a.M.

Marburg, 2021

Originaldokument gespeichert auf dem Publikationsserver der
Philipps-Universität Marburg
http://archiv.ub.uni-marburg.de

Dieses Werk ist lizenziert unter einer Creative Commons
Namensnennung
Nicht kommerzielle Nutzung
Keine Bearbeitungen
4.0 International Lizenz.

Die vollständige Lizenz finden Sie unter:
https://creativecommons.org/licenses/by-nc-nd/4.0/

Die Arbeit zur vorliegenden Dissertation wurde von November 2017 bis Mai 2021 unter der Betreuung von Herrn Dr. Georg Fritz an der Philipps-Universität Marburg in der Arbeitsgruppe *Computational Microbiology* angefertigt.

Vom Fachbereich Biologie der Philipps-Universität Marburg (Hochschulkennziffer 1180) als Dissertation angenommen am 29.06.2021

Erstgutachter: Dr. Georg Fritz
Zweitgutachter: Prof. Dr. Martin Thanbichler
Tag der Disputation: 22.07.2021

Publikationen

Teile dieser Arbeit wurden publiziert in:

Angelika Diehl, Thomas M. Wood, Susanne Gebhard, Nathaniel I. Martin, Georg Fritz. The cell envelope stress response of *Bacillus subtilis* towards laspartomycin C. *Antibiotics (Basel, Switzerland)*, 9(11):729, 2020.

weitere Publikationen:

Hannah Piepenbreier, ***Angelika Diehl***, Georg Fritz. Minimal exposure of lipid II cycle intermediates triggers cell wall antibiotic resistance. *Nature communications* 10(1):1–13, 2019.

Delia Casas-Pastor, ***Angelika Diehl***, Georg Fritz. Coevolutionary analysis reveals a conserved dual binding interface between extracytoplasmic function σ factors and class I anti-σ factors. *mSystems*, 5(4), 2020.

Abbreviations

α-MG	α-methyl glucopyranoside
AS	anti-σ factor
CDA	calcium dependent lipopeptide antibiotic
CESR	cell envelope stress response
ECF	extracytoplasmic function σ factor
GlcNAc	N-acetyl-glucosamine
IC	inhibitory concentration
MDK	minimal duration of killing
MIC	minimal inhibitory concentration
MurNAc	N-acetyl-muramic acid
OIC	observed inhibitory concentration
PBP	penicillin binding protein
PG	peptidoglycan
RNAP	RNA polymerase
UP	undecraprenyl-phosphate
UPP	undecraprenyl-diphosphate

List of Figures

List of Tables

Contents

Abstract

Modern medicine relies on the use of antibiotics to treat infectious diseases caused by bacteria and save millions of lives. But bacteria acquire resistances with an alarming rate, rendering many antibiotics ineffective. As such, wise use of antibiotics to prevent the emergence of resistance is of utmost importance.

To utilize antibiotics more efficiently environmental conditions and the general structure of biochemical pathways should also be taken in account as they can have significant impact on susceptibility. In this work, the susceptibility of the gram-positive bacterium *Bacillus subtilis* against cell envelope targeting antibiotics was analyzed. As a member of the Firmicutes phylum and due to the strong conservation of cell wall synthesis the findings gained here in *B. subtilis* provide valuable insight into the resistance of dangerous pathogenes of the same phylum like *Staphylococcus aureus* and *Clostridium tetani*.

First, the natural cell envelope stress response towards the novel antibiotic laspartomycin C was investigated. Interestingly, while the very similar antibiotic friulimicin B only induces the σ^M module, laspartomycin C additionally activates the Lia- and the two Bce-like resistance modules tested here. We hypothesize that these differences arise from small but impactful differences in the antibiotics structure that allow a multimerization of UP-bound friulimicin B on the one hand and cause a higher disturbance of the membrane by laspartomycin C on the other hand. The resistance conferred by these modules was further examined via deletion strains. None of the modules tested here provided any protection against either of the two antibiotics. For a potential use of these antibiotics as clinical drugs the lack of conferred resistance is promising. However, the induction of the natural resistance modules by laspartomycin C might indicate their impending evolution to provide full resistance and should be kept in mind in further studies.

Slow growth is associated with resistance against environmental stresses and antibiotics. In many cases this higher resistance is caused by a slower metabolism and therefore a slow damaging effect by the environmental stress or antibiotic. Besides the overall metabolic rate, the metabolism of bacteria is also heavily regulated in dependence

of growth rate. For instance, fast growing bacteria are significantly bigger in cell size and are therefore expected to require more cell wall material. As such, the emergence of bottlenecks was expected with the upregulation of its synthesis, which should ultimately lead to changes in susceptibility of cell wall targeting antibiotics dependent on growth rate.

Here, inhibitory concentrations of a diverse set of cell envelope targeting antibiotic were determined in a range of different growth rates. Contrary to our expectations, the resistance towards most tested cell envelope targeting antibiotics was independent of growth rate. Only the cell envelop targeting antibiotic bacitracin showed a growth rate depended change of the susceptibility with a 40% increase of the inhibitory concentration. Compared to ribosome-targeting antibiotics, which have been shown to increase by up to 500% in activity in the same growth rate range, this increase in resistance seems less substantial. This indicates a tight regulation of the cell wall synthesis machinery, that impedes the emergence of bottlenecks despite changing demands of cell wall material. As such, cell envelope targeting antibiotics are versatile tools in the combat against both slow-growing and chronic, as well as fast-growing and acute infections.

Zusammenfassung

In der modernen Medizin ist der Einsatz von Antibiotika unverzichtbar, um Infektionskrankheiten zu behandeln und Menschenleben zu retten. Jedoch erwerben Bakterien mit einer alarmierenden Rate Resistenzen gegen diese und drohen die bekannten Antibiotika unwirksam zu machen. Daher ist der gezielte Einsatz von Antibiotika zur Verhinderung der Entstehung von Resistenzen von größter Bedeutung.

Um Antibiotika effizienter einzusetzen, dürfen die Umweltbedingungen und die allgemeine Struktur der biochemischen Pathways nicht außer Acht gelassen werden, da sie erhebliche Auswirkungen auf die Antibiotikaaktivität haben können. In dieser Arbeit wurde die Empfindlichkeit des grampositiven Bakteriums *Bacillus subtilis* gegen Antibiotika, die die Zellhülle angreifen, analysiert. Als Angehöriger des Phylums Firmicutes und aufgrund der starken Konservierung der Zellwandsynthese liefern die hier gewonnenen Erkenntnisse in *B. subtilis* wertvolle Einblicke in die Resistenz gefährlicher Krankheitserreger desselben Phylums wie *Staphylococcus aureus* und *Clostridium tetani*.

Zuerst wurde die natürliche Stressreaktion der Zellhülle auf das neuartige Antibiotikum Laspartomycin C untersucht. Während das sehr ähnliche Antibiotikum Friulimicin B nur σ^M induziert, aktiviert Laspartomycin C zusätzlich das Lia- und beide der hier getesteten Bce-ähnlichen Module. Diese Unterschiede sind vermutlich auf kleine, aber wirkungsvolle Ungleichheiten in der Antibiotikastruktur zurückzuführen, die einerseits UP-gebundenem Friulimicin B ermöglichen zu multimerisieren und andererseits eine stärkere Störung der Membranstruktur durch Laspartomycin C bewirken. Die verliehene Resistenz dieser Module wurde mittels Deletionsstämmen weiter untersucht. Keines der hier getesteten Module bot einen Schutz gegen eines der beiden Antibiotika.

Für eine mögliche Verwendung dieser Antibiotika als klinische Arzneimittel ist das Ausbleiben einer Schutzwirkung durch diese Module vielversprechend. Die Induktion der natürlichen Resistenzmodule durch Laspartomycin C könnte jedoch auf ihre weitere Evolution in Richtung vollständiger Resistenz hinweisen, und sollte in weiteren Studien berücksichtigt werden.

Langsames Wachstum wird häufig mit Resistenzen gegen ungünstige Umweltbedingungen und Antibiotika in Verbindung gebracht. In vielen Fällen ist diese höhere Re-

sistenz bedingt durch einen langsamen Metabolismus, wodurch der schädigende Effekt durch ungünstige Umweltbedingungen und Antibiotika verlangsamt wird. Neben der allgemeinen Stoffwechselrate wird der Stoffwechsel von Bakterien in Abhängigkeit von der Wachstumsrate stark reguliert. Beispielsweise sind schnell wachsende Bakterien signifikant größer und daher wird erwartet, dass sie mehr Zellwandmaterial benötigen. Mit der Hochregulierung der Zellwandsynthese werden somit Engpässe erwartet, was zu Veränderungen der Empfindlichkeit gegen Zellwand-schädigende Antibiotika in Abhängigkeit von der Wachstumsrate führen sollten.

In der vorliegenden Arbeit wurden inhibitorische Konzentrationen verschiedener Zellhüllschädigender Antibiotika bei unterschiedlichen Wachstumsraten bestimmt. Unerwarteterweise erwies sich dabei die Aktivität der meisten Antibiotika als stabil. Allein das Zellhüll-schädigende Bacitracin zeigte einen Anstieg der inhibitorischen Konzentration um 40% in schnellem Wachstum. Verglichen mit Ribosom-schädigenden Antibiotika, die einen Anstieg um bis zu 500% in der gleichen Wachstumsratenspanne zeigten, ist diese höhere Resistenz jedoch zu vernachlässigen.

Diese Ergebnisse deuten auf eine strenge Regulierung der Zellwandsynthesemaschinerie hin, die das Auftreten von Engpässen trotz sich ändernder Anforderungen an Zellwandmaterial verhindert. Daher bieten sich Zellhüllschädigende Antibiotika als vielseitige Werkzeuge im Einsatz sowohl gegen langsam wachsende, chronische als auch gegen schnell wachsende, akute Infektionen an.

1. Introduction

Since the discovery of penicillin by Alexander Fleming in 1928 antibiotics have become vital tools in modern medicine [1]. As such, the rise of antibiotic resistance especially in clinical settings is deeply unsettling and the identification of novel antibiotics is of utmost importance. However, development of clinical antibiotic drugs is costly and only provides a small profit margin causing most pharmaceutical companies to abandon antibiotic research [1]. To prevent the total loss of antibiotic drugs it is necessary to use the existing ones wisely to reduce the development of resistances. For this, a detailed understanding of their interaction with their cellular targets and mode of action is essential.

As the outermost structure of gram-positive bacteria, the cell wall exhibits some very important qualities as a target for antibiotics such as essentiality, accessibility and conservation. However, protective mechanisms against cell wall targeting antibiotics are abundant in natural environments and further facilitate resistance in clinical settings [2]. While many of these are genetic resistance modules, intrinsic properties of the cell wall and its biosynthesis might also modify susceptibility [3].

The gram-positive bacterium *Bacillus subtilis* presents itself as an excellent model organism for a detailed analysis of cell envelope targeting antibiotics as its cell wall synthesis and natural resistance is well researched. Furthermore, as a member of the Firmicutes phylum and due to the high conservation of the cell wall structure and synthesis, the insights gained here can be transferred to dangerous pathogens such as *Staphylococcus aureus* and *Clostridium tetani*.

1.1. Cell wall components of gram-positive bacteria

The major component of bacterial cell wall is peptidoglycan (PG) - a large polymer consisting of long chains of alternating β-1-4 linked N-acetyl-glucosamine (GlcNAc) and N-acetyl-muramic acid (MurNAc) that are interlinked by short peptides anchored on MurNAc (Figure 1.1a). Recently, Pasquina-Lemonche et al. found that in *B. subtilis* the sugar-strands are synthesized along the short axis of the cylinder and circumferential at the poles, but this directionality gets lost quickly as the peptidoglycan matures [4].

Typical for a gram-positive bacterium the cell wall of *B. subtilis* is very thick with around 20 layers peptidoglycan, the main component of the cell wall [5].

Electron microscopy reveals *B. subtilis* surface to have a rough, almost fuzzy appearance (Figure 1.1b). This is caused by the phosphate-rich polymers lipo- and wall teichoic acids (LTA/WTA), which extend outwards and are attached to the cytoplasmic membrane or peptidoglycan respectively (Figure 1.1c,d) [6]. Both teichoic acids species are synthesized via distinct pathways and share common functions in e.g. regulation of peptidoglycan hydrolysis and metal ion homeostasis [6, 7]. Even though the large mesh-like structure of the cell wall is composed of peptidoglycan, teichoic acids can attribute up to 60% of the total cell wall weight [8]. As such teichoic acids play a secondary but crucial role as cell wall polymers in gram-positive bacteria.

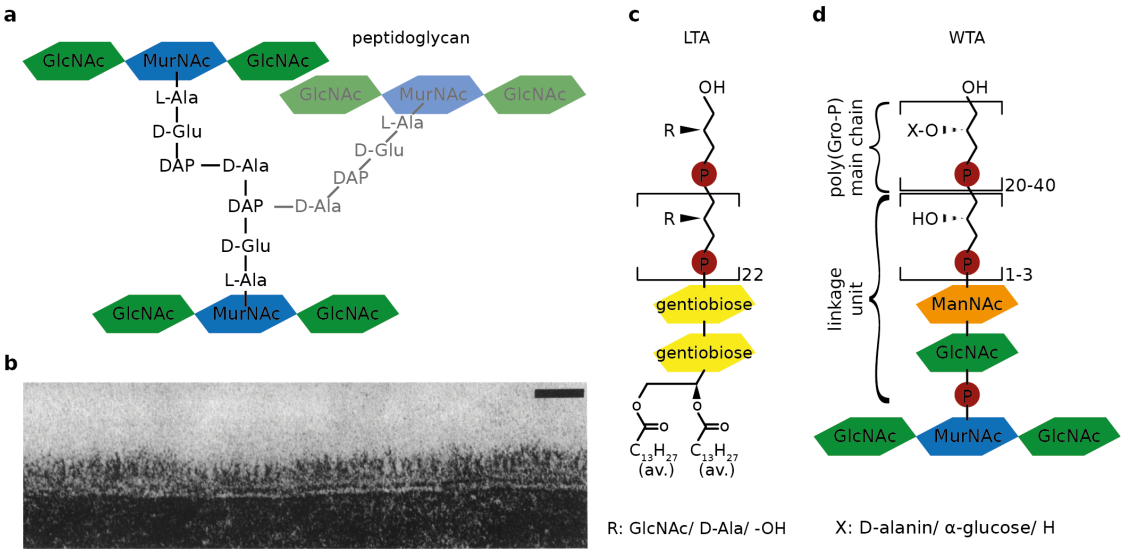

Figure 1.1.: Cell wall structure of *B. subtilis*. (a) Chemical structure of *B. subtilis* peptidoglycan. DAP: diaminopimelic acid. (b) Cross section of *B. subtilis* cell walls via electron microscopy. Reprinted from [9], with permission from American Society for Microbiology. (c) Lipoteichoic acid structure. (d) Wall teichoic acid structure. All structures are shown for *B. subtilis* (W168) and might vary in other organisms.

1.2. Peptidoglycan synthesis in *B. subtilis*

Peptidoglycan synthesis is a complex two-stage process: (1) the Mur pathway and (2) the lipid II cycle. The two stages are responsible for the cytosolic and the membrane-bound precursor synthesis, respectively. The Mur pathway produces the cytosolic precursor UDP-MurNAc-pentapeptide from UDP-GlcNAc [10, 11] and is thought to do so in excess under non-inhibiting conditions [12, 13]. However, during inhibition of the lipid II cycle

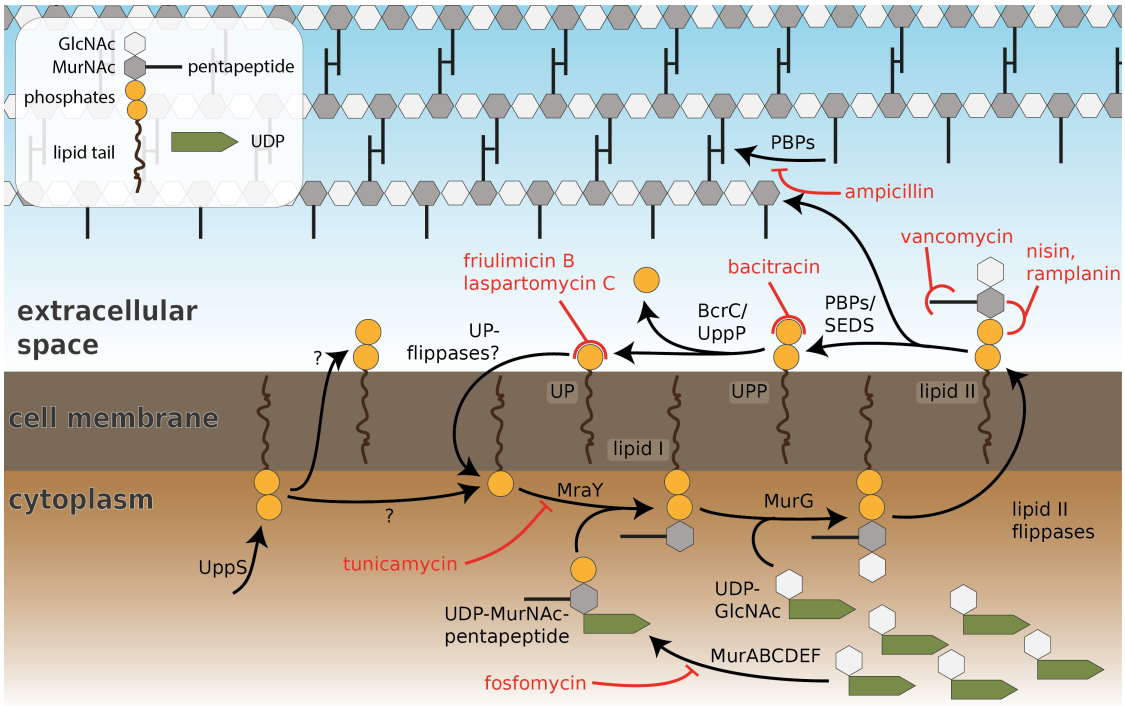

Figure 1.2.: Schematic overview of the lipid II cycle in *B. subtilis*. The lipid carrier UP is loaded with cytosolic PG precursors and subsequently flipped to the extracellular surface of the membrane. There the PG precursor is inserted into a growing PG strand via transglycosylation. The remaining lipid carrier is dephosphorylated to gain the initial UP. The nature of UP's flipping mechanism is still undetermined. The cytosolic precursors UDP-GlcNAc and UDP-MurNAc-pentapeptide are synthesized via the Mur pathway. Newly synthesized PG strands are crosslinked by PBPs. Lipid carrier is supplied in the form of UPP by UppS. Many of these steps can be inhibited by antibiotics, which are indicated in red. Modified from [17].

only the Mur intermediate UDP-MurNAc-tripeptide was found to accumulate while the final product UDP-MurNAc-pentapeptide did not [14]. Additionally, MurA, the first enzyme of the pathway, has been found to tightly bind a later intermediate (UDP-MurNAc) [15]. This indicates feedback inhibition mediated by the abundance of pathway intermediates of the Mur pathway [14, 15]. Other evidence suggests further regulation via RelA within the stringent response [16].

The lipid II cycle begins with the consecutive attachment of cytosolic PG precursors to the lipid carrier undecaprenyl-phosphate (UP) on the cytoplasmic surface of the membrane (Figure 1.2). The resulting lipid II molecules are subsequently flipped to the outer surface of the membrane, where the PG building block is detached and inserted into growing PG strands. Finally, the remaining lipid carrier is recycled and returned to the cytosolic side of the membrane.

The first cytosolic precursor to be attached to UP is MurNAc-pentapeptide. This produces lipid I, to which MurG attaches GlcNAc to yield lipid II. The lipid II flippases MurJ and Amj (Alternate to MurJ) mediate the translocation of lipid II to the extracellular surface [18–20]. While MurJ is considered the main flippase in normal growth, Amj is induced by σ^M (section 1.5.2) under cell wall stress and particularly in absence of functional MurJ (e.g. deletion or inhibition) [21]. Interestingly, Amj shares neither sequence nor structural homology with MurJ. This is thought to provide an extra layer of protection against antibiotics targeting this essential function [18, 21].

The resulting GlcNAc-MurNAc-pentapeptide is released from the lipid carrier by PG-glycosyltransferases and inserted into growing PG strands [22]. PG-glycosyltransferases can be found in the SEDS (shape, elongation, division, sporulation) family such as RodA and FtsW and class A (=bifunctional) Penicillin-binding proteins (PBPs) [22, 23]. The subsequent cross-linkage of pentapeptides is conducted by either associated class B PBPs in case of SEDS or the transpeptidation domain of class A PBPs. Recent work now points to SEDS being utilized in the regular PG synthesis for elongation and division, while class A PBPs are employed in PG repair [24]. While there is compelling evidence that SEDS proteins function as glycosyltransferases and MurJ and Amj have been found to translocate lipid II, there is also evidence that FtsW might be involved in the flipping step [8, 21, 25].

The resulting lipid carrier UPP is dephosphorylated by BcrC, UppP or YodM [26]. While BcrC and YodM are members of the PAP2 superfamily, UppP belongs to the BacA family and shows no homology to either BcrC or YodM [26]. BcrC seems to be the mayor UPP phosphatase under normal growth conditions, but is also upregulated during cell envelope stress and mediates resistance against bacitracin [27, 28]. UppP is able to perform UPP-dephosphorylation in a $\Delta bcrC$ background - although with a reduced growth rate [26–28]. However, UppP is essential for sporulation [28]. The third lipid phosphatase YodM can only support growth in the absence of BcrC and UppP when artificially overexpressed [26].

To initiate another round of the lipid II cycle, the dephosphorylated UP needs to be flipped back to the inner surface of the membrane. Interestingly, so far no potential UP-flippase has been identified. The slow flipping rate, however, might indicate a passive flipping mechanism [3, 29].

Lipid carrier is replenished in the form of UPP by UppS in the cytoplasm [29–31]. This harbors the problem that the newly synthesized UPP is located on the cytoplasmic side of the membrane while all known UPP-phosphatases are located on the extracellular surface. So far, it has not been elucidated how the lipid carrier is fed into the lipid II cycle, but there are two major hypotheses: (1) a UPP-phosphatase could facilitate dephosphorylation of UPP in the cytoplasm or (2) UPP could be flipped to the extracellular

surface to then be dephosphorylated there [29].

In addition to its usage in the lipid II cycle, UP is also utilized as a lipid carrier in the synthesis of wall teichoic acids, which underlines its importance for cell envelope synthesis [6].

1.3. Elongasome and divisome

The rod shape of a typical *B. subtilis* cell requires a careful organization of the cell wall synthesis apparatus. This organization has to be two-fold: spatial to achieve the rod shape and temporal to ensure a balance between growth and division. For this, *B. subtilis* contains two cytoskeleton proteins that serve as a scaffold for enzymes involved in peptidoglycan synthesis - MreB, which is involved in elongation [32, 33], and FtsZ, which is required for cell division [34]. The two cell wall synthesis complexes surrounding these scaffolds are termed elongasome and divisome, respectively [35]. As they incorporate the main enzymes responsible for the incorporation of PG building blocks into the peptidoglycan sacculus, their localization and timing greatly influence the eventual shape of the cell [35].

The elongasome contains three actin-like MreB proteins (MreB, MreBH and Mbl), which polymerize along the cell membrane and colocalize with the essential proteins MreC, MreD, RodZ and PG hydrolases as well as the SEDS protein RodA and PBPs [32, 33]. The latter of which catalyze the last two steps (transglycosylation and transpeptidation) of PG synthesis. While PbpH is the most commonly found PBP in the elangosome it can be replaced by Pbp2a in e.g. *pbpH* deletion mutants [32]. The whole complex moves circumferentially around the short axis of the cell. This has been show to be driven by peptidoglycan synthesis as any inhibition of the lipid II cycle also slows down MreB movement [32, 33].

The cytoskeleton of the divisome consists of FtsZ, a tubulin-like GTPase that polymerizes at the future division site (midcell in *B. subtilis*) to form the so called (Fts)Z-ring [34]. These FtsZ polymers move circumferentially around the cell by treadmilling, which describes the polymerization of FtsZ proteins at one end of the structure while dissociating from the other. This treadmilling of FtsZ was recently shown to drive circumferential PG synthesis [36–38]. To achieve the correct localization of the FtsZ-ring many bacterial species have been found to utilize regulators such as the Min-system of *Escherichia coli*, which inhibits FtsZ polymerization in polar regions through an oscillating system [39]. In *B. subtilis* the Min-system also locally inhibits FtsZ polymerization but functions in a more stationary way [40]. For this, MinD binds to DivIVA, which localizes at negatively

curved membranes found at the cell poles and after constriction at the new division site [40]. Another cue of FtsZ polymerization in *B. subtilis* seems to be closely connected to open complex formation of DNA replication, which is initiated by DnaA, as a blockage leads to an off-center FtsZ-ring formation [41].

The assembly of a mature divisome can be divided into two consecutive steps. In the early stages FtsZ multimerizes with its membrane-anchor FtsA, which are subsequently stabilized by ZapA and EzrA [42]. In a later stage GpsB, FtsL, DivIB, FtsW, Pbp2B and DivIVA are recruited [42]. Of these, FtsW is thought to detach PG building blocks from lipid II and insert it into growing PG strands via transglycosylation, after which Pbp2B crosslinks the pentapeptides [22, 23, 42]. While Pbp2B is the most common PBP in the divisome, others, such as Pbp1a, can take its place [34].

1.4. Cell wall targeting antibiotics

As an essential structure that is easily accessible the cell wall is often targeted by antibiotics. In this section some noteworthy antibiotics targeting the PG synthesis will be introduced (Table 1.1).

Table 1.1.: Antibiotics used in throughout this thesis. CDA: calcium dependent lipopeptide antibiotic. [1] +: gram-positive bacteria, -: gram-negative bacteria. *: in a deletion strain of the main resistance determinant, *bceAB*, as used throughout this work.

antibiotic	class	active against[1]	cellular target	reported MIC in *B. subtilis*
ampicillin	β-lactam	+/-	PBPs	0.06 µg/ml [22]
bacitracin	cyclilc peptide	+	UPP	8-16µg/ml* [43]
friulimicin B	CDA	+	UP	1.5 µg/ml [44]
laspartomycin C	CDA	+	UP	8 µg/ml [45]
nisin	lantibiotic (type A)	+	lipid II	125 µg/ml [46]
ramoplanin	glycolipodepsipeptide	+	lipid II	1.25 µg/ml [47]
tunicamycin	nucleoside antibiotic	+	MraY	5 µg/ml [48]
vancomycin	glycopeptide	+/-	lipid II	0.5 µg/ml [49] 0.25 µg/ml [22]

1.4.1. Lipid II binding antibiotics

As the last membrane-bound precursor in the lipid II cycle before insertion of the peptidoglycan building block into the sacculus, lipid II is an attractive target for antibiotics. Some of these antibiotics will be described here in more detail to represent the variety of binding sites and mechanisms.

The glycolipodepsipeptide ramoplanin directly binds to the pyrophosphate moiety of lipid II [5]. While a depolarization of the membrane has been found to occur at high concentrations of ramoplanin in *Staphylococcus aureus* [50] the main mechanism of action is presumed to be blockage of the lipid II pool [3]. By sequestering lipid II ramoplanin impedes the transglycosylation step of the lipid II cycle and therefore PG synthesis [3].

Just like ramoplanin the type A lantibiotic nisin binds to the pyrophosphate moiety of lipid II via its N-terminal peptide rings [51]. However, binding and sequestering of lipid II is not the only mechanism nisin employs. The C-terminal rings mediate the clustering of 4 lipid II and 8 nisin molecules, creating a pore in the bacterial membrane [52]. The subsequent depolarization of the membrane and loss of cytoplasmic solutes potentiates nisin activity [53]. Furthermore, nisin has been found to increase fluidity and reduce dipole potential in an eukaryotic membrane model [54].

The glycopeptide vancomycin has also been found to bind lipid II [5]. In contrast to nisin and ramoplanin, vancomycin recognizes the pentapeptide chain, which is also present in nascent peptidoglycan [55]. In *E. coli* vancomycin decreases the cross-linkage of peptidoglycan, indicating nascent peptidoglycan to be its primary target [55]. In *B. subtilis* however, exposure to vancomycin leads to an accumulation of lipid II, indicating the membrane-bound lipid carrier as the primary target [56].

1.4.2. Bacitracin

The branched cyclic dodecylpeptide bacitracin is a narrow spectrum antibiotic, which is active against gram-positive cocci and bacilli [57]. It does so by binding and sequestering UPP in a Zn^{2+}-dependent manner [58, 59]. This inhibits UPP dephosphorylation and decreases the free lipid carrier availability. Ultimately, this slows down the lipid II cycle and therefore inhibits PG synthesis [3]. Due to its nephrotoxicity and potential to cause anaphylactic reactions it is no longer recommended by the Food and Drug Administration (FDA, US) as treatment by injection of infants, but bacitracin can still be used topically or ophthalmically [60].

1.4.3. β-lactams

β-lactam antibiotics such as ampicillin primarily inhibit the transpeptidase domains of high molecular weight penicillin binding proteins (PBPs) and thereby prevent the maturation/cross-linkage of peptidoglycan strands [61]. With prolonged exposure to β-lactams the bacterial cell wall loses stability, which ultimately leads to lysis, as old peptidoglycan is constantly degraded by autolysins to allow for growth [22, 62].

1.4.4. Calcium-dependent lipopeptide antibiotics

Both friulimicin B and laspartomycin C are calcium-dependent lipopeptide antibiotics consisting of a 10 amino acid cyclic core and a N-terminal fatty acid tail [63, 64]. Both antibiotics were found to sequester UP. Interestingly, laspartomycin C has been described to bind UP more efficiently (K_D 7.3±3.8 nM) than friulimicin B (K_D 210 nM) but needs higher concentrations for its antibiotic activity (Table 1.1) [63–65]. Friulimicin B entered clinical trials in 2007. However, these were stopped due to toxic effects [66].

The only calcium-dependent lipopeptide antibiotic that is currently in clinical use is daptomycin, which has recently been found to bind phosphatidylglycerol to subsequently multimerize [67–69]. Due to the multimerization and daptomycin's bulky lipid tail fluid lipids cluster around the lipid-bound antibiotic, which increases the overall rigidity of the remaining cellular membrane [68, 69]. This change in membrane liquid state might decrease the affinity of peripheral membrane proteins such as MurG leading to their detachment and consequent inhibition of activity [69].

1.4.5. Tunicamycin

Tunicamycin consists of uracil, the C_{11} sugar tunicamine, N-acetylglucosamine and a fatty acid and inhibits the PNPT superfamily of enzymes, which consists of prenyl sugar transferases [48, 70]. In gram-positive bacteria these include several enzymes involved in cell envelope synthesis - most notably MraY, which catalyzes the synthesis of lipid I (Figure 1.2), and TagO, which is involved in wall teichoic acid synthesis [8, 70].

MraY has been crystallized in the presence of tunicamycin revealing the mode of action [71]. Tunicamycin binds its target in a wide cytoplasmic binding cavity, mimicking MraY's substrate MurNAc [71]. Since the human MraY/TagO-homologue GTP is also inhibited by tunicamycin a medicinal use is not possible. However, current research is ongoing to modify tunicamycin in a way that allows effective MraY inhibition, while reducing affinity for human GTP [72].

1.4.6. Fosfomycin

The phosphonic acid antibiotic fosfomycin is a broad-spectrum antibiotic targeting MurA, which catalyzes the first step of cytosolic PG precursor synthesis [10, 73]. As MurA resides in the cytoplasm, fosfomycin has to cross the bacterial membrane to inhibit PG synthesis. This transport has been found to be mediated by a specific sugar transporter making the uptake and with it the antibiotic action directly dependent on the utilized carbon source [10, 73].

This selection of cell wall targeting antibiotics already provides an insight into the great diversity that can be found here. The majority seem to target easily accessible structures, although some antibiotics such as tunicamycin and fosfomycin reach their active sites via the cytoplasm. Furthermore, the inhibition of the lipid II cycle is predominately achieved via sequestering of lipid carrier molecules.

1.5. Effects on antibiotic susceptibility

As diverse as antibiotics are many bacterial species have developed mechanisms to reduce their susceptibility towards them. These mechanisms are as diverse as the antibiotics and range from the more commonly known genetic resistances to general principles in the interactions between antibiotic and target. Furthermore, not all effects on antibiotic susceptibility are in fact resistance but somewhat different mechanisms. These will be described here.

1.5.1. Mechanisms reducing antibiotic susceptibility

Resistance Resistance describes the ability of a microbial culture to grow and proliferate while being exposed to an antibiotic [74]. Usually, resistance is measured via the minimal inhibitory concentration (MIC), which represents the lowest antibiotic concentration that prevents growth [74]. As such, a higher MIC indicates higher resistance (Figure 1.3a).

Most changes that lead to resistance are genetic, like acquisition of resistance genes (e.g. β-lactamases, modules described in section 1.5.2) or the mutation of a binding pocket in the antibiotics target. However, there are also some cases where changes in the metabolism have an impact on resistance. One example for this is fosfomycin, which is imported via two sugar transporters in *E. coli*. One of these (hexose-6-phosphate transporter) is strongly affected by carbon catabolite repression, which means that the transporter is inactive in presence of glucose [10, 73]. Therefore, *E. coli* is much more resistant in glucose-containing media due to the reduced import rate of fosfomycin. As fosfomycin's target MurA resides in the cytoplasm this can have a great impact on the MIC.

Another example for this is the work of Greulich and colleagues about ribosome targeting antibiotics and the growth-dependent bacterial susceptibility [75]. They have found that due to the growth rate-dependent shift in ribosome content the efficiency of ribosome-targeting antibiotics can vary dependent on their mode of binding at different growth rates (section 1.5.4).

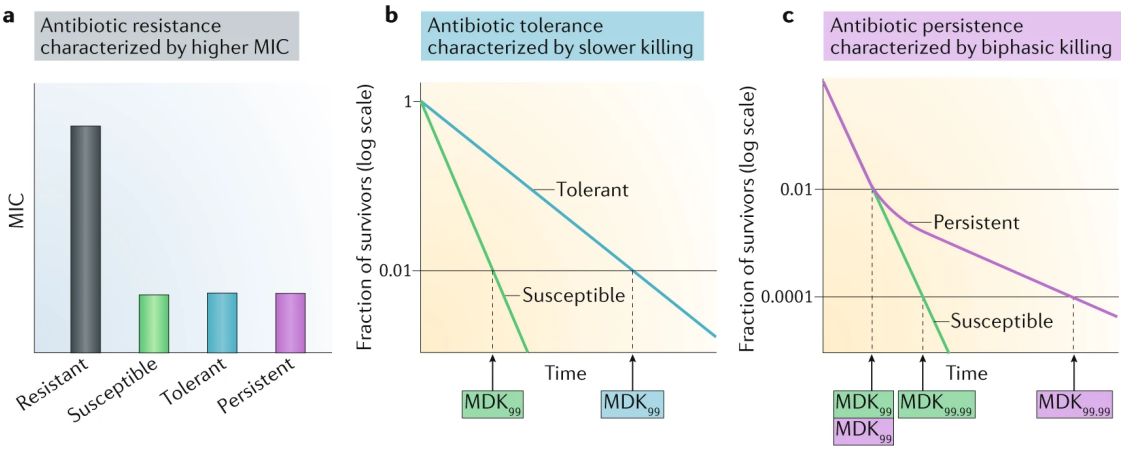

Figure 1.3.: Antibiotic resistance, tolerance and persistence. (a) Resistance is best recognized by an increase of the antibiotic concentration needed to kill a bacterial culture. Both tolerant and persistent bacteria are killed by the same concentration of antibiotic as susceptible bacteria. (b) While the antibiotic concentration needed to kill tolerant bacteria stays the same, they are able to survive for longer. This increases the minimal duration of killing (MDK). (c) Only a small portion of a culture consists of persistent cells while most others are susceptible. Only when this majority of susceptible cells are killed will the increased MDK of persistent cells become apparent. This results in a biphasic killing curve. Reprinted from [74], with permission from Springer Nature.

Tolerance In 1944 slow-growing bacterial cultures were shown to die more slowly than fast-growing cells [76–78]. This phenomenon has been termed tolerance [74]. It is important to note that in contrast to resistance it only refers to the time it takes a culture to die to a certain extent and does not indicate a change in the concentration needed to kill the culture. As tolerance is defined via the duration of killing it can only be determined for bactericidal antibiotics [74]. To determine the degree of tolerance it is advised to measure the minimal duration of killing (MDK_{99}) of a large fraction (99%) of the initial culture (Figure 1.3b) [74].

Persistence A distinct type of tolerance is the increased duration of killing of a subpopulation of a clonal bacterial culture. These surviving bacteria are termed persisters and are generally recognized by a diphasic killing curve (Figure 1.3c) [74]. Similar to tolerant cells, persisters are usually characterized by dormancy as well as a reduced metabolism and ATP levels [74]. Persistant bacteria are particularly problematic as they cannot be eliminated by antibiotics and are the most common cause for relapsing and chronic infections [79, 80].

While persistence is a transient phenomenon that cannot be inherited, several factors have been identified that promote the formation of persister cells [81]. Many of these factors can be caused by the environment as e.g. the SOS response of *E. coli* [82] or the

depletion of nutrient in mid-exponential phase [83]. However, certain genetic factors can modify the amount of cells in a population that enter a persistant state [81]. For instance, the deletion of a global regulator often results in a 10-fold decrease of persister-formation [81]. Similarly, many toxin-antitoxin modules can induce the formation of persister cells and their deletion reduces the amount of persister cells in a culture [81]. However, the mechanisms of persistence are highly redundant as all tested strains still produced persisters [81].

1.5.2. Cell envelope stress response of *B. subtilis*

As so many antibiotics are targeting the cell wall synthesis it will not come as a surprise that most bacteria have developed genetic resistance mechanisms to combat them. The model organism *B. subtilis* is no exception to this. A summary of cell envelope stress response (CESR) modules in *B. subtilis* is given in Table 1.2.

Table 1.2.: CESR modules of *B. subtilis*. [1]: 2CS: two-component system, T: ABC-transporter, I:inhibitory protein

module	type[1]	function	inducers	references
Ape	2CS+T	protection from eukaryotes	eukaryotic anti-microbial peptides	[84, 85]
Bce	2CS+T	bacitracin resistance	bacitracin, certain lipid II-binding antibiotics	[86, 87]
Lia	2CS+I	cell membrane and wall homeostasis	some PG-targeting antibiotics, alkaline pH, detergents	[88–90]
Psd	2CS+T	nisin resistance	lipid II-binding antibiotics, bacitracin	[91]
σ^M	ECF	cell wall homeostasis	salt, acid, heat, cell wall antibiotics, superoxide stress	[92–94]
σ^V	ECF	protection from lytic enzymes	lysozyme	[95]
σ^W	ECF	cell membrane homeostasis	PG synthesis inhibitors, alkali stress, detergents	[92, 96, 97]
σ^X	ECF	protection from cationic antimicrobial peptides	β-lactams, lantibiotics, bacitracin	[93, 98]

Two-component systems

Two-component systems are basic stimulus-response coupling mechanisms and consist of a membrane-bound, stimulus-sensing histidine-kinase and a cognate, cytoplasmic response regulator that induces cellular changes when activated [99]. Typically histidine-kinases consist of a N-terminal ligand binding domain that is responsible for signal-sensing and a C-terminal kinase domain, responsible for signal transduction. Additional domains, especially transmembrane domains, are also very common [100]. Under inducing conditions the histidine-kinase autophosphorylates and the phosphate moiety is subsequently transferred to the response-regulator, which activates its output domain [101]. This output domain can often bind DNA and therefore regulate transcription [101].

The CESR of *B. subtilis* contains four unusual two-component systems as the involved histidine-kinase does not possess a stimulus-sensing domain. Instead these are functionally linked to additional proteins [102]. The Lia module is regulated by an inhibiting, third component while the Bce-like modules associate with ABC transporters that are able to sense and remove certain cell envelope targeting antibiotics from their membrane-bound targets [102].

The Lia module Under non-inducing conditions the histidine-kinase LiaS is kept inactive by LiaF [88, 103]. However, in presence of specific cell envelope targeting antibiotics, alkaline pH or detergents this inhibition ceases and LiaS autophosphorylates [103]. This phosphate group is subsequently transferred to the response regulator protein LiaR, which then activates transcription of at least 10 genes [88]. As the Lia module is autoregulated this includes *liaFSR*. However, the main target is *liaIH* [88]. LiaI has been shown to freely diffuse in small patches in the membrane in absence of cell wall damage but to locate in distinct spots during cell envelope stress [90]. Under these circumstances LiaI becomes static and recruits LiaH. The emerging LiaIH patches are thought to occur beneath holes in the cell wall to stabilize the membrane and prevent tears [90]. The sensing mechanism of the Lia module is still unknown although many different inducers have been identified [89, 104, 105].

Bce-like modules Bce-like resistance modules are commonly found in Firmicutes and *B. subtilis* is no exception [106, 107]. Here, three modules namely BceRSAB [86], PsdRSAB [91] and ApeRSAB (formerly YxdRSAB) [84] have been described. The best characterized Bce-like module so far is BceRSAB in *B. subtilis*. In contrast to the Lia module BceS does not interact with an inhibitory protein but rather an ABC transporter complex - BceAB [108]. Resistance is achieved by a target-protection mechanism where an an-

tibiotic is detached from its target in an ATP-dependent manner by BceAB [87, 109]. This process activates the histidine-kinase BceS via a flux-sensing mechanism [43, 108, 110]. After subsequent phosphorylation of BceR this response-regulator activates the transcription of BceAB. This ensures that the expression of further BceAB transporters to combat an ongoing antibiotic challenged can be matched exactly to the demand [43]. Related modules are expected to function similarly.

While the BceRSAB module is primarily activated by UPP-bound bacitracin some lipid II-binding antibiotics have also been shown to induce the system [91, 111]. PsdRSAB also reacts to bacitracin but is more specialized to lipid II-binding antibiotics [91] and the ApeRSAB module seems to be specialized to eukaryotic antimicrobial peptides [84, 85]. Both the BceRSAB and PsdRSAB modules are also induced by so-called cannibalism toxins that a subpopulation of *B. subtilis* synthesizes at the beginning of stationary phase [111]. These cannibalism toxins are thought to allow the producing cells to scavenge nutrients from their unprepared siblings to postpone sporulation [90, 111].

Extracytoplasmic function σ factors

In bacteria the RNA polymerase (RNAP) complex requires σ factors for promoter recognition and activation of transcription. To achieve differential expression each cell contains various σ factors that recognize distinct promoters [112]. Most transcription for everyday growth is regulated by housekeeping σ factors of the σ^{70} family. However, transcription required for specific circumstances is initiated by other σ factors such as members of the σ^{56} family or σ factors of the σ^{70} family with a reduced set of up to four conserved regions (σ_1-σ_4) [113, 114]. Of these regions only σ_2 and σ_4 are essential for σ factor function as they accomplish RNAP binding and promoter recognition [114]. The most minimalistic σ^{70} factors only contain these two domains and are often involved in the signal transduction of extracytoplasmic signals [115]. These so-called extracytoplasmic function σ factors (ECFs) are involved in the sensing and subsequent reaction to different signals ranging from oxidative or reductive stress to iron homeostasis [112]. Regulation of these ECFs is diverse, however the most common regulation is performed by so-called anti-σ factors (AS), which sequester their cognate ECF under non-inducing conditions to keep them inactive [116].

Four ECF-AS pairs in *B. subtilis* are known to be active in the CESR [92, 98]. While each of them seems to play a specific role in the CESR their scope of inducers and regulons overlap [98].

σ^W is most effectively induced by membrane-active agents such as detergents and activates the transcription of 60-90 genes - dependent on the inducer [98]. One of

the notable targets is metallothiol transferase FosB, which confers resistance against fosfomycin, an inhibitor of cytosolic PG precursor synthesis [117]. Furthermore, σ^W contributes to the resistance against pore-forming lantibiotics such as nisin by expression of the membrane-stabilizing phage-shock protein PspA [96, 97]. Another important target of σ^W is the fatty acid biosynthesis operon *fabHa-fabF*. Here, σ^W activity leads to changes in the abundance of the expressed proteins and ultimately to a decrease in membrane fluidity [118].

σ^V confers resistance against lysozyme via induction of the *dltA* operon and the peptidoglycan O-acetyltransferase OatA [95, 98].

σ^M regulates the expression of 60 or more genes of which most are involved in the core machinery of cell division and cell wall synthesis [98]. These genes can be divided into three groups of different function: (1) Genes encoding proteins of the core cell wall synthesis machinery, such as components of the elangosome (MreBCD, RodA) and divisome (DivIB, DivIC, MinCD) as well as enzymes producing PG precursors (Ddl, MurB, MurF) [119]. (2) Genes encoding enzymes with redundant functions, which might fill in if the primary gene/protein is inhibited. For instance, this is the case for the lipid II translocase Amj, which is functionally redundant to MurJ, the lipid II flippase, and LtaSa, an alternative to LtaS, which catalyzes the elongation of lipoteichoic acids [21, 119]. (3) The third group includes genes with regulatory functions such as AS controlling σ^M as well as synthases for nucleotide second messengers and the transition state regulator Abh [98].

σ^X represents a second layer of resistance against β-lactam antibiotics, nisin and bacitracin (after σ^M) [98]. By activating the *dltA* and *pssA* operons (D-alanylation of teichoic acids and synthesis of neutral lipids, respectively) σ^X reduces the net negative charge of the cell envelope, which protects the cell from cationic antimicrobial peptides [120].

Besides genetic resistance factors described in this section other mechanisms exist that enable bacterial cultures to survive higher antibiotic concentrations. Two of them shall be explain in the following section.

1.5.3. Antibiotic evasion mechanisms

Inoculum effect Often antibiotic activity is reduced in high cellular densities [121–124]. This phenomenon is termed inoculum effect and can have multiple origins. For instance, bacterial strains which harbor β-lactamase can survive higher concentrations of β-lactams at higher densities [122]. This is achieved by the higher total production of β-lactamase in dense populations. Other resistance determinants, such as an

acetyltransferase of the pathogen *Providencia stuartii* that inactivates aminoglycoside antibiotics, need to be produced in high number to be effective [123]. Here, the bacteria have implemented a quorum sensing mechanism, with which they monitor their density, to only activate the energy intensive production of the resistance determinant in sufficiently dense populations [123]. Nevertheless, even in the absence of resistance genes, the inoculum effect can be observed in bacterial cultures. As shown by García and colleagues high cellular densities alone can lead to an overall increased resistance against certain disinfectants due to a decrease of active component per cell [124].

Minimal exposure of targets For a long time researchers were puzzled by the much lower in vivo activity of many cell wall targeting antibiotics than the in vitro binding affinity data suggested. This phenomenon has been observed for many species and antibiotic compounds. Neither yet undiscovered resistance genes nor inactivation of the antibiotic in vivo could fully explain it [3, 47, 49, 53, 91, 125–129]. To determine if a general property of the strongly conserved PG synthesis pathway is the cause for the in vivo efficacy gap Hannah Piepenbreier, a former colleague and collaborator, developed a mathematical model of the lipid II cycle. Interestingly, a stark imbalance of lipid carrier pool sizes was revealed with the vast majority of lipid carrier being present as UPP (Figure 1.4) [3].

Since the molecular targets as well as the equilibrium dissociation constants (K_D) of friulimicin, bacitracin, vancomycin, nisin and ramoplanin are known they were easily integrated into the mathematical model. Starting with bacitracin, which binds the largest lipid carrier pool UPP, the concentration needed to reduce the PG synthesis rate by 50% (IC_{50}=1.8 μM) coincided with both, the K_D-value (1 μM) and the MIC. Under closer examination it turned out that at the IC_{50} bacitracin sequesters enough UPP in a complex to reduce the total lipid carrier pool by half.

The model predicted that while nisin sequesters 50% of lipid II molecules at concentrations around the K_D (0.015 μM) it reduces the total lipid carrier pool only by around 1% as it targets the much smaller lipid carrier pool of lipid II. Since the lipid II cycle has a very fast turn-over rate of around $1.9 \cdot 10^6$ molecules/min the lipid II pool is quickly replenished and PG synthesis is virtually undisturbed. To block 50% of total lipid carrier a 700-fold higher concentration of nisin is required. Not only does this high concentration lead to a 50% reduction of PG synthesis in the model (IC_{50}=10.1 μM) but it is also in the same order of magnitude as the experimental MIC (4.77 μM).

The same mechanism applies to the other lipid II binders, ramoplanin and vancomycin as well as the UP-binding friulimicin B [3].

The above described examples and findings demonstrate that the in vivo efficacy gap

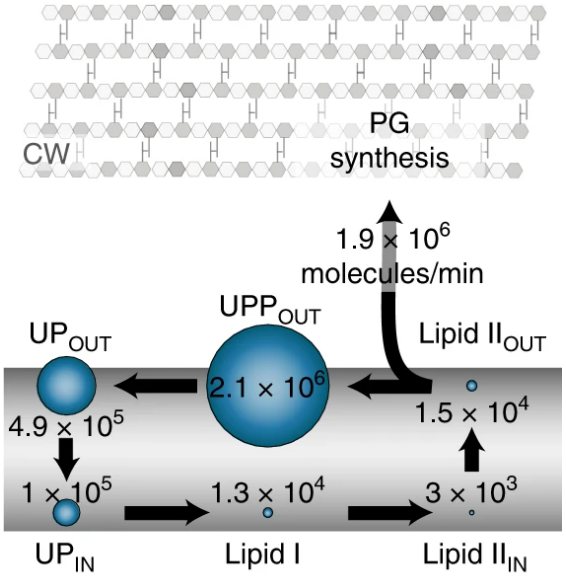

Figure 1.4.: Distribution of lipid carrier pool sizes in *B. subtilis* and rate of PG synthesis. A mathematical model predicts a highly irregular distribution of lipid carrier pool sizes in the lipid II cycle. Reprinted from [3], with permission from Springer Nature.

arises from vastly different lipid carrier pool sizes. Therefore, bacteria are able to protect themselves against many cell wall targeting antibiotics by keeping the vast majority of lipid carrier in a not targeted version [3].

1.5.4. Cellular adaptions to growth conditions

Bacteria have to adjust most of their metabolism to the ever changing environment. As this entails most potential targets of antibiotics their efficacy can change accordingly. This also holds true for pathogens causing infectious diseases [130]. In the medical environment, infections caused by slow growing bacteria are often particularly problematic to control as antibiotic treatments are often ineffective [131, 132]. This is often caused by a widespread tolerance of slow growing bacteria against antibiotic attacks [131, 133]. However, the resistance of bacteria against specific antibiotics can also vary depending on growth rate [75].

The following section addresses the multifaceted ways in which bacteria adapt to their surroundings and how this can effect antibiotic susceptibility.

Adaption of macromolecular composition to growth conditions

To outcompete other microorganisms in their natural environment bacteria have evolved to utilize nutrients very quickly and efficiently. The most obvious change in bacterial

growth caused by a shift into richer media is a faster rate at which the cellular mass doubles in - the growth rate. Furthermore, RNA, DNA and protein mass per cell increases with growth rate [134]. However, the cellular changes are more tightly regulated than a simple overall increase of cell material.

It is well known that bacteria can grow with much shorter division times than they need to replicate their genome [135]. To ensure that every daughter cell receives a fully functional genome these bacteria start a new round of genome replication before completing the previous round. This so-called multifork replication has been shown e.g. in *E. coli* with an average of 6.7 origins per cell at a doubling time of 20 min [134]. Obviously, this increases the amount of total DNA per cell in fast growth and can lead to a rise in copy number of genes close to the replication origin [134, 136].

While the total protein amounts per cell increases in fast growth, not all proteins are affected by this in the same way [134, 137]. In fact, the fraction of ribosomal proteins has been shown to increase linearly with growth while the metabolic fraction of proteins declines accordingly [138]. To see how gene expression is modulated by changes in growth rate, Klumpp and colleagues have built a mathematical model, which included the cellular copy number of the gene, transcription rate per copy of the gene, mRNA degradation rate, translation rate per mRNA, protein degradation rate and cell volume [139]. Their model predicted that even though the number of constitutively expressed mRNA and proteins per cell increases, the final protein concentration is reduced linearly in faster growth due to the simultaneous increase in cell volume/mass [139]. This correlation is only slightly modulated by gene copy number but transcriptionally regulated genes can be affected differently. The regulators of transcription are also subject to the same decreased production in fast growth as constitutively expressed gene products. This decreased regulator concentration in cells at high growth rates leads to a stronger decline in production of positively regulated genes as their activators are not present in sufficient numbers [139]. For negatively regulated genes, the opposite is true as the reduced inhibitor concentration struggles to stop transcription. The authors found that in case of highly cooperative repressors even a positive growth rate dependence of negatively regulated genes takes place [139].

Not only transcription is dependent on growth rate but also translation as Borkowski et al. have found in *B. subtilis* [140]. While the overall translation efficiency is reduced in fast growth, gene-specific translation initiation regions can have a strong impact on this efficiency [140].

With the bacterial cytoplasm being very densely packed [141] it comes to no surprise that increased amounts of DNA, RNA and protein per cell are accompanied with larger cell sizes and therefore higher volumes. In fact, every $2 \cdot 10^9$ amino acid residues of protein have been found to lead to approximately $1\,\mu m^3$ increase in volume in bacteria [134]. Interestingly, while both *E. coli* and *B. subtilis* are rod-shaped bacteria this change in volume is not acquired in the same manner. While *E. coli* grows in both, length and width, *B. subtilis* increases its volume only via elongation but maintains a nearly constant width [142, 143]. Of course, this increase in size entails a matching increase in cell volume and cell surface.

While the rate of all major anabolic pathways depends on growth rate only fatty acid synthesis was show to have a direct impact on on cell size [144]. This was shown by the addition of oleic acids to *E. coli* perturbed in RNA or protein biosynthesis via antibiotics. Here, the addition of the fatty acid partly corrected the size defects induced by the antibiotics [144]. This shows that the availability of fatty acids is a major limiting factor for cell size. Similar data in *B. subtilis* and *Saccharomyces cerevisiae* suggests a strong conservation of this dependency [144].

Antibiotic susceptibility at different growth rates

With so many changes to the bacterial cell in dependence of the growth rate researchers wondered early on how these can affect antibiotic susceptibility. β-lactams were one of the first antibiotics to be investigated [76]. While Lee et al. and many groups after that measured a reduction in antibiotic activity in slow-growing bacteria [76–78, 145], their assays were ultimately set up to measure tolerance [78]. Unlike resistance, tolerance describes the change of duration of antibiotic activity (section 1.5.1). However, to my knowledge the resistance i.e. the concentration needed for lysis/growth inhibition has not been measured for any cell wall targeting antibiotics in dependence of growth rate.

The first comprehensive investigation of the changes in intrinsic resistance (i.e. in absence of genetic resistance determinants) caused by adaptions to varying growth rates of any type of antibiotics focused on ribosome targeting antibiotics. Greulich et al. found that the growth rate can have a varying effect on the activity of ribosome targeting antibiotics [75]. They showed that the transiently binding antibiotics tetracycline and chloramphenicol were less effective against slow-growing cells while the two aminoglycosides streptomycin and kanamycin, which bind nearly irreversibly to the 30S ribosomal complex, inhibit slow-growing cells more effectively [75]. It stands to reason, that these changes in susceptibility are caused by the changes in ribosomal abundance described above. However, there is a second, opposing trend connected to the high ribosome con-

centration in fast-growing cells: The higher the ribosomal concentration under unperturbed conditions the less this ribosomal pool can be increased in response to antibiotic attack. With the help of a mathematical model, the authors were able simulate these opposing trends and found that the ribosomal content has a higher impact on irreversibly binding antibiotics such as streptomycin and kanamycin, while the ability to increase said content by a large factor has a higher effect on reversible binding antibiotics such as tetracycline and chloramphenicol [75].

1.6. Aims and Objectives

The threat of active resistance mechanisms, such as resistance genes, on modern healthcare is widely recognized as one of the most pressing issues of our time. However, intrinsic passive resistance mechanisms, such as metabolic adjustments or the general structure of pathways that decrease susceptibility, are equally important to consider in the clinical administration of antibiotics to fully utilize their potential while reducing the risk of spreading resistance. In this work, the impact of active and passive resistance mechanisms of *B. subtilis* against cell envelope targeting antibiotics will be investigated.

The first aim of the project is to review the natural cell envelope stress response and conferred resistance of the involved resistance modules toward the novel antibiotic laspartomycin C. To do this, we will analyze the induction of the various resistance modules and measure the susceptibility of the wild type and strains carrying a deletion of the respective resistance modules. The results will be compared with the stress response and conferred resistance against friulimicin B, a related antibiotic with the same target.

Furthermore, we aim to explore the influence of growth rate on the susceptibility towards cell envelope targeting antibiotics. Here, an assay to accurately measure the susceptibility towards cell envelope targeting antibiotics will be developed to minimize the influence of nutrient quality of the media as well as the expected reduction of reaction time during slow growth. Susceptibility of *B. subtilis* will be determined with adjusted IC measurements at different growth rates.

In addition I aim investigate several smaller research projects. These include:

- Analyzing the effect of amino acids on growth rate, stationary phase stress response and antibiotic susceptibility as amino acid availability can have significant effects on the metabolism.
- Investigating the degradation rate of selected cell wall targeting antibiotics to gain an understanding of its influence on antibiotic activity.
- Exploring the conferred resistance of a putative tunicamycin resistance gene against tunicamycin as its activity has only been shown in overexpression.
- Determining how inoculum size affects nisin activity.
- Analyzing the effect of enzyme activity reduction in the lipid II cycle on susceptibility towards cell wall targeting antibiotics.

2. Results

2.1. CESR of *Bacillus subtilis* towards laspartomycin C

These results were published in *Antibiotics* (Basel, Switzerland) in 2020 and are printed here with permission. I contributed by planning and performing the experiments, analyzing the data and writing the manuscript [17]. The referenced figures in the summary can be found in the publication.

2.1.1. Summary

Laspartomycin C is a novel antibiotic that blocks PG synthesis by sequestering the lipid carrier UP. While its biochemical properties have been well researched [45, 63, 66], the cellular stress responses induced by laspartomycin C have not been investigated so far. Here, the stress response of *B. subtilis* after laspartomycin C attack was compared with the stress response generated by a challenge with friulimicin B, which also sequesters UP and belongs to the same family of cyclic calcium-dependent lipopeptides.

As bacteria only need to protect themselves and induce stress response systems at antibiotic concentrations damaging to the cell, the induction of all stress response modules was not compared at their absolute concentration but relative to their antibiotic action. For this, the inhibitory concentration leading to a 50% growth reduction (IC_{50}) was determined for both antibiotics. Growth was measured via OD_{600} 10 h after antibiotic challenge. Here, the susceptibility towards friulimicin B (IC_{50} 1.6 µg/ml) was higher than towards laspartomycin C (IC_{50} 7.3 µg/ml).

First the induction of σ^M, the only module activated by friulimicin B [44], was examined with a stain expressing a luciferase reporter gene under the control of a σ^M regulated promoter (P_{bcrC}). Interestingly, laspartomycin C generated a higher response of the σ^M-regulon with a 3.5-fold increase than friulimicin B with only a 2-fold increase in luminescence (Figure 5). Intrigued by this stronger induction more CESR modules of *B. subtilis* (section 1.5.2) were examined for their inducibility by laspartomycin C. Consistend with previous reports friulimicin B did not generate a response [44]. However, laspartomycin C induced the Lia, Bce and Psd modules to an intermediate degree in

experimental setups similar to the one described above (Figures 6, 7).

As laspartomycin C induces these modules the question arose whether they also confer resistance against this novel antibiotic. For this, the IC_{50} of strains carrying deletions of either a target of the resistance module (*bcrC* in case of $\sigma^{M \text{ and } Lia}$) or the resistance determinants themselves (in case of Bce and Psd) was determined. Interestingly, none of the investigated strains were more susceptible towards laspartomycin C than the wild type (Figure 8). This indicates that the modules tested here do not provide any resistance against laspartomycin C, despite being induced.

The differential induction of cell envelope stress response modules in *B. subtilis* by friulimicin B and laspartomycin C are fascinating as these two antibiotics differ only in their lipid tail as well as some moieties in the peptide ring (Figure 2). Here, these differences are hypothesized to alter the antibiotics polymerization-state and interaction with surrounding membrane lipids, which might enable the sensing of laspartomycin C by resistance modules (Figure 9).

The absence of conferred resistance by stress response modules of *B. subtilis* is reassuring for a potential application of laspartomycin C in clinical settings. However, the sensing ability of these modules might be a first step in their evolution to actually confer resistance. The knowledge gained here of triggered natural resistance modules can guide further research and the clinical development of laspartomycin C as a drug.

antibiotics

MDPI

Article

The Cell Envelope Stress Response of *Bacillus subtilis* towards Laspartomycin C

Angelika Diehl [1,2], Thomas M. Wood [3,4], Susanne Gebhard [5], Nathaniel I. Martin [3] and Georg Fritz [2,*]

1 LOEWE Centre for Synthetic Microbiology, Philipps-Universität Marburg, Hans-Meerwein-Strasse 6, 35032 Marburg, Germany; angelika.diehl@synmikro.uni-marburg.de
2 School of Molecular Sciences, The University of Western Australia, Crawley 6009, WA, Australia
3 Biological Chemistry Group, Institute of Biology Leiden, Leiden University, Sylviusweg72, 2333 BE Leiden, The Netherlands; t.m.wood@biology.leidenuniv.nl (T.M.W.); n.i.martin@biology.leidenuniv.nl (N.I.M.)
4 Department of Chemical Biology & Drug Discovery, Utrecht Institute for Pharmaceutical Sciences, Utrecht University, Universiteitsweg 99, 3584 CG Utrecht, The Netherlands
5 Milner Centre for Evolution, Department of Biology and Biochemistry, University of Bath, Bath BA2 7AY, UK; sg844@bath.ac.uk
* Correspondence: georg.fritz@uwa.edu.au

Received: 29 September 2020; Accepted: 21 October 2020; Published: 23 October 2020

Abstract: Cell wall antibiotics are important tools in our fight against Gram-positive pathogens, but many strains become increasingly resistant against existing drugs. Laspartomycin C is a novel antibiotic that targets undecaprenyl phosphate (UP), a key intermediate in the lipid II cycle of cell wall biosynthesis. While laspartomycin C has been thoroughly examined biochemically, detailed knowledge about potential resistance mechanisms in bacteria is lacking. Here, we use reporter strains to monitor the activity of central resistance modules in the *Bacillus subtilis* cell envelope stress response network during laspartomycin C attack and determine the impact on the resistance of these modules using knock-out strains. In contrast to the closely related UP-binding antibiotic friulimicin B, which only activates ECF σ factor-controlled stress response modules, we find that laspartomycin C additionally triggers activation of stress response systems reacting to membrane perturbation and blockage of other lipid II cycle intermediates. Interestingly, none of the studied resistance genes conferred any kind of protection against laspartomycin C. While this appears promising for therapeutic use of laspartomycin C, it raises concerns that existing cell envelope stress response networks may already be poised for spontaneous development of resistance during prolonged or repeated exposure to this new antibiotic.

Keywords: laspartomycin C; friulimicin B; *Bacillus subtilis*; cell wall inhibition; stress response

1. Introduction

The cell envelope is both the bacterium's first line of defence against harmful substances and an essential structure to counteract the internal turgor pressure. As many antibiotics exploit the accessibility of the cell envelope, bacteria have evolved numerous countermeasures to protect themselves against these constant attacks. In Gram-positive bacteria in particular, the biosynthesis pathway of peptidoglycan (PG), the lipid II cycle, is a key antibiotic target [1,2] (Figure 1). As a cyclic pathway, the blockage at any point of the cycle is sufficient to bring PG synthesis to a halt [1], and consequently, all externally exposed cycle intermediates are inhibited by one or several antibiotics (Figure 1). While antibiotics targeting lipid II and undecaprenyl pyrophosphate (UPP) are widely

Antibiotics **2020**, *9*, 729

used in therapeutic and commercial applications, e.g., vancomycin, nisin and bacitracin, currently no antibiotics targeting undecaprenyl phosphate (UP) are in use.

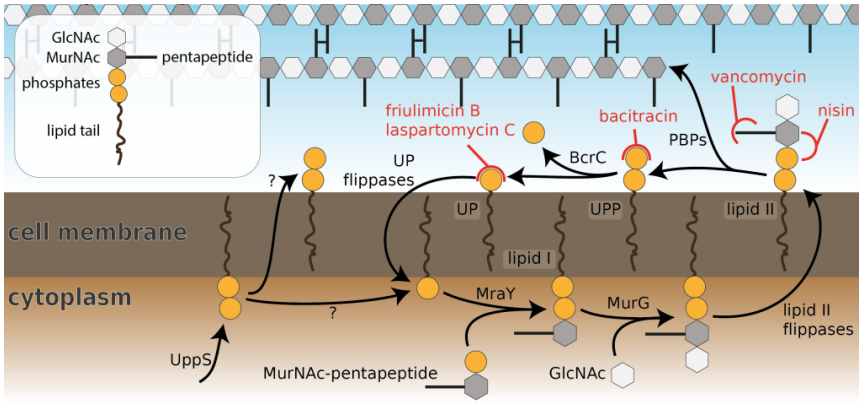

Figure 1. Schematic overview of the lipid II cycle of *Bacillus subtilis*, including lipid carrier molecules, involved enzymes and selected antibiotics that target cell wall synthesis. The cell wall precursor lipid II is assembled on the cytoplasmic side of the membrane and then flipped. After insertion of the GlcNAc-MurNAc pentapeptide into the growing peptidoglycan, the lipid carrier UPP is recycled via dephosphorylation by BcrC. The generated lipid carrier UP is subsequently flipped back to the cytoplasmic side of the membrane to begin a new cycle. The lipid carrier is supplied by UppS in the form of UPP on the cytoplasmic side of the membrane; it remains to be elucidated whether newly synthesized UPP is fed into the cycle by dephosphorylation on the cytoplasmic side of the membrane or by flipping. Example antibiotics that target lipid carrier pools on the periplasmic side of the membrane are indicated in red.

First hopes to exploit UP as a novel drug target against Gram-positive bacteria were based on friulimicin B—a naturally occurring cyclic lipopeptide produced by the actinomycete *Actinoplanes friuliensis* (Figure 2) [3]. However, clinical trials with friulimicin B were soon discontinued due to unfavourable pharmacokinetic properties [4]. While these properties can, in principle, be altered by introducing small chemical modifications in the polypeptide structure, this is difficult for friulimicin B, which is currently obtained naturally by extensive extraction from *A. friuliensis* [3]. Recently, laspartomycin C, another cyclic calcium-dependent lipopeptide, has been obtained by total chemical synthesis and was shown to also bind to UP as a drug target (Figure 2) [5,6]. In principle, the chemical synthesis of laspartomycin C allows for easier modification of the peptide's pharmacokinetics, making this a promising route to develop a clinically relevant drug. However, while laspartomycin C has been examined in great detail biochemically [5,7,8], little is known about potential bacterial defence and stress response mechanisms against this novel antibiotic. Such an understanding is key to assess the risk of antibiotic resistance evolution and to develop early strategies to prevent cross resistance from stress responses triggered by any potential off-target binding in vivo.

Bacillus subtilis is a Gram-positive soil bacterium that is naturally exposed to a large range of antimicrobial peptides produced by competing environmental bacteria. The intricate cell envelope stress response (CESR) network protecting *B. subtilis* against these attacks (Figure 3) has become a model system for studying antibiotic resistance mechanisms in Gram-positive bacteria. Here, we set out to perform a comprehensive analysis of the *B. subtilis* CESR towards laspartomycin C and to compare it to the response against the structurally related friulimicin B [5]. Previously, friulimicin B was shown to induce the activity of several extra cytoplasmic function (ECF) σ factors involved in the CESR, with the greatest effect seen in σ^M and σ^V activation [9]. Under non-inducing conditions the anti-sigma factors YhdL/YhdK keep σ^M in an inactive state, but release it during cell envelope stress [10].

Antibiotics **2020**, *9*, 729

The free σ factor recruits RNA polymerase to specific target promoters to activate transcription of genes encoding general cell wall homeostatic mechanisms. The most noteworthy target of σ^M is *bcrC* [11], which encodes the UPP phosphatase BcrC—an integral component of the lipid II cycle that catalyzes the dephosphorylation of UPP to UP (Figure 1). Interestingly, during friulimicin B challenge, *bcrC* has been found to be one of the most highly induced genes [9], and it may play a role in friulimicin B resistance in combination with its function in replenishing the UP pool.

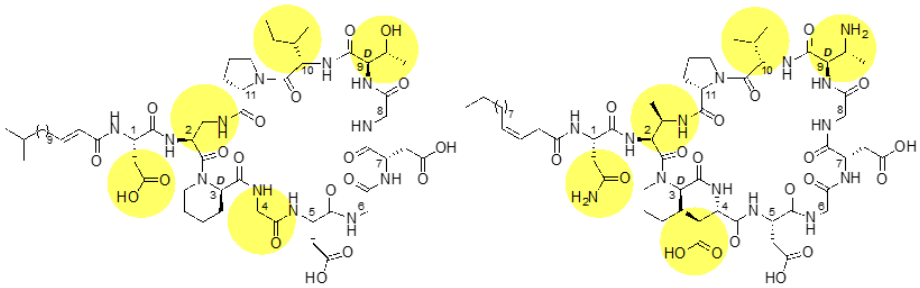

Figure 2. Structures of laspartomycin C and friulimicin B. The lipid tails of the two lipopeptides differ, as laspartomycin C bears a 15-carbon tail containing a *trans* alpha-beta unsaturated moiety while friulimicin B contains a 14-carbon *cis*-beta gamma unsaturated lipid. Other notable differences include the amino acids at positions 1, 2, 4, 9 and 10 (highlighted), which are Asp, diaminoproionic acid (Dap), Gly, D-*allo*-Thr, and Ile, respectively, in laspartomycin C and Asn, 2*S*,3*R*-diaminobutyric acid (Dab), L-*threo*-3-methyl-aspartate (MeAsp), 2*R*,3*R*-D-Dab and Val, respectively, in friulimicin B.

Another module involved in the CESR is the two-component system LiaRS, which is kept inactive by LiaF under non-inducing conditions [12]. During antibiotic attack on the lipid II cycle, e.g., by bacitracin, or upon membrane perturbation, this inhibition ceases and LiaS phosphorylates the response regulator LiaR. In turn, LiaR activates 10 genes including its main targets *liaI* and *liaH* [12]. During cell envelope stress, the two encoded proteins, LiaI and LiaH, colocalize in small patches on the cell membrane and are thought to stabilize the membrane underneath holes in the peptidoglycan layer [13]. Although the Lia module has been shown to respond to a large range of different stressors [14–16], the actual trigger has not been identified yet. However, it is generally believed that the system indirectly senses the damage on the cell envelope rather than directly detecting the diverse range of stressors [13,17].

The third and last type of CESR modules in *B. subtilis* are the Bce-like systems BceRSAB [21], PsdRSAB [22] and ApeRSAB (formerly YxdRSAB) [23]. Bce-like systems are widespread in Firmicutes bacteria, including important pathogens such as *Staphylococcus aureus* and *Enterococcus faecalis* [24,25]. They consist of a two-component system that is functionally linked to an ABC transporter, with the best studied example being the BceRSAB module from *B. subtilis* (Figure 3). Here, the transport permease BceB directly interacts both with the ATP-binding protein BceA and with the histidine kinase BceS [26]. BceAB likely confers resistance by a target protection mechanism [27], detecting the antibiotic bacitracin in complex with its cellular target UPP and removing bacitracin from UPP under ATP hydrolysis [18].The activity of BceAB then triggers activation of the histidine kinase BceS [19,26], which phosphorylates the response regulator BceR, leading to transcription activation of *bceAB* [20].

While it is known that friulimicin B does not activate any resistance modules of the *Bacillus subtilis* CESR apart from σ^M and σ^V [9], no such research has been done for laspartomycin C. Here, we found that while laspartomycin C triggers induction of the σ^M response similar to friulimicin B, it also strongly activates other resistance modules involved in the CESR, leading us to investigate their role in potential laspartomycin resistance.

Antibiotics **2020**, *9*, 729

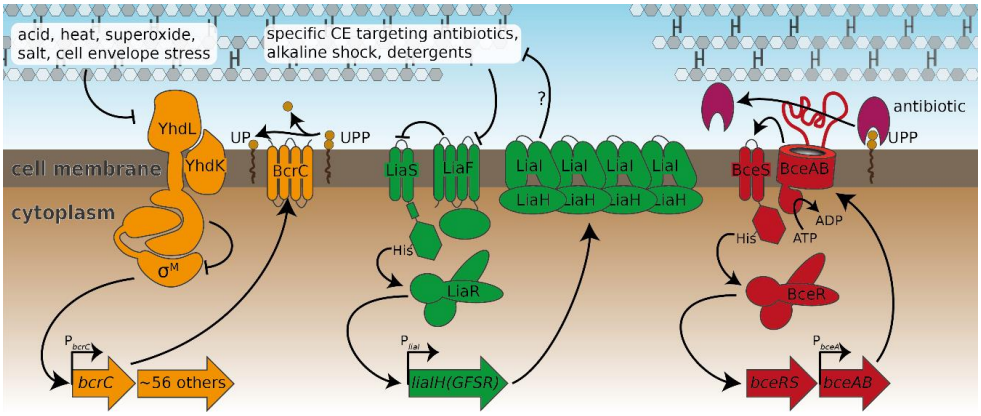

Figure 3. The three major cell envelope stress response modules of *B. subtilis* analysed in this study. The σ^M module (left) is kept inactive under non-inducing conditions by its anti-σ factors YhdL/YhdK [10]. Upon exposure to, e.g., acids or cell envelope stress, σ^M is released and free to guide RNA polymerase to its target promoters such as P_{bcrC} [11]. The Lia module (middle) senses a plethora of external stresses through a yet-undetermined sensing mechanism. Upon stress sensing, the inhibition of the two-component system LiaS/LiaR by LiaF ceases [12], which subsequently allows increased expression of the genes involved in the signaling cascade as well as *liaI* and *liaH*. The Bce module (right) is shown as a representative of all bce-like modules of *B. subtilis*. Here, the ABC-transporter BceAB is thought to remove the antibiotic bacitracin from its target, UPP [18]. BceAB activity stimulates the two-component system BceS/BceR and thereby leads to the increased production of BceAB [19,20]. Regulation patterns are depicted with arrows; arrowheads and T-heads indicate activation and inhibition, respectively. Operons activated by the resistance modules are shown as thick arrows.

2. Results

2.1. Laspartomycin C Induces a Slightly Stronger Response of the σ^M Regulon than Friulimicin B

The UPP phosphatase BcrC catalyzes a key reaction in the lipid II cycle, and is therefore highly expressed during normal growth [21,28]. Upon blockage of UP by friulimicin B, the increased activity of σ^M leads to a further boost in *bcrC* expression [9], thus possibly contributing to friulimicin B resistance. Given that laspartomycin C also targets the UP pool, we reasoned that it may likewise trigger the induction of the σ^M response, leading to upregulation of *bcrC*. To compare the σ^M response towards the two antibiotics, we used a strain of *B. subtilis* W168 harbouring a genomically integrated luciferase reporter under the control of the P_{bcrC} promoter [11]. When exponentially growing cells of this strain were challenged with either of the antibiotics, the P_{bcrC} promoter was most active between 30 min and 1 h after antibiotic challenge (Figure 4a,b). Figure 4c shows the dose dependency of luciferase activity, monitored 30 min after antibiotic addition. Here it turned out that while the P_{bcrC} promoter reached a plateau in activity at 3 µg/mL friulimicin B and beyond, laspartomycin C maximally activated the P_{bcrC} promoter at the higher concentration of 5 µg/mL (Figure 4c). While this suggests that the σ^M response is marginally more sensitive to friulimicin B than laspartomycin C, the P_{bcrC} response was slightly stronger for laspartomycin C (3.5-fold induction) compared to friulimicin B (2-fold induction).

Antibiotics **2020**, *9*, 729

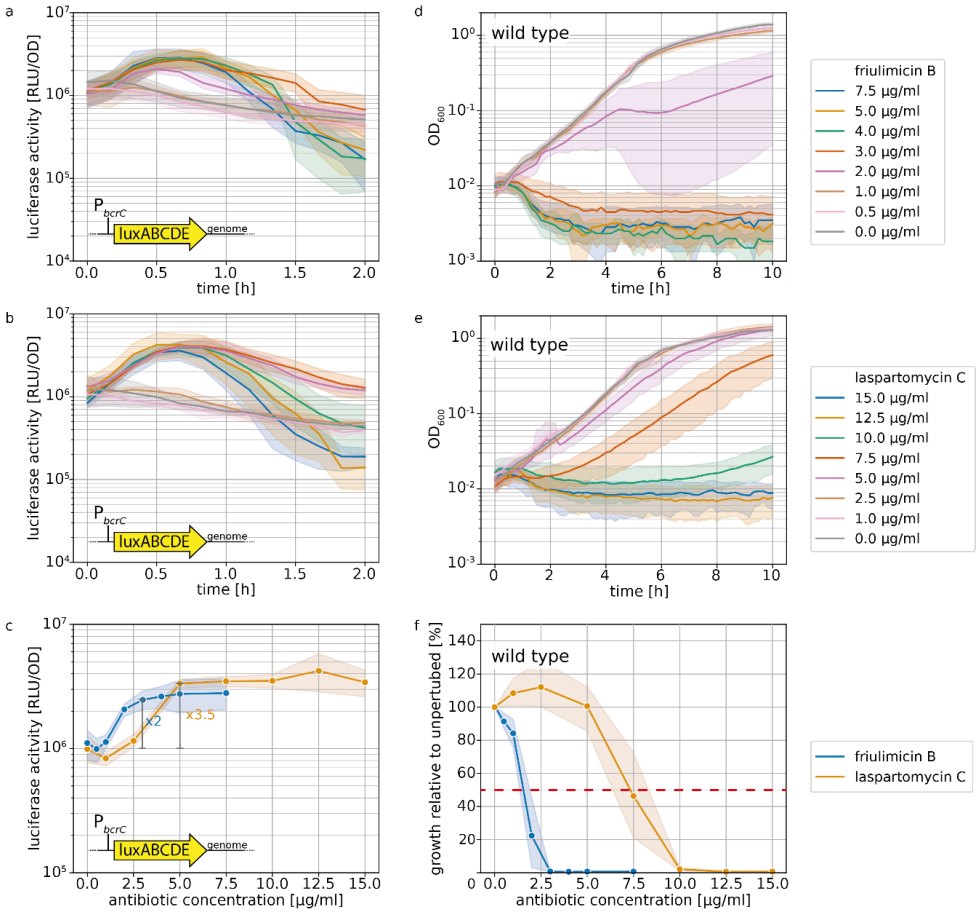

Figure 4. σ^M stress response as shown by *bcrC* promoter activation and growth during friulimicin B and laspartomycin C attack. (**a**,**b**) Expression of *bcrC* over time in dependency of different concentrations of friulimicin B (**a**) or laspartomycin C (**b**). (**c**) Dose dependency of the σ^M stress response 30 min after antibiotic challenge. Blue and orange lines depict the P_{bcrC} promoter response generated by friulimicin B and laspartomycin C, respectively. The fold change over basal activity is shown at the beginning of the plateau. (**d**,**e**) Growth after antibiotic challenge with friulimicin B (**d**) or laspartomycin C (**e**). (**f**) Dose dependency of the growth relative to an unperturbed culture 10 h after antibiotic challenge. IC_{50} values were determined as the antibiotic concentration reducing bacterial growth by 50% (red dashed line), which was 1.6 and 7.3 µg/mL for friulimicin B and laspartomycin C, respectively. Shaded areas depict 95% confidence intervals.

It had been reported previously that *B. subtilis* was more sensitive to friulimicin C than laspartomycin B, with MIC values of 0.078 and 8 µg/mL, respectively [8,9]. To test whether this was also true for exponentially growing cells under the conditions in our reporter gene experiments, we next tested the effect of both antibiotics on cell growth following challenge in the exponential growth phase (Figure 4d,e). The results confirmed that friulimicin B was more potent than laspartomycin C, with 5 µg/mL friulimicin B completely inhibiting cell growth, while 5 µg/mL laspartomycin C only marginally affected cells (Figure 4d,e). Closer examination showed that a 50% reduction in growth after 10 h (IC_{50}, used as proxy for MIC) was achieved at 1.6 µg/mL friulimicin B, which was significantly lower than the IC_{50} for laspartomycin C—7.3 µg/mL (Figure 4f).

For effective protection, it is vital that resistance modules sense and respond to an antibiotic challenge before significant damage accrues. However, as IC_{50} values can vary widely between

Antibiotics **2020**, *9*, 729

antibiotics, the critical concentration at which an antibiotic challenge needs to be sensed varies just as much. Therefore, we reasoned that the sensitivity of the σ^M response should be considered relative to the IC_{50} of the respective antibiotic, allowing us to place the regulation into a better physiological context. For this, we normalized the P_{bcrC} dose–response curves in Figure 4c to the IC_{50} values. Growth kinetics of the strain harbouring the P_{bcrC} reporter are shown in Figure S1. This showed that laspartomycin C maximally activated the σ^M stress response at concentrations around the IC_{50} value, while full induction by friulimicin B required concentrations exceeding the IC_{50} at least 2-fold (Figure 5). As such, we conclude that laspartomycin C is actually the more potent inducer of σ^M under physiological relevant conditions, i.e., at antibiotic concentrations below the IC_{50} value.

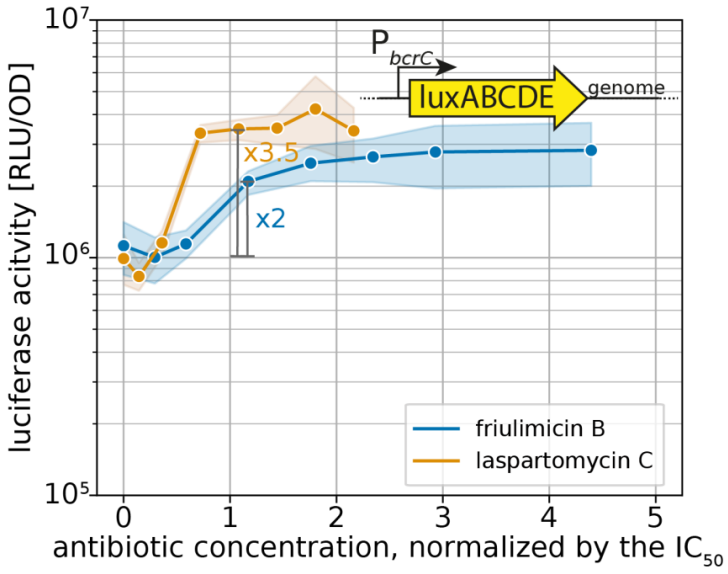

Figure 5. Sensitivity-normalized dose-dependent activation of the σ^M stress response as shown by *bcrC* promoter induction during friulimicin B and laspartomycin C attack. The antibiotic concentration is shown in relation to the IC_{50} of the respective antibiotic. The induction at the IC_{50} is indicated in grey, and the fold change is given. The induction at the IC_{50} is indicated in grey, and the fold change is given. Measurements were taken 30 min after antibiotic challenge. Shaded areas depict 95% confidence intervals.

2.2. Probing the Broader CESR against Laspartomycin C Shows Induction of the LiaFSR Module

We next wanted to test whether laspartomycin C also activates other CESR modules of *B. subtilis*. The Lia system responds to a broad range of cell envelope-perturbing agents as described above [29,30]. Given this broad inducer spectrum, it was surprising that the UP-binding antibiotic friulimicin B did not activate the Lia system [15]. Based on our observation that laspartomycin C was a more potent inducer of the σ^M response than friulimicin B, we wondered whether this antibiotic could elicit a Lia response, or whether the Lia system generally did not react to UP-binding compounds.

To gain insight into the response of the Lia system toward laspartomycin C, we monitored the activity of P_{liaI}, the main target promoter of the LiaFRS sensing module [12], via a luciferase-reporter fusion integrated into the genome of *B. subtilis* W168. We assessed luciferase activity at a time point close to the maximal induction of P_{liaI} (30 min after antibiotic challenge), and plotted these activities as a function of the respective IC_{50}-normalized antibiotic concentration to directly analyse the physiologically relevant sensitivity of the Lia module (Figure 6). Growth kinetics of the strain harbouring the P_{liaI} reporter are shown in Figure S2.

Antibiotics **2020**, *9*, 729

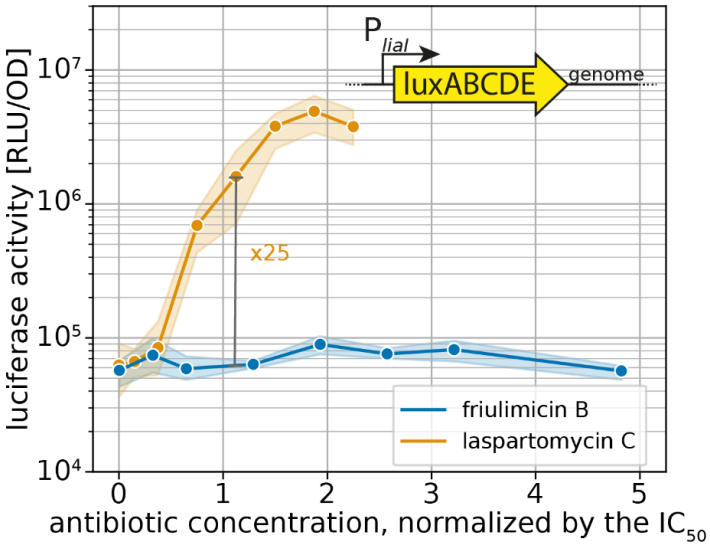

Figure 6. Sensitivity-normalized dose-dependent stress response of the Lia module as shown by *liaI* promoter activation during friulimicin B and laspartomycin C attack. The relative antibiotic concentration in respect of their IC_{50} is given. The induction at the IC_{50} is indicated in grey, and the fold change is given. Measurements were taken 30 min after antibiotic challenge. Shaded areas depict 95% confidence intervals.

In agreement with earlier studies [9,15], friulimicin B did not activate the Lia response in our experiments (Figure 6). In contrast, laspartomycin C led to a 25-fold P_{liaI} induction (maximal induction at 2xMIC: 80-fold). This shows that the Lia response can indeed be triggered by UP-binding antibiotics. The laspartomycin C response represents an intermediate induction of the Lia module, as the strongest inducer known so far—bacitracin—activates the promoter 100-fold around the IC_{50} in our setup (Figure S3). These results further suggest that the higher sensitivity towards laspartomycin C was not specific for just the σ^M resistance module but rather a more general phenomenon. Moreover, our result show that laspartomycin C, but not friulimicin B, can be sensed by several CESR modules.

2.3. Induction of Specific CESR Modules by Laspartomycin C

In contrast to the Lia response, the Bce-like modules of *B. subtilis* have a much more specific inducer spectrum, which made us wonder how these will respond to laspartomycin C [17]. The two best-understood modules, Bce and Psd, likely sense antibiotics in complex with their membrane-anchored target. So far, most of the Bce- and Psd-inducing antibiotics bind to the diphosphatic lipid carriers UPP and lipid II [22]. Given that laspartomycin C and friulimicin B block the monophosphatic UP molecule, it was unclear whether these antibiotics would be able to trigger activation of the Bce-like CESR modules. Since the Ape module is less understood, we restricted our analysis to the Bce and Psd modules and studied their activity via genomically integrated luciferase cassettes under the control of the P_{bceA} and P_{psdA} promoters in *B. subtilis* W168 using the previously described setup. Growth kinetics of the strains harbouring the P_{bceA} and P_{psdA} reporters are shown in Figures S4 and S5, respectively.

Dose–response curves 30 min after antibiotic challenge show that friulimicin B activated neither the Bce (Figure 7a) nor the Psd module (Figure 7b). Laspartomycin C, however, induced P_{bceA} 25-fold at the IC_{50} (=maximal induction) (Figure 7a). While this response was weaker than the full induction of P_{bceA} under bacitracin stress (~170-fold) [18], it still showed a pronounced activation. Similarly, the Psd module was activated 25-fold by laspartomycin C around IC_{50} (maximal induction: 30-fold) (Figure 7b). The observation that laspartomycin C, but not friulimicin B, activates these systems

Antibiotics **2020**, *9*, 729

suggests that, while both antibiotics are able to bind to UP, only laspartomycin C can be recognized by the transporter and trigger its activity.

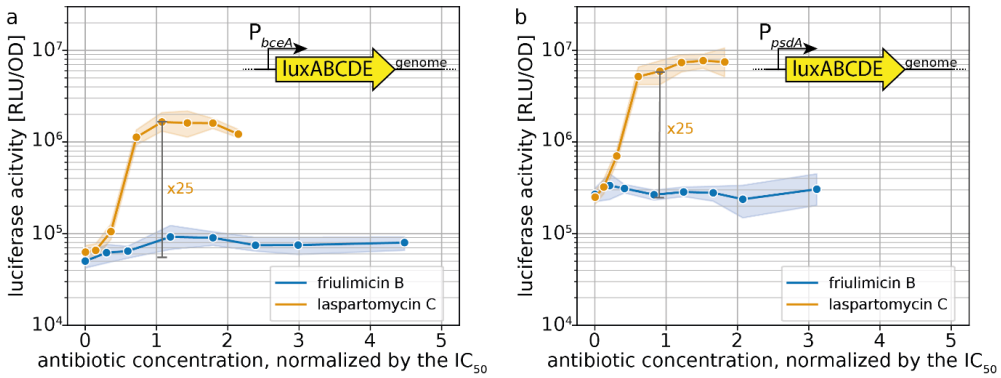

Figure 7. Sensitivity-normalized dose-dependent stress response of bce-like modules as shown by P_{bceA} (**a**) and P_{psdA} (**b**) promoter activation during friulimicin B and laspartomycin C attack. The relative antibiotic concentration in respect of their IC_{50} is given. The induction at the IC_{50} is indicated in grey, and the fold change is given. Measurements were taken 30 min after antibiotic challenge. Shaded areas depict 95% confidence intervals.

2.4. Acitvated Resistance Modules do not Protect against Laspartomycin C Attack

After establishing that laspartomycin C induces all three types of CESR modules in *B. subtilis*, we next asked whether the activated target genes conferred any protection against the antibiotic. Therefore, we determined the IC_{50} of laspartomycin C in wild-type *B. subtilis* W168, and in strains carrying deletions of each of the modules or their key target genes, i.e., Δ*bcrC*, Δ*liaIH*, Δ*bceRSAB* and Δ*psdRSAB* (Table S1), using the methodology described above. Surprisingly, none of the tested deletion strains showed a significant reduction in the IC_{50} of laspartomycin C and friulimicin B (Student's t test, $p > 0.001$) (Figure 8), suggesting that none of the induced genes actually contributed to protection of the cell against these antibiotics. Note that growth in the absence of the antibiotics was not affected by any of the deletions (Figure S6). Growth kinetics of all deletion strains challenged with laspartomycin C or friulimicin B are shown in Figures S7 and S8, respectively.

Given the complexity of the laspartomycin C stress response, it was possible that deletion of a single resistance determinant may not be sufficient to cause a detectable change in laspartomycin C sensitivity. A similar observation was made previously in the bacitracin stress response of *B. subtilis*, where the contribution of the Lia system to resistance was masked by the strong resistance mediated by BceAB, and a protective effect of Lia could only be observed when both *bceAB* and *liaIH* were deleted. To examine potential redundancy of the resistance modules during laspartomycin C challenge, we next tested the susceptibility of strains with deletions of two resistance modules combined. However, even in these double-deletion strains, no increase in susceptibility was detected (Student's t test, $p > 0.001$) (Figure 8). This indicates that none of these resistance modules, even though strongly expressed, can protect *B. subtilis* against laspartomycin C.

Antibiotics **2020**, *9*, 729

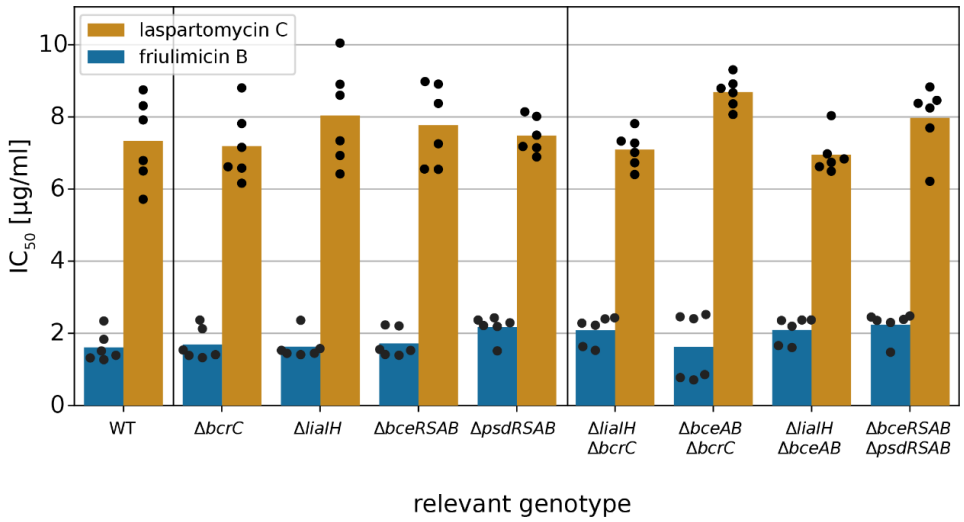

Figure 8. Impact of CESR modules on friulimicin B and laspartomycin C resistance. IC_{50} values were measured 10 h after antibiotic challenge in wild-type *B. subtilis* and deletion strains of CESR modules. The IC_{50} values of the wild-type strain were 1.6 and 7.3 µg/mL for friulimicin B and laspartomycin C, respectively. Bars represent the averaged IC_{50} over six biological replicates. Black dots show single replicates. Neither deletions of single CESR modules nor the combination of any two deletions changed the IC_{50} significantly (Student's t-test: $p > 0.001$; unequal variance).

3. Discussion

As a proxy for the potential of resistance development by the novel cyclic calcium-dependent lipopeptide laspartomycin C, we here assessed its ability to trigger elements of the CESR of *B. subtilis*. This was compared to the response to the better-characterized antibiotic friulimicin B, which shares similarities in chemical structure with laspartomycin C. Here, we found significant differences, as friulimicin B only triggered the induction of the σ^M component of the CESR, while laspartomycin C produced a stronger σ^M response and additionally activated both the Lia and Bce-like modules. Since the two antibiotics are closely related and bind the same target—UP—this was highly surprising.

3.1. Novel Clues on CESR Signal Perception

While the σ^M and Lia modules have been broadly referred to as "damage-sensing" systems [31], their specific triggers are currently unknown. Possible cues include the sensing of perturbations in the peptidoglycan layer, in the membrane [31], or an altered abundance of lipid II cycle intermediates [13] by some unknown mechanism. Since friulimicin B and laspartomycin C both bind to, and hence sequester, UP, it is likely that both antibiotics have similar effects on the abundance of the other lipid II cycle intermediates, i.e., decreased levels of UPP, lipid I and lipid II. The similarity in the σ^M response triggered by both antibiotics (2-fold induction by friulimicin B vs. 3.5-fold induction by laspartomycin C) might be reflective of such effects. This could be compatible with the σ^M module detecting changes in pool levels of lipid II cycle intermediates. Interestingly, however, we detected a strongly differential response of the Lia module toward the two antibiotics (no induction by friulimicin B vs. 25× induction by laspartomycin C). One might therefore argue that the Lia module is less likely to sense a reduction in lipid II cycle intermediates, as such a reduction should be very similar for both antibiotics. While we cannot provide a definitive answer to this question, the differential responses elicited by friulimicin B and laspartomycin C may be able to serve as novel tools to elucidate the physiological triggers of the Lia module and potentially of σ^M.

In contrast to the indirect (damage-)sensing mechanism employed by the Lia and σ^M systems, the Bce-like modules are known to directly sense the antibiotic–target complexes, where the target is typically a diphosphatic lipid carrier (UPP or lipid II) [22]. Although it is still unknown which parts of the antibiotic–target complex these modules react to [18,22,32], individual modules specifically respond to a small set of antibiotics and often discriminate between very similar peptides. For example, of the two globular lantibiotics mersacidin and actagardine, only the latter induces the Psd module [22]. Recently, the two cannibalism toxins Sdp and Skf were also shown to induce the Bce and Psd modules [33]. Here, the membrane-anchored immunity protein SdpI was essential for induction of both modules, suggesting that the two toxins might be sensed in complex with SdpI. With laspartomycin C, we show here that the inducer spectrum of the Bce and Psd modules also extends to antibiotics targeting the monophosphatic lipid carrier UP. This unfolding promiscuity of compounds recognized by Bce-like systems may offer insights into the mode of action of these unique resistance transporters. The antibiotics appear to be only recognized in complex to their cellular target. However, this cellular target can apparently be either diphosphatic (UPP, lipid II) or monophosphatic (UP) lipid carriers, and even proteins (SdpI). This observation potentially extends the notion that Bce-like transporters act by target protection of cell wall synthesis [18,34], to target protection of the extracellular face of the membrane more generally, where the transporters are responsible for removing membrane- and cell wall-perturbing compounds.

3.2. Differential Sensing of Friulimicin B and Laspartomycin C

While the calcium-dependent lipopeptide antibiotics friulimicin B and laspartomycin C share structural similarity, there are also a number of differences in the sidechains of the constituent amino acids and in the length and orientation of their lipid tails (Figure 2). Most notable among these differences is the presence of neutral Gly and D-*allo*-Thr residues at positions 4 and 9, respectively, in laspartomycin C, while these positions are filled by L-*threo*-3-methyl-aspartate (MeAsp) and 2*R*,3*R*-D-Dab, respectively, in friulimicin B. The crystal structure of laspartomycin C bound to geranyl phosphate indicates that residues 4 and 9 are solvent accessible [8]. Given that friulimicin B has acidic and basic residues at these positions, it may be possible that intermolecular salt bridges are formed between neighbouring friulimicin B–UP complexes. This in turn might lead to multimerization on the bacterial cell surface. Should friulimicin B form such multimeric structures, it may be that individual friulimicin B molecules become less accessible to the sensory machinery of resistance modules (Figure 9a). In contrast, given that laspartomycin C features neutral residues at positions 4 and 9, it may be less likely to form higher-order complexes. In this case, the more disperse laspartomycin C molecules might be more accessible to direct sensing by Bce-like modules (Figure 9b). Ongoing structural investigations are aimed at clarifying this hypothesis.

This model, however, only explains the differing responses towards the two antibiotics for resistance modules with a direct sensing mechanism. For damage-sensing modules, the differential responses are much more difficult to explain. As the trigger of σ^M is very controversial [35] and the induction of the P_{bcrC} promoter by the two antibiotics did not show marked differences (<2-fold), we believe that strong conclusions about a differential σ^M response towards laspartomycin C and friulimicin B are not warranted based on our data. In contrast, the trigger of the Lia module is less hazy as it is generally believed to be either discrepancies in lipid carrier pool sizes or membrane perturbations [13,31]. As the former model is not in line with the differential Lia response towards friulimicin B and laspartomycin C, as described above, we favour a model in which the Lia module senses membrane perturbations. However, the exact nature of these perturbations remains enigmatic [13]. Within this model for Lia function, the observation that friulimicin B is not an inducer of the Lia response can be rationalised by predicting that friulimicin B would trigger less severe membrane perturbations than laspartomycin C. Such differences may arise, for instance, due to the longer and trans-configurated lipid tail of laspartomycin C, which creates a bulkier structure on the membrane surface than friulimicin B. This bulkiness might prevent membrane lipids from organizing in an orderly

Antibiotics **2020**, *9*, 729

fashion and could lead to the accumulation of more fluid lipids around UP–laspartomycin C complexes, thereby preventing gaps in the membrane. This mode of action has previously been observed in the related cyclic calcium-dependent lipopeptide daptomycin, which also binds to a lipid in the cellular membrane—phosphatidylglycerol [36–38]. Due to its bulky lipid tail, fluid lipids cluster around daptomycin—a process that is further amplified by daptomycin multimerization [36]. This clustering has been shown to cause a depletion of fluid lipids in the remainder of the cellular membrane and increases overall membrane rigidity [38]. Since daptomycin also induces the Lia module, we propose that the depletion of fluid lipids from the membrane and/or the accompanied increase in membrane rigidity might be the molecular trigger for the induction of the LiaFSR signaling system [9,36]. A similar mechanism can be envisioned for laspartomycin C (Figure 9b), although future experiments will be needed to further corroborate such a model.

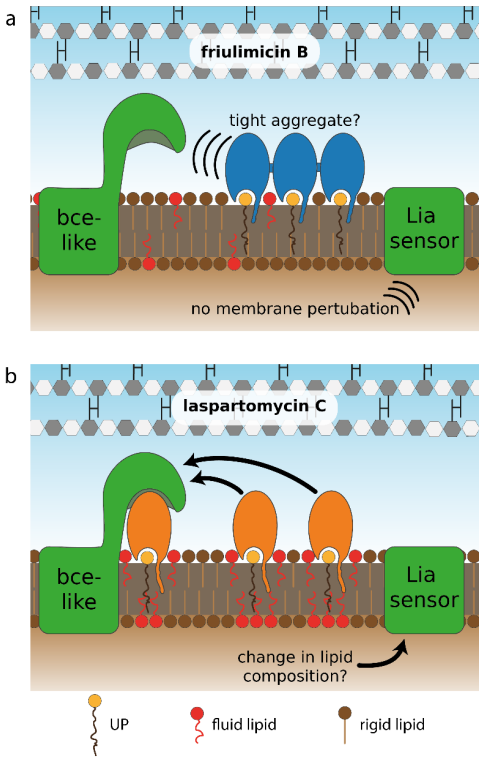

Figure 9. Hypothetical model for differential sensing of friulimicin B and laspartomycin C by Bce-like direct sensors and the LiaFSR damage sensor. (**a**) The proposed ionic interactions between neighbouring friulimicin B molecules may lead to formation of antibiotic–UP aggregates. Such tight packing of antibiotic–UP complexes could prevent the sensory complexes BceAB–BceRS and PsdAB–PsdRS from binding to the friulimicin B–UP complexes, thus interfering with the direct sensing of the Bce-like systems. (**b**) For laspartomycin C, in contrast, the bulkier lipid tail and the absence of salt-bridging amino acids in its peptide ring might suggest that it forms freely diffusing, non-aggregating complexes with UP. These complexes may be more amenable to interaction with the BceAB–BceRS and PsdAB–PsdRS sensory complexes, as suggested by the fact that BceAB detects both the antibiotic and the lipid carrier in the bacitracin–UPP complex [18]. Likewise, the bulkier lipid tail of laspartomycin C might trigger changes in membrane lipid composition, e.g., by depleting fluid lipids from other parts of the membrane, serving as potential trigger for the induction of the LiaFSR system. Such lipid re-arrangements could be absent for friulimicin B, when present in the tightly aggregated form as in (**a**), serving as a potential explanation why friulimicin B does not activate the LiaFSR system.

3.3. Lacking Antibiotic Protection is Widespread in Bce-like Resistance Modules and may Precede the Spontaneous Evolution of Resistance

One intriguing finding of this study was that even though laspartomycin C induces the expression of the Bce and Psd modules, none of these systems conferred detectable resistance against this novel antibiotic. Interestingly, similar observations have been made for other inducers of Bce-like resistance modules in *B. subtilis*. For instance, while the Bce module is most highly induced by both bacitracin and the lipid II-binding antibiotic mersacidin, it confers a high level of resistance against bacitracin (30-fold change in susceptibility) but only moderate resistance against mersacidin (4-fold change in susceptibility) [22]. Further, the aforementioned cannibalism toxins SdpC and SkfA are strong inducers of BceAB and PsdAB expression, but neither of the modules confers resistance against these toxins [33]. Similarly, the PsdRSAB module is induced by lipid II-binding antibiotics, such as actagardine and gallidermin [22], but despite actagardine being the strongest known inducer of *psdAB* expression, PsdAB does not confer any detectable actagardine resistance [22]. This indicates that the strength of induction of Bce-like modules by an antibiotic does not necessarily correlate with the level of protection conferred.

Astoundingly, the same lack of protection against laspartomycin C, despite clear induction responses, was observed for every resistance module we tested in this study. Thus, it seems that the path to a fully functional resistance module is a two-step process: (1) sensing of the antibiotic leading to gene expression and (2) effectively counteracting the antibiotics. In the case of the Bce-like modules, both functions are presumably carried out by the transporters, BceAB or PsdAB [21,39,40]. We have shown previously that signaling is proportional to transporter activity [20], and thus signaling and resistance should also be directly coupled. However, the proposed target protection mechanism of BceAB action may provide some clues as to the observed discrepancy between gene expression and level of resistance. As discussed above, the physiological substrate for the transporter is the antibiotic in complex with its cellular target, and the energy from ATP hydrolysis is presumably used to break the antibiotic–target interactions and free the target [18,27]. For this process to lead to effective protection, BceAB activity has to result in an equilibrium shift towards free target that is sufficient to allow cell wall synthesis to continue. The freeing of the target therefore has to be fast relative to the renewed binding of the antibiotic. However, according to our current understanding of flux-dependent signaling, activation of the kinase will occur in proportion to ATP hydrolysis [19,20,26], irrespective of whether this results in effective freeing of the target. Conceptually, signaling should therefore be simpler to achieve, requiring only recognition of the substrate–target complex by the transporter, whereas resistance additionally requires suitable kinetic properties of the transporter to facilitate target protection.

Given our findings, a potential route for the evolution of resistance against other/novel antibiotics by Bce-like modules may present itself. Considering the wide range of antibiotics that can be sensed by Bce-like modules it is relatively likely that a novel antibiotic could also induce these systems, as we observed here for laspartomycin C. As this already accomplishes the first step towards a functional resistance module, it is conceivable that continued selection pressure, for example through clinical use of a new antibiotic, would easily result in mutations that improve transport kinetics to the point where the antibiotic is effectively removed from its target and resistance is achieved. While experimental evolution of laspartomycin C resistance in *B. subtilis* was beyond the scope of this study, it will be interesting to test this in the future, should larger quantities of laspartomycin C become available.

Since Bce-like resistance modules are widespread in Firmicutes bacteria, including in important pathogens such as *S. aureus* and *E. faecalis*, the fact that laspartomycin C is able to induce these modules poses a considerable risk that resistance against this antibiotic might develop faster than for an antibiotic not already recognized as an inducer [24,25]. As such, further development of laspartomycin C as a clinical drug candidate must address these inducing properties and eliminate them if possible. More generally, testing a novel antibiotic for induction of known resistance systems may provide a

Antibiotics **2020**, *9*, 729

fast, initial laboratory test for gauging the risk for developing resistance by adaptation from known resistance systems.

4. Materials and Methods

4.1. Bacterial Strains and Growth Conditions

All strains used in this study are listed in Table 1. *B. subtilis* was routinely grown in MOPS media [41] with added glucose (1.8% (*w*/*v*)) and tryptophan (0.05% (*w*/*v*)) at 37 °C and agitation at 220 rpm. Bacterial growth was monitored as optical density at a wavelength of 600 nm (OD_{600}). Solid media contained 1% (*w*/*v*) agar. Selective media contained chloramphenicol (5 µg/mL), tetracycline (12.5 µg/mL) or kanamycin (5 µg/mL).

Table 1. Strains used in this study.

***B. subtilis* Strain**	**Source/Reference**
W168 trpC2	Laboratory stock
W168 P_{bcrC}-lux	[31]
W168 P_{liaI}-lux	[31]
W168 P_{bceA}-lux	[31]
W168 P_{psdA}-lux	[33]
W168 *bcrC*::kan	[31]
W168 Δ*liaIH*	[31]
W168 Δ*bceRSAB*	[20]
W168 Δ*psdRSAB*	Intermediate strain to produce TMB1518 [42]
W168 Δ*liaIH bceAB*::kan	[31]
W168 Δ*liaIH bcrC*::tet	[31]
W168 *bceAB*::kan *bcrC*::tet P_{liaI}-lux	This work

4.2. Luciferase Reporter and IC_{50} Determination Assay

Stationary cultures were diluted 1:50 in fresh media and incubated for 5 h at 37 °C and 220 rpm. The cultures were subsequently diluted to OD_{600} 0.01 and loaded onto a black 96-well plate. Antibiotic dilutions were added and measurements (OD_{600} and luminescence) were taken every 10 min for 12 h in a CLARIOstar reader (BMG Labtech, Germany) at 37 °C. Lids were used to reduce evaporation. Cultures were agitated in between measurements in the corner well meandering mode at 300 rpm. All experiments were performed with the addition of 1.25 mM $CaCl_2$. All experiments were performed in six biological replicates, but the P_{liaI} promoter activity, which was measured in five replicates.

4.3. Data Processing

All data were analysed with custom scripts using Python. Measurements were smoothed using a median filter (window size = 3). Luminescence output was normalized to cell density by dividing each data point by its corresponding blank-corrected OD_{600} value (RLU/OD). Dose response was measured after one hour. The IC_{50} is defined as the minimal antibiotic concentration reducing the OD_{600} by 50% in comparison to unperturbed growth and was measured 10 h after antibiotic challenge. The true IC_{50} was estimated via a linear fit between the measured concentrations neighbouring the IC_{50}.

Supplementary Materials: The following are available online at http://www.mdpi.com/2079-6382/9/11/729/s1, Figure S1: Kinetics of growth and luminescence of a *B. subtilis* strain harbouring the lux cassette under the P_{bcrC} promoter, Figure S2: Kinetics of growth and luminescence of a *B. subtilis* strain harbouring the lux cassette under the P_{liaI} promoter, Figure S3: Response of the Lia module in response to bacitracin challenge in our setup, Figure S4: Kinetics of growth and luminescence of a *B. subtilis* strain harbouring the lux cassette under the P_{bceA} promoter, Figure S5: Kinetics of growth and luminescence of a *B. subtilis* strain harbouring the lux cassette under the P_{psdA} promoter, Figure S6: Unperturbed doubling time of all strains used in this study, Figure S7: Growth kinetics of deletion strains challenged with laspartomycin C, and Figure S8: Growth kinetics of deletion strains challenged with friulimicin B.

Author Contributions: Conceptualization, A.D., S.G., N.I.M. and G.F.; methodology, A.D., T.M.W., N.I.M. and G.F.; software, A.D.; validation, A.D. and G.F.; formal analysis, A.D.; investigation, A.D.; resources, A.D., T.M.W. and N.I.M. and G.F.; data curation, A.D. and G.F.; writing—original draft preparation, A.D. and G.F.; writing—review and editing, all authors; visualization, A.D. and T.M.W.; supervision, S.G., N.I.M. and G.F.; project administration, S.G., N.I.M. and G.F.; funding acquisition, S.G., N.I.M. and G.F. All authors have read and agreed to the published version of the manuscript.

Funding: This research was funded by the German Research Foundation (DFG), grant number FR3673/1-2 to G.F. Work in S.G.'s laboratory was funded by the Biotechnology and Biological Sciences Research Council (BBSRC; BB/M029255/1). Funding for research in N.I.M.'s laboratory was provided by the European Research Council (ERC consolidator grant, grant agreement no. 725523). The APC was funded by The University of Western Australia.

Acknowledgments: We are grateful to Thorsten Mascher (TU Dresden, Germany) for the gift of friulimicin C and for sharing many of the bacterial strains used in this study.

Conflicts of Interest: The authors declare no conflict of interest. The funders had no role in the design of the study; in the collection, analyses, or interpretation of data; in the writing of the manuscript, or in the decision to publish the results.

References

1. Piepenbreier, H.; Diehl, A.; Fritz, G. Minimal exposure of lipid II cycle intermediates triggers cell wall antibiotic resistance. *Nat. Commun.* **2019**, *10*, 2733. [CrossRef] [PubMed]
2. Breukink, E.; de Kruijff, B. Lipid II as a target for antibiotics. *Nat. Rev. Drug Discov.* **2006**, *5*, 321–332. [CrossRef] [PubMed]
3. Schneider, T.; Gries, K.; Josten, M.; Wiedemann, I.; Pelzer, S.; Labischinski, H.; Sahl, H.G. The lipopeptide antibiotic Friulimicin B inhibits cell wall biosynthesis through complex formation with bactoprenol phosphate. *Antimicrob. Agents Chemother.* **2009**, *53*, 1610–1618. [CrossRef] [PubMed]
4. Wood, T.M.; Martin, N.I. The calcium-dependent lipopeptide antibiotics: Structure, mechanism, & medicinal chemistry. *Medchemcomm* **2019**, *10*, 634–646.
5. Kleijn, L.H.J.; Oppedijk, S.F.; 't Hart, P.; van Harten, R.M.; Martin-Visscher, L.A.; Kemmink, J.; Breukink, E.; Martin, N.I. Total Synthesis of Laspartomycin C and Characterization of Its Antibacterial Mechanism of Action. *J. Med. Chem.* **2016**, *59*, 3569–3574. [CrossRef]
6. Corcilius, L.; Elias, N.T.; Ochoa, J.L.; Linington, R.G.; Payne, R.J. Total Synthesis of Glycinocins A-C. *J. Org. Chem.* **2017**, *82*, 12778–12785. [CrossRef]
7. Wood, T.M.; Bertheussen, K.; Martin, N.I. The contribution of achiral residues in the laspartomycin family of calcium-dependent lipopeptide antibiotics. *Org. Biomol. Chem.* **2019**. [CrossRef]
8. Kleijn, L.H.J.; Vlieg, H.C.; Wood, T.M.; Sastre Toraño, J.; Janssen, B.J.C.; Martin, N.I. High-resolution crystal structure reveals molecular details of target recognition by the calcium-dependent lipopeptide antibiotic laspartomycin C. *Angew. Chem. Int. Ed Engl.* **2017**. [CrossRef]
9. Wecke, T.; Zühlke, D.; Mäder, U.; Jordan, S.; Voigt, B.; Pelzer, S.; Labischinski, H.; Homuth, G.; Hecker, M.; Mascher, T. Daptomycin versus Friulimicin B: In-depth profiling of *Bacillus subtilis* cell envelope stress responses. *Antimicrob. Agents Chemother.* **2009**, *53*, 1619–1623. [CrossRef]
10. Yoshimura, M.; Asai, K.; Sadaie, Y.; Yoshikawa, H. Interaction of *Bacillus subtilis* extracytoplasmic function (ECF) sigma factors with the N-terminal regions of their potential anti-sigma factors. *Microbiology* **2004**, *150*, 591–599. [CrossRef] [PubMed]
11. Cao, M.; Helmann, J.D. Regulation of the *Bacillus subtilis bcrC* bacitracin resistance gene by two extracytoplasmic function sigma factors. *J. Bacteriol.* **2002**, *184*, 6123–6129. [CrossRef] [PubMed]
12. Jordan, S.; Junker, A.; Helmann, J.D.; Mascher, T. Regulation of LiaRS-dependent gene expression in *Bacillus subtilis*: Identification of inhibitor proteins, regulator binding sites, and target genes of a conserved cell envelope stress-sensing two-component system. *J. Bacteriol.* **2006**, *188*, 5153–5166. [CrossRef] [PubMed]
13. Domínguez-Escobar, J.; Wolf, D.; Fritz, G.; Höfler, C.; Wedlich-Söldner, R.; Mascher, T. Subcellular localization, interactions and dynamics of the phage-shock protein-like Lia response in *Bacillus subtilis*. *Mol. Microbiol.* **2014**, *92*, 716–732. [CrossRef] [PubMed]
14. Wecke, T.; Bauer, T.; Harth, H.; Mäder, U.; Mascher, T. The rhamnolipid stress response of *Bacillus subtilis*. *FEMS Microbiol. Lett.* **2011**, *323*, 113–123. [CrossRef] [PubMed]

15. Wolf, D.; Kalamorz, F.; Wecke, T.; Juszczak, A.; Mäder, U.; Homuth, G.; Jordan, S.; Kirstein, J.; Hoppert, M.; Voigt, B.; et al. In-depth profiling of the LiaR response of *Bacillus subtilis*. *J. Bacteriol.* **2010**, *192*, 4680–4693. [CrossRef] [PubMed]
16. McAuley, S.; Vadia, S.; Jani, C.; Huynh, A.; Yang, Z.; Levin, P.A.; Nodwell, J.R. A Chemical Inhibitor of Cell Growth Reduces Cell Size in *Bacillus subtilis*. *ACS Chem. Biol.* **2019**, *14*, 688–695. [CrossRef]
17. Radeck, J.; Fritz, G.; Mascher, T. The cell envelope stress response of *Bacillus subtilis*: From static signaling devices to dynamic regulatory network. *Curr. Genet.* **2017**, *63*, 79–90. [CrossRef]
18. Kobras, C.M.; Piepenbreier, H.; Emenegger, J.; Sim, A.; Fritz, G.; Gebhard, S. BceAB-type antibiotic resistance transporters appear to act by target protection of cell wall synthesis. *Antimicrob. Agents Chemother.* **2019**, *2019/12/25*, 835702. [CrossRef]
19. Koh, A.; Gibbon, M.J.; van der Kamp, M.W.; Pudney, C.R.; Gebhard, S. Conformation control of the histidine kinase BceS of *Bacillus subtilis* by its cognate ABC-transporter facilitates need-based activation of antibiotic resistance. *Mol. Microbiol.* **2020**. [CrossRef]
20. Fritz, G.; Dintner, S.; Treichel, N.S.; Radeck, J.; Gerland, U.; Mascher, T.; Gebhard, S. A new way of sensing: Need-based activation of antibiotic resistance by a flux-sensing mechanism. *MBio* **2015**, *6*, e00975. [CrossRef]
21. Rietkötter, E.; Hoyer, D.; Mascher, T. Bacitracin sensing in *Bacillus subtilis*. *Mol. Microbiol.* **2008**, *68*, 768–785. [CrossRef]
22. Staroń, A.; Finkeisen, D.E.; Mascher, T. Peptide antibiotic sensing and detoxification modules of *Bacillus subtilis*. *Antimicrob. Agents Chemother.* **2011**, *55*, 515–525. [CrossRef] [PubMed]
23. Müller, A.; Wolf, D.; Gutzeit, H.O. The black soldier fly, *Hermetia illucens*—A promising source for sustainable production of proteins, lipids and bioactive substances. *Z. Naturforsch. C* **2017**, *72*, 351–363. [CrossRef] [PubMed]
24. Dintner, S.; Staroń, A.; Berchtold, E.; Petri, T.; Mascher, T.; Gebhard, S. Coevolution of ABC transporters and two-component regulatory systems as resistance modules against antimicrobial peptides in Firmicutes Bacteria. *J. Bacteriol.* **2011**, *193*, 3851–3862. [CrossRef]
25. Joseph, P.; Fichant, G.; Quentin, Y.; Denizot, F. Regulatory relationship of two-component and ABC transport systems and clustering of their genes in the Bacillus/Clostridium group, suggest a functional link between them. *J. Mol. Microbiol. Biotechnol.* **2002**, *4*, 503–513. [PubMed]
26. Dintner, S.; Heermann, R.; Fang, C.; Jung, K.; Gebhard, S. A sensory complex consisting of an ATP-binding cassette transporter and a two-component regulatory system controls bacitracin resistance in *Bacillus subtilis*. *J. Biol. Chem.* **2014**, *289*, 27899–27910. [CrossRef]
27. Wilson, D.N.; Hauryliuk, V.; Atkinson, G.C.; O'Neill, A.J. Target protection as a key antibiotic resistance mechanism. *Nat. Rev. Microbiol.* **2020**, *18*, 637–648. [CrossRef]
28. Mascher, T.; Margulis, N.G.; Wang, T.; Ye, R.W.; Helmann, J.D. Cell wall stress responses in *Bacillus subtilis*: The regulatory network of the bacitracin stimulon. *Mol. Microbiol.* **2003**, *50*, 1591–1604. [CrossRef]
29. Mascher, T.; Zimmer, S.L.; Smith, T.-A.; Helmann, J.D. Antibiotic-inducible promoter regulated by the cell envelope stress-sensing two-component system LiaRS of *Bacillus subtilis*. *Antimicrob. Agents Chemother.* **2004**, *48*, 2888–2896. [CrossRef]
30. Kepplinger, B.; Morton-Laing, S.; Seistrup, K.H.; Marrs, E.C.L.; Hopkins, A.P.; Perry, J.D.; Strahl, H.; Hall, M.J.; Errington, J.; Allenby, N.E.E. Mode of Action and Heterologous Expression of the Natural Product Antibiotic Vancoresmycin. *ACS Chem. Biol.* **2018**, *13*, 207–214. [CrossRef]
31. Radeck, J.; Gebhard, S.; Orchard, P.S.; Kirchner, M.; Bauer, S.; Mascher, T.; Fritz, G. Anatomy of the bacitracin resistance network in *Bacillus subtilis*. *Mol. Microbiol.* **2016**, *100*, 607–620. [CrossRef]
32. Gebhard, S.; Mascher, T. Antimicrobial peptide sensing and detoxification modules: Unravelling the regulatory circuitry of *Staphylococcus aureus*. *Mol. Microbiol.* **2011**, *81*, 581–587. [CrossRef]
33. Höfler, C.; Heckmann, J.; Fritsch, A.; Popp, P.; Gebhard, S.; Fritz, G.; Mascher, T. Cannibalism stress response in *Bacillus subtilis*. *Microbiology* **2016**, *162*, 164–176. [CrossRef] [PubMed]
34. Chang, G. Multidrug resistance ABC transporters. *FEBS Lett.* **2003**, *555*, 102–105. [CrossRef]
35. Asai, K. Anti-sigma factor-mediated cell surface stress responses in *Bacillus subtilis*. *Genes Genet. Syst.* **2018**, *92*, 223–234. [CrossRef]
36. Müller, A.; Wenzel, M.; Strahl, H.; Grein, F.; Saaki, T.N.V.; Kohl, B.; Siersma, T.; Bandow, J.E.; Sahl, H.-G.; Schneider, T.; et al. Daptomycin inhibits cell envelope synthesis by interfering with fluid membrane microdomains. *Proc. Natl. Acad. Sci. USA* **2016**, *113*, E7077–E7086. [CrossRef] [PubMed]

37. Grein, F.; Müller, A.; Scherer, K.M.; Liu, X.; Ludwig, K.C.; Klöckner, A.; Strach, M.; Sahl, H.-G.; Kubitscheck, U.; Schneider, T. Ca2+-Daptomycin targets cell wall biosynthesis by forming a tripartite complex with undecaprenyl-coupled intermediates and membrane lipids. *Nat. Commun.* **2020**, *11*, 1455. [CrossRef] [PubMed]
38. Mescola, A.; Ragazzini, G.; Alessandrini, A. Daptomycin Strongly Affects the Phase Behavior of Model Lipid Bilayers. *J. Phys. Chem. B* **2020**. [CrossRef] [PubMed]
39. Crow, A.; Greene, N.P.; Kaplan, E.; Koronakis, V. Structure and mechanotransmission mechanism of the MacB ABC transporter superfamily. *Proc. Natl. Acad. Sci.* **2017**, *114*, 12572–12577. [CrossRef] [PubMed]
40. Mavrici, D.; Marakalala, M.J.; Holton, J.M.; Prigozhin, D.M.; Gee, C.L.; Zhang, Y.J.; Rubin, E.J.; Alber, T. *Mycobacterium tuberculosis* FtsX extracellular domain activates the peptidoglycan hydrolase, RipC. *Proc. Natl. Acad. Sci. USA* **2014**, *111*, 8037–8042. [CrossRef] [PubMed]
41. Neidhardt, F.C.; Bloch, P.L.; Smith, D.F. Culture Medium for Enterobacteria. *J. Bacteriol.* **1974**, *119*, 736–747. [CrossRef] [PubMed]
42. Gebhard, S.; Fang, C.; Shaaly, A.; Leslie, D.J.; Weimar, M.R.; Kalamorz, F.; Carne, A.; Cook, G.M. Identification and characterization of a bacitracin resistance network in *Enterococcus faecalis*. *Antimicrob. Agents Chemother.* **2014**, *58*, 1425–1433. [CrossRef] [PubMed]

Publisher's Note: MDPI stays neutral with regard to jurisdictional claims in published maps and institutional affiliations.

© 2020 by the authors. Licensee MDPI, Basel, Switzerland. This article is an open access article distributed under the terms and conditions of the Creative Commons Attribution (CC BY) license (http://creativecommons.org/licenses/by/4.0/).

2.2. Growth rate dependency of cell wall targeting antibiotics

Depending on the stage of infection, growth behaviors of pathogens differ widely with e.g. rapid growth in an acute stage of the disease but rather slow-growth in chronic infections [146]. Together with the growth rate, the metabolic state of bacteria is carefully balanced and needs to be readjusted continuously during growth [136, 138, 147, 148]. A reduction of metabolic activity has often been shown to diminish susceptibility towards antibiotics with e.g. stationary cultures, which have exhausted available nutrients and show no net growth. This is especially worrisome in pathogens such as *Klebsiella pneumoniae* and *Mycobacterium tuberculosis*, which were described to become tolerant in stationary cultures against ampicillin and ciprofloxacin, as well as ofloxacin, sulbactam-ampicillin, rifampin, and isoniazid, respectively [149, 150]. But also single cells with a reduced metabolic activity can exhibit higher tolerance of antibiotics as so-called persister cells [79]. For instance, single *E. coli* cells with an active SOS-response caused by DNA damage were shown to be tolerant against ciprofloxacin, which targets DNA topoisomerases [82]. While many examples of this dependency between growth rate, metabolic state and antibiotic susceptibility are known [74, 78, 81], more sophisticated dependencies of resistance on growth rate could arise from the cellular organization of targeted pathways. Recently, an interesting growth dependence of ribosome targeting antibiotics has been found. Greulich et al. showed that their activity can be both positively or negatively correlated with growth rate [75]. The directionality of the trend depends on the binding affinity of the antibiotic to the ribosome and is caused by the simultaneous increase of ribosome content in fast growth and the decreasing potential to build more ribosome (section 1.5.4, for more detail).

Research about the growth rate dependency of cell wall targeting antibiotics showed that higher growth rate promoting media also increased the rate of killing by penicillin [76]. Since then, the same effect has been observed for other penicillin-like antibiotics [62, 145, 151, 152]. However, this phenomenon does not represent resistance but rather tolerance, which describes the prolonged duration a bacterial culture can survive at antibiotic concentrations above its MIC as indicated by an increased rate of killing [74, 78]. To my knowledge, the resistance of any cell wall targeting antibiotic has not been examined in its dependency on the growth rate to date.

An optimal dosage of antibiotics is key to prevent the further development genetic resistances as to low concentrations fail to clear infections while to high concentrations might leak into the environment and create an evolutionary benefit for resistant bacteria [153, 154]. As the growth rate of pathogens can differ [146] a changing susceptibility

dependent on growth rate could strongly influence this optimal dosage. Here, I set out to examine the antibiotic susceptibility under varying growth rates for cell envelope targeting antibiotics. For this, a range of antibiotics were tested that target the cell wall synthesis via different routes, namely inhibition of PBPs and MraY as well as sequestration of external lipid carriers.

2.2.1. Modulating growth rate with α-methyl glucopyranoside

One of the easiest ways to cultivate cultures at different rates is to change nutrient quality with e.g. more kinds of amino acids to achieve faster growth rates or carbon sources of different energy content [75, 155–157]. However, drastic changes in media composition can have other drastic effects on the metabolism and can occur when widely different media are used in the same assay such as the complex media tryptic soy broth (TSB) and defined media such as minimal MOPS media. Similarly, the addition of more and more kinds of amino acids for faster growth also alters the metabolic landscape drastically as each supplied amino acid represses the biosynthesis machinery of its own production [158]. This causes interference at many points of the metabolism, each of which could cause growth rate independent changes and could lead to artifacts. To avoid these effects a technique that only interferes at one point in the metabolism would be preferable. For this, I used the glucose analogue α-methyl glucopyranoside (α-MG) to regulate growth rate in media containing glucose as the sole carbon source. α-MG competes with glucose for import by the permease PtsG (Figure 2.1a) but once inside the cell it cannot be catabolized [159, 160]. PtsG is the main but not the only transporter of glucose so that α-MG can inhibit most but not all import [160, 161]. If glucose is used as the sole carbon source the growth rate is reduced by α-MG in a concentration-dependent manner as shown with *E. coli* [162].

Minimal MOPS media with glucose as the sole carbon source was substituted with varying concentrations of α-MG and exponential growth of *B. subtilis* was recorded. This led to slower growth with increasing α-MG concentration (Figure 2.1b). Quantification of growth rate showed that the addition of α-MG reduced the growth rate from 0.88±0.06 h^{-1} at 0% (w/v) α-MG to 0.32±0.02 h^{-1} at 3.6% (w/v) α-MG (Figure 2.1c).

When media containing fructose as the sole carbon source was used, addition of α-MG lead to a small decrease of growth rate, however, not in a concentration-dependent manner (Figure 2.1c, d). This marks fructose supplemented MOPS media as an excellent control to ensure that any changes in the susceptibility are due to a diminished growth rate and not by other effects caused by α-MG addition.

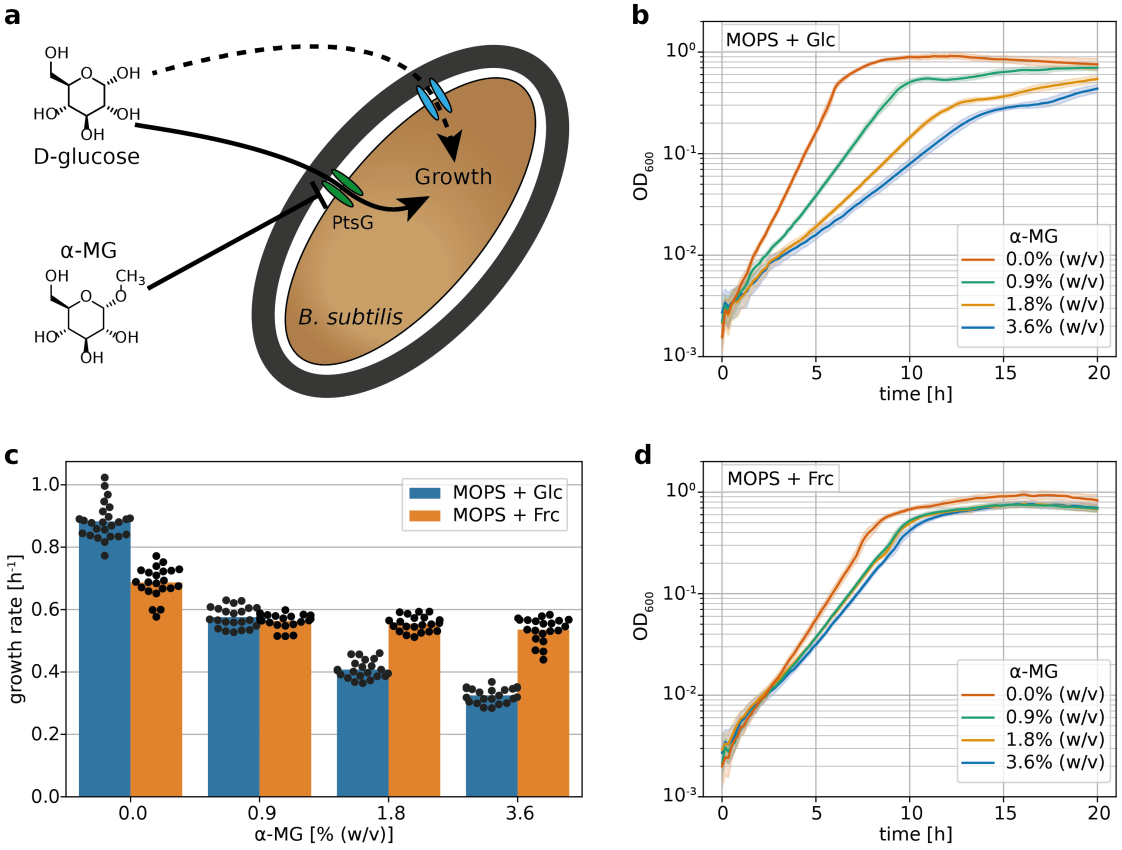

Figure 2.1.: Growth inhibition by α-MG. (a) Under normal growth conditions most of the glucose is imported via the sugar transporter PtsG. Addition of α-MG slows down growth since it competes with glucose for import but cannot be utilized any further. Due the activity of minor glucose transporters the growth rate cannot be reduced indefinitely by α-MG [160, 161]. (b,d) Growth curves of *B. subtilis* in minimal MOPS media supplemented with glucose (b) and fructose (d) (n≥22). (c) Growth rate as induced by α-MG addition. (n≥20)

2.2.2. Inhibition pattern of cell envelope targeting antibiotics

Here, a diverse set of cell envelope targeting antibiotics was examined for their growth rate dependent activity. Therefore, great care had to be taken in choosing an assay that accurately measures susceptibility in all growth conditions for all antibiotics. For this, it was necessary to gain a detailed understanding of the inhibition patterns produced by the antibiotics used here.

To examine the intrinsic, passive resistance a *B. subtilis* W168 carrying unmarked deletions of all three endogenous Bce-like modules (bceRS-bceAB, psdRS-psdAB, and yxdJK-yxdLM-yxeA (Δ3bce)) was used in the following experiments. Cultures of this strain were grown in minimal MOPS media with glucose for several generations to reach steady-state exponential growth, in which all properties of the culture (cell number, total mass, DNA etc.) increase exponentially at the same rate [163]. These were then

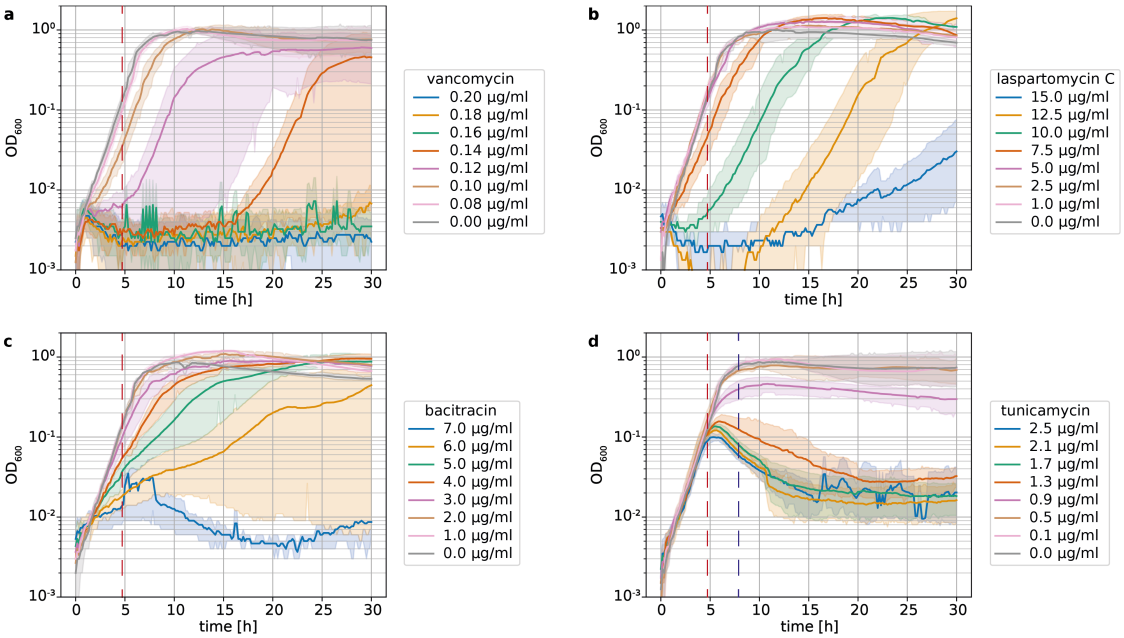

Figure 2.2.: Pattern of inhibition by cell wall targeting antibiotics. Growth curves of the fastest growth condition challenged with vancomycin (a), laspartomycin (b), bacitracin (c) or tunicamycin (d) at t=0. Dashed lines in red and blue indicate 6 and 10 doublings after antibiotic challenge, respectively. Shaded areas depict 95% confidence intervals. (n≥3)

challenged with antibiotics and their growth (OD_{600}) was monitored every 10 min. The resulting growth curves showed that most of the antibiotics used here did not modulate the growth rate as described for those that target ribosomes (Table 2.1) [75]. Instead, in most cases a lag phase was induced, the duration of which was concentration dependent as shown here for vancomycin (Figure 2.2a). This was also the case for ampicillin, nisin and ramoplanin (Table 2.1, Figure S.1). Laspartomycin C exhibited a combined inhibition pattern with a lag phase and a growth rate reduction – both concentration dependent (Figure 2.2b). The lag phase induction seems to be a recurring inhibition pattern of cell envelope targeting antibiotics, as it covers a great diversity of targets with lipid carriers of the lipid II cycle (UP and lipid II) as well as the transpeptidation activity of PBPs. Bacitracin, which targets the most abundant lipid carrier of the cycle (UPP) [3], did not induce a lag phase but reduced the growth rate (Figure 2.2c). Finally, tunicamycin, which inhibits MraY activity, showed the most distinct inhibition pattern with a very rapid lysis/ growth rate reduction event after about 5 doublings of unperturbed growth (Figure 2.2d).

Inhibition patterns observed in the absence of α-MG are observed in all α-MG concentrations tested here, as shown by the modulation of growth rate (Figure S.2).

Table 2.1.: Pattern of inhibition of the cell envelope targeting antibiotics tested here. *: IC_{50} as measured in MOPS with glucose as the sole carbon without the addition of α-MG.

antibiotic	cellular target	IC_{50} in MOPS + Glc*	pattern of inhibition
ampicillin	PBPs	0.08 µg/ml	induces lag phase
bacitracin	UPP	3.48 µg/ml	modulates growth rate
laspartomycin C	UP	6.56 µg/ml	modulates growth rate and induces lag phase
nisin	lipid II	32.7 µg/ml	induces lag phase
ramoplanin	lipid II	0.27 µg/ml	induces lag phase
tunicamycin	MraY	2.24 µg/ml	growth arrest/lysis after initial growth
vancomycin	lipid II	0.09 µg/ml	induces lag phase

2.2.3. Design of a suitable assay for growth rate dependent susceptibility

With the gained knowledge about the inhibition patterns of the antibiotics used here a suitable assay was selected. As some of the antibiotics were not bactericidal, a killing assay as used by most other studies on growth rate dependent activity of cell envelope targeting antibiotics was not suitable [62, 76, 145, 151, 152]. Similarly, measuring the reduction of growth rate as used for ribosome targeting antibiotics [75] was inappropriate, since only bacitracin solely reduces the growth rate in a concentration dependent manner.

As all antibiotics lead to a reduction of growth (OD_{600}) after a given time, a refined IC assay was used. For this, growth curves of *B. subtilis* after antibiotic challenge were monitored as before in the various media. Then, the antibiotic concentration reducing

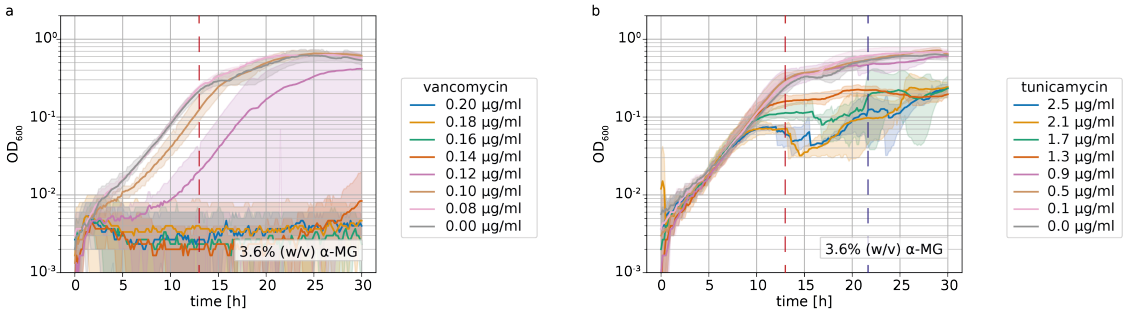

Figure 2.3.: Inhibition by vancomycin (a) and tunicamycin (b) in slow growth. Growth curves of the slowest growth condition challenged with vancomycin (a) or tunicamycin (b) at t=0. Dashed, red and blue lines indicate 6 and 10 doublings after antibiotic challenge, respectively. Shaded areas depict 95% confidence intervals. (n≥3)

growth by 50% (IC_{50}) was determined after a given incubation time. To compare fast and slow-growing cultures without bias it was important that the cultures were in the same state when this measurement was taken. If an absolute incubation time such as 5 h was used, fast growing cultures have reached a higher OD_{600} than slow-growing cultures and therefore might be in a different growth phase and in another metabolic state. Furthermore, if a time point is chosen mid exponential phase in the fastest growth condition, slow-growing cultures were not developed enough to accurately measure an IC_{50} as shown here for vancomycin (Figures 2.2a & 2.3a, at the 5 h mark).

To compare the susceptibility at similar growth stages in all conditions the IC_{50} was determined 6 doublings after antibiotic challenged as calculated by the growth rate of an unperturbed culture in the same condition (red dashed line, Figures 2.2a & 2.3a). This ensures a comparable growth phase and metabolic state across all conditions and allows the activity of growth rate modulating and lag-phase inducing antibiotics as well as any hybrid forms to be measured without introducing a bias. Due to the unique inhibition pattern of tunicamycin, the IC_{50} could not be measured after 6 doublings in most conditions, as the antibiotic takes effect around this time (red dashed line, Figure 2.2d & 2.3b). Since the inhibition becomes more apparent at later stages, the IC_{50} was measured after 10 doublings (beginning of stationary phase) instead (blue dashed line, Figure 2.2d & 2.3b).

2.2.4. Susceptibility towards cell wall targeting antibiotics is largely independent of growth rate

When measuring the susceptibility using the assay described above, a striking invariability in activity of most cell wall targeting antibiotics became apparent (Figure 2.4a). The only significant change in antibiotic activity was seen in bacitracin with an IC_{50} of 3.48±0.29 µg/ml in fast growth and IC_{50} of 2.19±0.39 µg/ml in slow growth (Figure 2.4b).

The average IC_{50} of ampicillin increased almost 2-fold from 0.08±0.02 µg/ml in fast growth to 0.16±0.05 µg/ml in slow growth (Figure 2.4c). However, a similar trend was observed in the fructose control (Figure 2.5).

Likewise, tunicamycin showed an insignificant decrease in susceptibility in slow growth with 1.42±0.31 µg/ml compared to 0.92±0.14 µg/ml in fast growth (Figure 2.4d). But a similar change from 2.23±0.25 µg/ml with 3.6% (w/v) α-MG to 1.10±0.07 µg/ml without α-MG is observed in fructose supplemented MOPS media, in which α-MG had a smaller effect on growth rate (Figure 2.5).

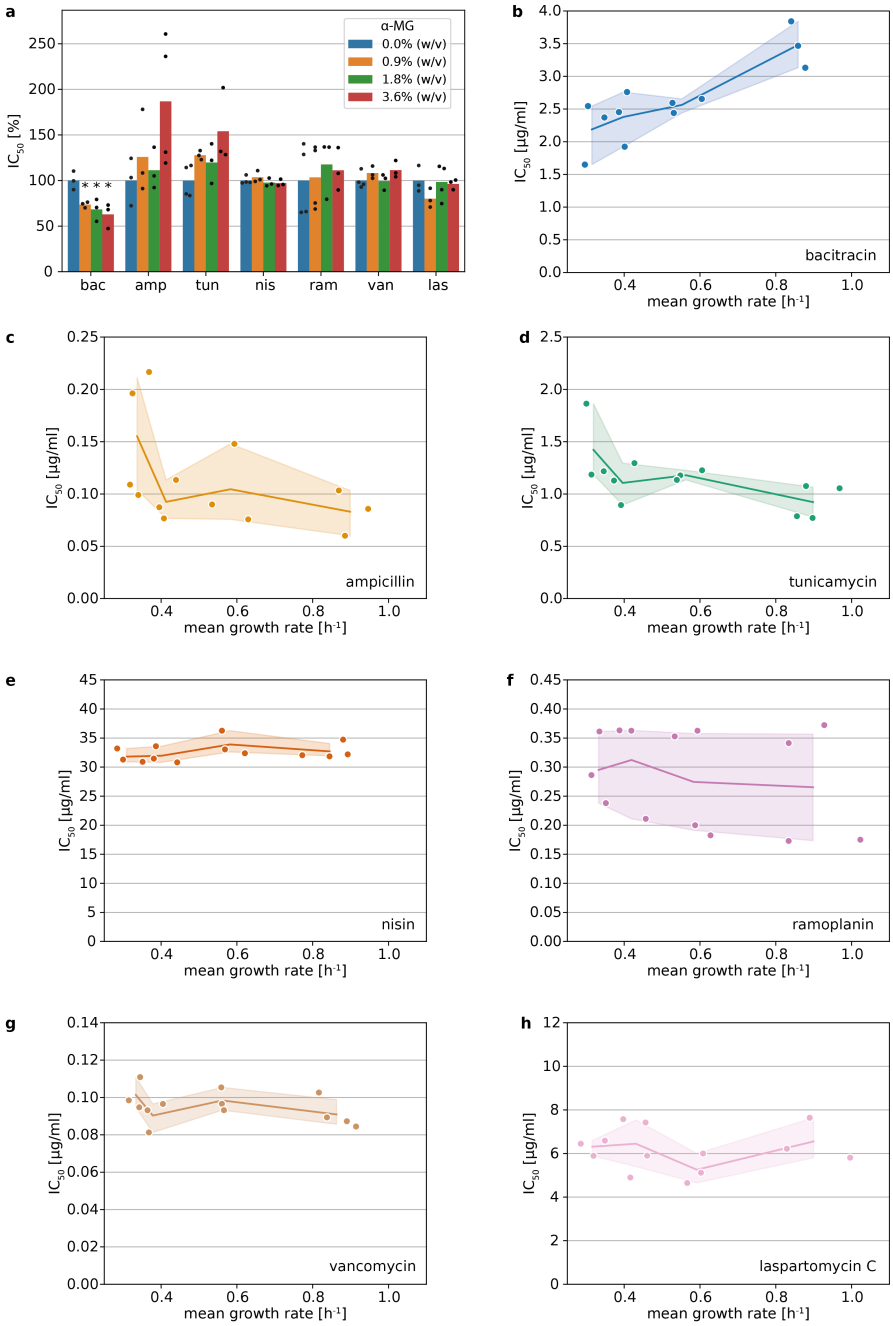

Figure 2.4.: Susceptibility towards cell wall antibiotics at different growth rates induced by α-MG. (a) Dependence of the IC_{50} on α-MG concentration. Bars show the averaged IC_{50}. Black dots show single replicates. Statistical significance was calculated in relation to the fastest growth condition using unpaired t-tests (*: $p<0.05$, equal variance). (b-c, e-h) Dependence of the IC_{50} on growth rate 6 doublings after antibiotic challenge. (d) Dependence of tunicamycin's IC_{50} on growth rate 10 doublings after antibiotic challenge. Lines show the averaged IC_{50}. Shaded areas display 95% confidence intervals. Dots show single replicates. ($n \geq 3$)

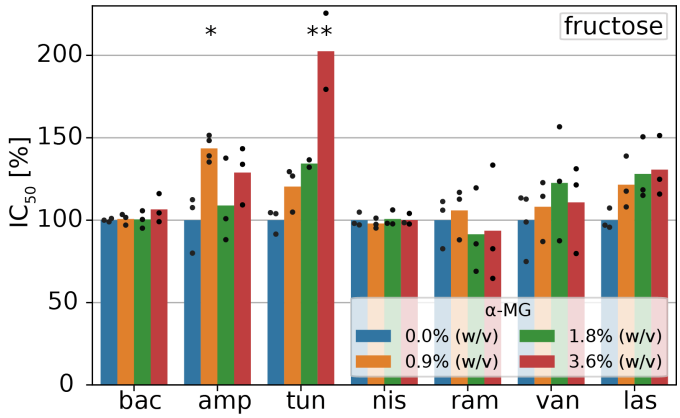

Figure 2.5.: Susceptibility towards cell envelope targeting antibiotics at different α-MG concentration in fructose supplemented media. Dependence of the IC_{50} on α-MG concentration. Bars show the averaged IC_{50}. Black dots show single replicates. Statistical significance was calculated in relation to the fastest growth condition using unpaired t-tests (*: $p<0.05$, equal variance). Absolute values of susceptibility are given in table S.1. ($n\geq3$)

Interestingly, all lipid II binding antibiotics tested (nisin, ramoplanin and vancomycin) as well as laspartomycin C showed no change in activity (Figure 2.4e-h). It is to note that no significant changes in antibiotic activity were observed in the fructose-control other than with tunicamycin and ampicillin (Figure 2.5).

2.2.5. Media composition can have drastic effects on susceptibility

To see whether media composition has indeed as high of an influence on resistance as suspected and to broaden the range of growth rates tested, susceptibility was also measured in LB media. Due to its diverging nutritional value and type, LB media might promote a distinct metabolic state that can influence susceptibility. In the setup used here *B. subtilis* grew with a growth rate of $1.26\,h^{-1}$ in LB. The trend of increasing resistance with growth rate observed with α-MG of bacitracin was continued as the IC_{50} increased from 3.48 µg/ml in MOPS media without α-MG to 3.75 µg/ml in LB media (Figure 2.6b). The IC_{50} of both ampicillin and tunicamycin are similarly in the same range as measured in MOPS media without α-MG at 0.07 µg/ml and 1.00 µg/ml, respectively (Figure 2.6a, f). However, *B. subtilis* displayed a stark increase of the resistance towards laspartomycin C, nisin, ramoplanin and vancomycin from the fasted growth condition in MOPS to LB media, although these antibiotics did not show a growth rate dependency before (Figure 2.6). While the IC_{50} of nisin and ramoplanin roughly doubles to 65.53 µg/ml and 0.48 µg/ml in LB, resistance towards laspartomycin C and vancomycin increases about 3-fold with IC_{50} of 18.41 µg/ml and 0.30 µg/ml, respectively.

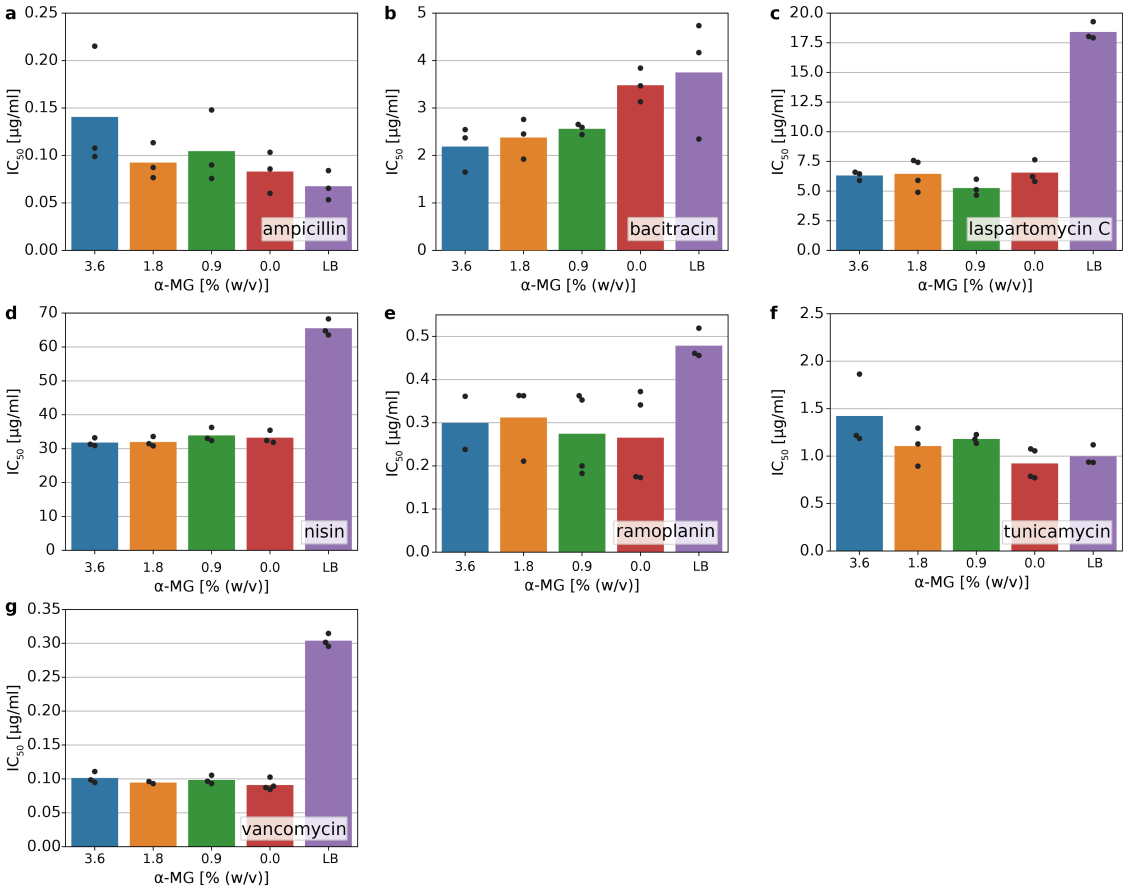

Figure 2.6.: Susceptibility in LB media differs drastically from the growth rate trend observed in MOPS media. Dependence of the IC_{50} on growth rate 6 doublings (a-e, g) or 10 doublings (f) after antibiotic challenge. Bars show the averaged IC_{50}. Dots show single replicates. (n≥3)

2.2.6. Conclusion

To measure the growth rate dependent susceptibility towards cell envelope targeting antibiotics, we developed an assay that (1) reduces nutritional effects of the media besides growth rate on the metabolism and (2) ensures the same metabolic state of all conditions for unbiased view of susceptibility.

Overall, a striking independence of susceptibility towards cell envelope targeting antibiotics was found with the notable exception of bacitracin, to which *B. subtilis* showed a 40% total increase in resistance over the entire growth rate range tested. While the increase of resistance against bacitracin is significant the dependency is rather small when compared to ribosome-targeting antibiotics which show a 500% total increase in resistance over a similar range of growth rates.

As cell size increases with faster growth [142], which entails an increase in cell sur-

face area and therefore PG demand, a high level of regulation is necessary to adjust the PG synthesis machinery. As seen for ribosomes, this regulation can lead to different susceptibilities towards antibiotics with changing growth rates [75]. As such a redistribution of lipid carrier pool sizes or the emergence of other bottlenecks was also expected for cell envelope targeting antibiotics. The nearly constant susceptibility across growth rates seen here indicates a finely tuned and stable regulation of PG synthesis.

As a proof of concept susceptibility was also tested LB media, which differs drastically in nutritional composition from the other media used. Here, *B. subtilis* showed a continuous trend between growth rate in MOPS media and LB towards some antibiotics (ampicillin, bacitracin and tunicamycin). However, other antibiotics (lipid II binders and laspartomycin C) displayed a considerable increase in the IC_{50} between MOPS media and LB. The growth rate promoted by LB media exceeds the growth rate achieved by any MOPS media tested here and the sudden increase of resistance with even faster growth could be due to a dependency of higher order or the combination of opposing trends. However, as the two media differ so drastically in nutritional composition this difference might also be an artifact caused by a different metabolic state.

2.3. Further insight into the susceptibility towards cell envelope targeting antibiotics

During this work several other scientific questions around the resistance of *B. subtilis* towards cell envelope targeting antibiotics presented themselves. For instance, while α-MG was chosen in section 2.2 to modulate growth rate, many other studies alter nutrient quality - especially amino acid content - to this end. Here, I investigated the effect of selected amino acids on growth, the response of the Lia module and antibiotic susceptibility. Furthermore, the origin of the common regrowth inhibition pattern of cell envelope targeting antibiotics described in section 2.2.2 is investigated with a focus on antibiotic degradation. The effect of inoculum size on nisin activity is examined. Moreover, the effect of a reduced activity of single enzymatic functions in the lipid II cycle on susceptibility was investigated with a combination of mathematical modeling and experimental techniques. Finally, the conferred resistance of *tmrB*, a potential tunicamycin resistance gene, is determined.

2.3.1. Effect of amino acids

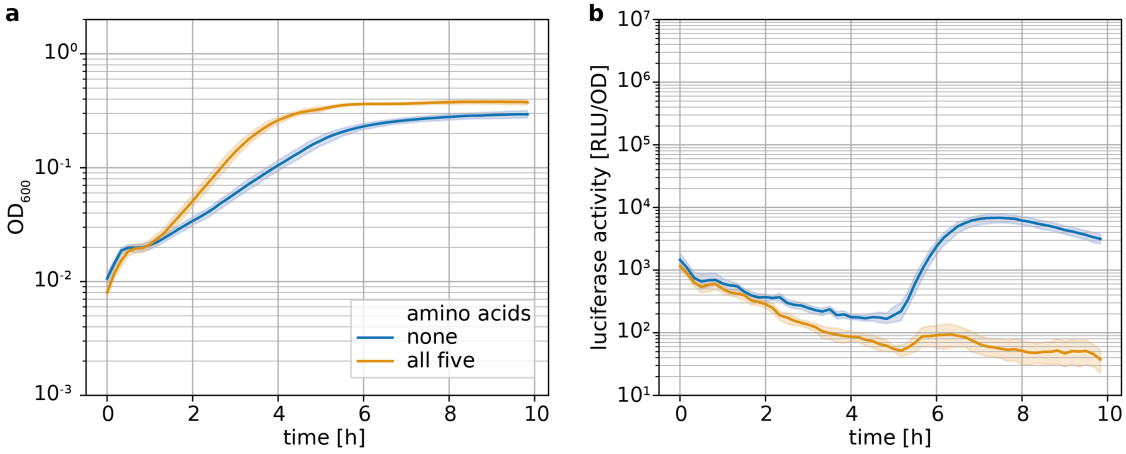

Figure 2.7.: Growth and Lia-response in presence and absence of amino acids. Time dependent growth (a) and Lia response as shown by the *liaI* promoter (b) in presence and absence of amino acids. Shaded areas depict 95% confidence intervals. (n=10)

Many studies utilize nutrient quality as a means to modulate bacterial growth rate [75, 155–157]. During preliminary testing inconsistencies of the stationary phase stress response of most CESR modules, a well described phenomenon in *B. subtilis* growth, became apparent [111, 164]. This stress response has been found to be induced by so called cannibalism toxins, which are produced by a subpopulation of the culture to lyse their unprepared siblings and utilize the released nutrients in order to delay

the initiation of sporulation - a committed step to a lengthy and energy-intensive process [90, 111]. These cannibalism toxins include sporulation delaying protein (SDP), sporulation killing factor (SKF) and YydF, the latter of which has been shown to almost exclusively trigger a Lia response [165, 166].

When growing a *B. subtilis* strain (Δ3bce) containing a Lia reporter (P_{liaI}-lux) in minimal MOPS media the addition of five amino acids (arginine, histidine, methionine, proline, threonine) had various effects. Not only grew *B. subtilis* better with the addition of amino acids (Figure 2.7a) but the stationary phase stress response was eliminated (Figure 2.7b). As this stress response is consistently induced in both minimal media (MSCE) as well as (protein-)rich media (LB) [88, 111] this outcome was highly unexpected. To determine whether this was a collective effect of the added amino acids or caused by a specific single amino acid I supplemented the media with each amino acid individually and repeated the experiment. The 5 amino acid mix increased growth rate 1.8-fold (Figure 2.8a). Methionine, proline and threonine did not show a significant change in growth rate compared to the condition without amino acids. Arginine showed the only significant positive effect on growth rate, however, it only increased it 1.2-fold. Histidine even decreased the growth rate 1.2-fold.

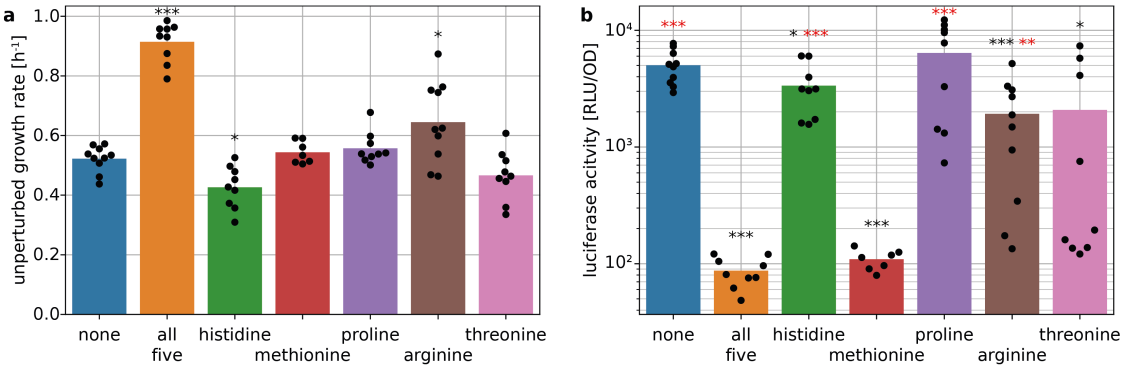

Figure 2.8.: Effect of selected amino acids on growth rate (a) and Lia response (b) in *B. subtilis*. Stationary phase stress response was measured at the respective entry into stationary phase (5 doubling times after the begin of measurement). Black dots show single replicates. Statistical significance was calculated in relation to the condition without (black (a&b)) and with all five amino acids (red (b)) using two-sided unpaired t-tests (*: p<0.05, **: p<0.01, ***: p<0.001, equal variance). (n≥7)

By measuring the luminescence 5 doubling times after the beginning of the experiment (as calculated by the growth rate) I was able to extract a near maximal stationary phase stress response for all conditions. This was a more reliable method than a fixed time due to the varying growth rates (data not shown). With both histidine and proline the *liaI* promoter was induced to the same level as in the absence of amino acids

(Figure 2.8b). Addition of methionine led to the elimination of the stationary stress response as with the 5 amino acid mix. Arginine and threonine showed a high variation between replicates ranging from nearly uninduced levels to a full stress response. As such, methionine seems to be the main component in the elimination of the stationary phase stress response.

This elimination of the stationary phase stress response could be caused by one of three mechanisms: changes in the metabolism caused by availability of methionine might (1) enable a higher intrinsic resistance to cell envelope stress and therefore antibiotics targeting the cell envelope, (2) inhibit Lia induction or (3) inhibit synthesis of cannibalism toxins. To test the first two hypotheses I challenged the *B. subtilis* strain used before with three well-described cell envelope targeting antibiotics, which also induce the Lia module (bacitracin, nisin and vancomycin), in presence and absence of the five amino acids.

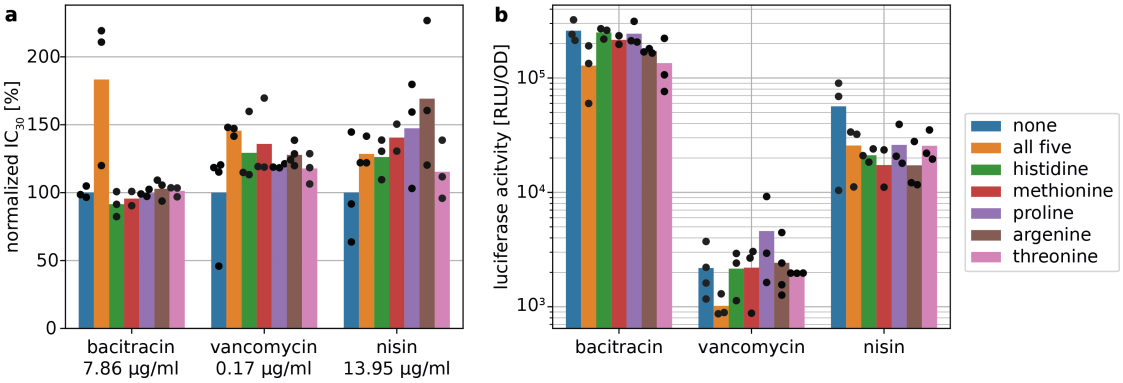

Figure 2.9.: Presence of amino acids affects neither susceptibility against cell envelope targeting antibiotics nor the antibiotic-induced Lia response. (a) The IC_{30} of key cell envelope targeting antibiotics in the presence of different amino acids was determined 3 doubling times after antibiotic challenge. All IC_{30} values were normalized by the IC_{30} measured without the addition of amino acids, which is given underneath the x-axis. (b) The Lia response induced by theses antibiotics was measure 30 min after antibiotic challenge. Depicted are only measurements taken with antibiotic concentrations just below the IC_{30} (bacitracin: 3.0 µg/ml,vancomycin: 0.1 µg/ml, nisin: 10 µg/ml). Black dots show single replicates. Neither susceptibility nor Lia response is significantly altered by addition of any amino acids ($p>0.05$, equal variance). ($n\geq 2$)

For this, exponentially growing cultures with the respective amino acids were challenged with antibiotic and growth (OD_{600}) was measured every 10 min for the following 10 h. To resolve the susceptibility the inhibitory concentration leading to a growth reduction to 30% of an unperturbed culture (IC_{30}) was determined during mid-exponential phase (3 doubling times after antibiotic challenge). This did not reveal any significant ($p<0.05$) changes in the IC_{30} (Figure 2.9a). However, the IC_{30} of bacitracin showed a not statistically significant increase by 80% in presence of all five amino acids.

Next, I investigated the Lia response towards these antibiotics in presence of amino acids. The Lia response measured 30 min after antibiotic challenge was chosen for this analysis, as it has been described to be close to maximal at this point [88, 89]. To show the data more clearly the Lia response induced only by the antibiotic concentration just below the IC_{30} is shown here. No significant changes between the presence or absence of amino acids were observed (Figure 2.9b). This also reflects the induction of the full range of antibiotic concentrations tested (Figure S.3).

Since neither susceptibility nor the induction of the Lia-response is affected by amino acids, both a higher resistance against antibiotics and an inhibition of the Lia-response are unlikely effects of amino acid addition. It would be interesting to see in the future, if supplementing amino acids can inhibit the synthesis of cannibalism toxins at the beginning of stationary phase in *B. subtilis*.

2.3.2. Degradation of selected cell wall targeting antibiotics

As described before in section 2.2, bacterial cultures challenged with certain cell wall targeting antibiotics regrow with an unperturbed growth rate after a concentration-dependent lag period (Figure 2.2a & S.1). This could be caused by a gradual deterioration of antibiotics above inhibitory levels as longer periods are necessary to reach sub-inhibitory levels the higher the initial concentration is. A high degradation rate could therefore lead to the fast-paced regrowth pattern we observe for many antibiotics. These experiments were performed by Dr. Jamie Tedeschi, who I instructed in microbiological lab work.

To see whether degradation plays a large role for cell wall targeting antibiotics, the half-life time of some of the antibiotics was determined in standard MOPS minimal media in absence of a bacterial culture. The antibiotics include ramoplanin and nisin as they exhibit the regrowth pattern and bacitracin, which is included as a control. The antibiotic was diluted with MOPS media and incubated as they would with a growing bacterial culture (37°C, 700 rpm) to replicate those conditions. After incubation times between 0-16 h a steady-state exponentially growing *B. subtilis* culture (Δ3*bce*) was added and growth (OD_{600}) was monitored every 10 min (Figure 2.10a). The concentration of active, i.e. not degraded antibiotic that induces a reduction of e.g. 30% in growth is constant for each antibiotic. This concentration of active antibiotic is determined with a control that skips the incubation step as the inhibitory concentration that reduces growth to 30% of an unperturbed culture 5 h after antibiotic challenge (IC_{30}). The observed inhibitory concentration (OIC) is determined correspondingly in samples with incubation times of

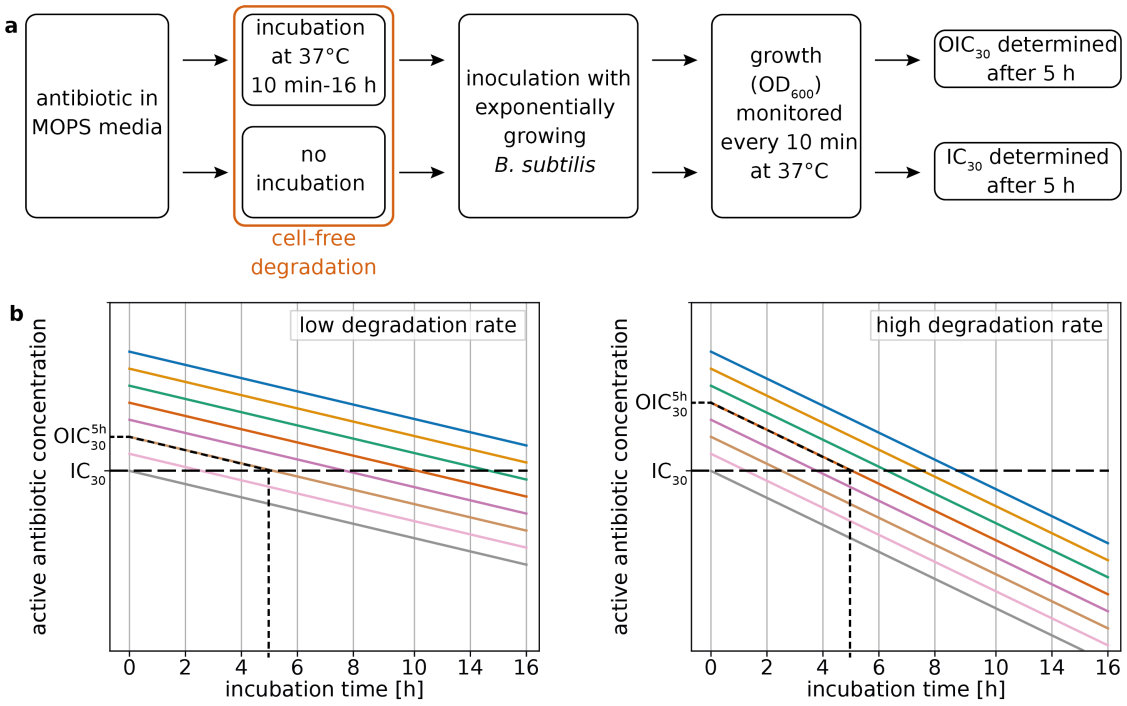

Figure 2.10.: Experimental procedure and data analysis of antibiotic degradation. (a) Flowchart of the experimental procedure to determine degradation of antibiotics. Antibiotics were incubated in MOPS media for 10 min to 16 h. The antibiotic-containing media was subsequently inoculated with exponentially growing *B. subtilis* culture and growth was monitored every 10 min. The OIC_{30} was determined after 5 h. The IC_{30} of the same antibiotics were determined as a control with the same experimental procedure, but skipping the incubation step. (b) Exemplary dependence of IC_{30} and OIC_{30} at low (left) and high (right) degradation rate of the antibiotic. Notice the higher OIC_{30}^{5h} at higher degradation rate.

the antibiotic between 10 min and 16 h. As the initial concentration of antibiotic in the media is known, the rate of degradation of each antibiotic can be determined via the difference of IC_{30} and OIC_{30} (Figure 2.10b).

In the control without prior incubation of the antibiotic the IC_{30} was determined as 3.3 µg/ml, 20.9 µg/ml and 0.38 µg/ml for bacitracin, nisin and ramoplanin, respectively (Figure 2.11a). In case of bacitracin prolonged incubation of up to 16 h had little impact on the OIC_{30}^{16h} as it showed only a 1.2-fold increase relative to the control without pre-incubation. However, this incubation period had a much stronger effect on nisin, which displays a 5.8-fold increase of the OIC_{30}^{16h}. Interestingly, this degradation does not appear to take place at a constant rate but within the first 40 min in particular as the OIC_{30}^{40min} was almost as high as after 16 h of incubation (117.4 µg/ml to 120.7 µg/ml). For better visualization the half-life time of the antibiotic in the first 40 min and the subsequent ~15 h of incubation was calculated (Figure 2.11b). Indeed, while the half-life time of

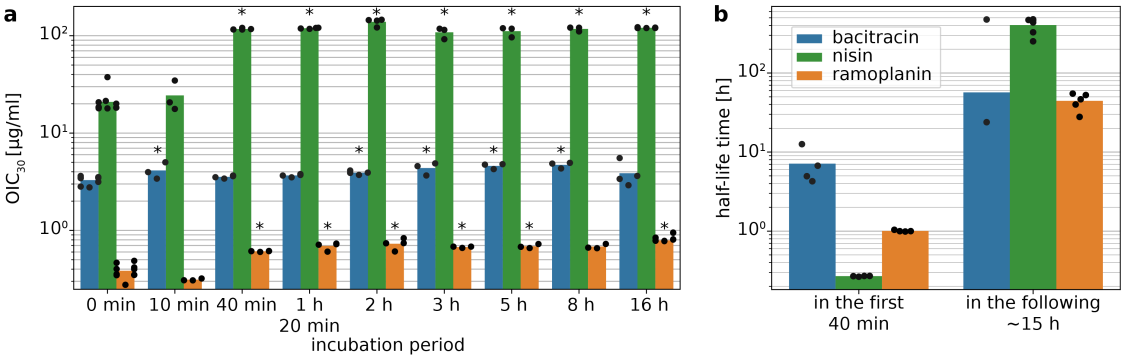

Figure 2.11.: Ramoplanin and nisin show a diphasic degradation pattern in MOPS minimal media. (a) OIC_{30} was measured 5 h after inoculation. Statistical significance was calculated in relation to no prior incubation using two-sided unpaired student's t-tests (*: p<0.05, equal variance). (b) Half-life times calculated between measurements of incubation times 0 h and 40 min as well as 40 min and 16 h. Bars represent the average. Black dots show single replicates. (n≥3)

nisin was 0.27 h in the first 40 min, degradation slowed down afterwards to 403.7 h. Ramoplanin showed a similar behavior as nisin with a 2.1-fold increase of the OIC_{30}^{16h}. Most of this was degraded within the first 40 min as can be seen on the half-life times of 1.0 h and 44.4 h in the first 40 min and the following ~15 h, respectively.

This diphasic degradation pattern of nisin and ramoplanin hints towards an active degradation process when they first come in contact with MOPS minimal media. Due to the absence of bacteria during the incubation step, a biological degradation of these antibiotics is improbable. However, the degradation could be caused by the pH level of the medium or by a reaction of the antibiotics with a compound in the medium.

2.3.3. Inoculum effect of nisin

As shown in the previous section, time can have a significant effect on antibiotic activity through degradation. However, when an infection is left untreated and the pathogen is free to replicate, the additional time of growth can also have an effect on antibiotic susceptibility. The longer the infection is untreated, the higher is the cellular density of the pathogens. This can generate an inoculum effect as García et al. found that the concentration of disinfectant needed to effectively kill a bacterial culture increases with the density of the culture [124]. This dependency is caused by a reduced amount of disinfectant per cell at high cellular densities. Several cell envelope targeting antibiotics sequester lipid II cycle intermediates, which have to be blocked by approx. 50% for an inhibitory effect [3]. As such, an increase in cell number could dilute the available antibiotic to a point were less then 50% of lipid II cycle intermediates are blocked per cell at antibiotic concentrations, which are inhibitory to less dense cultures. As this makes

a similar inoculum effect possible for lipid carrier targeting antibiotics, the susceptibility towards the lipid II-binding antibiotic nisin was determined at different inoculum sizes. For this the IC_{30} of a *B. subtilis* culture was determined at different initial cellular densities.

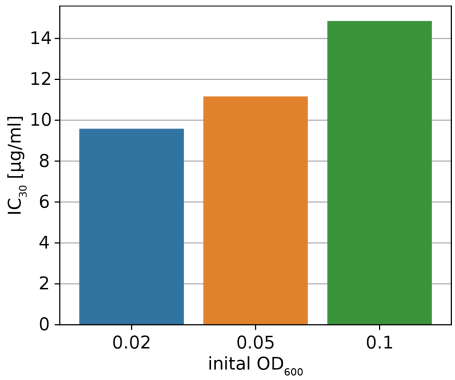

Figure 2.12.: Resistance towards nisin increases drastically at high cell densities. IC_{30} of cultures challenged with nisin at OD_{600} 0.02 to 0.1 measured after 5 h. The IC_{30} increases 1.5-fold from OD_{600} 0.02 to 0.1. (n=1)

Indeed, the IC_{30} 5 h after nisin challenge increased from 9.6 µg/ml at OD_{600} 0.02 to 14.9 µg/ml at OD_{600} 0.1. While further replicates are required for a reliable data set these results show a clear increase of the IC_{30} of about 1.5-fold with a 5-fold increase of inoculum size. As described by García et al. this is presumably not caused by antibiotic deactivation but a distribution of the antibiotic across a higher concentration of lipid carrier that would have to be sequestered for effective inhibition [124]. This indicates that biologically relevant changes in the availability of lipid carrier might affect the activity of antibiotics that target them. This is further investigated in the following section.

2.3.4. Lipid II deletion mutants and the effect on susceptibility

The mechanism of action of antibiotics targeting the lipid II cycle is generally to bind and sequester a lipid carrier to reduce the total substrate in the cycle and slow it down consequentially. We have found that the efficiency of an antibiotic to slow down the PG synthesis rate not only scales directly with the binding affinity to its target but also with the target pool size [3]. This means that the higher the portion of the targeted to the total lipid carrier pool the more efficient can the antibiotic block PG synthesis [3]. While the distribution of lipid carriers is fixed in unperturbed wild-type bacteria it can be modulated by addition of other antibiotics or the deletion of genes involved in the lipid II cycle. To examine this further, Hannah Piepenbreier modified the mathematical model of the lipid II cycle used in [3] to predict the antibiotic concentrations needed to

reduce PG synthesis by 50% dependent on a reduction of enzymatic function in UPP-dephosphorylation and transglycosylation (Figure 2.13; Hannah Piepenbreier, personal communication).

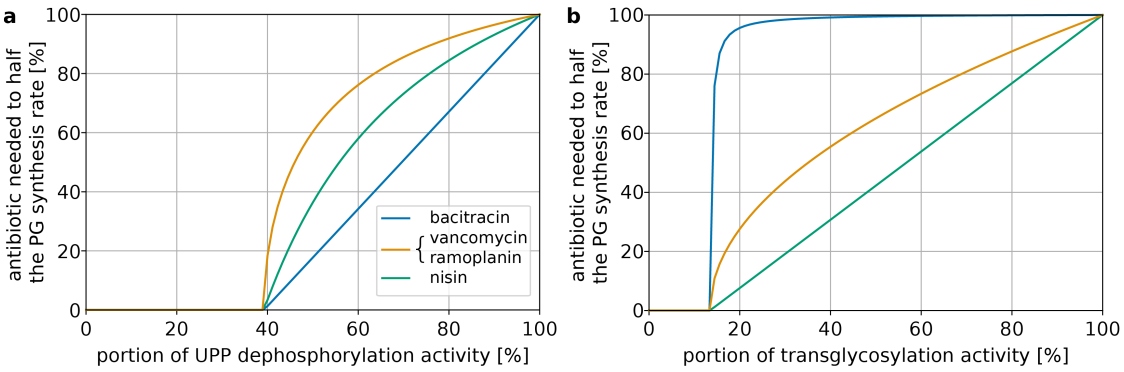

Figure 2.13.: Reduction of (a) UPP-dephosphorylation and (b) transglycosylation functions deferentially affect susceptibility towards PG synthesis targeting antibiotics according to the model. The relative reduction of antibiotic concentration needed to reduce PG synthesis by half is plotted against a reduction in enzymatic activity. Personal communication: Hannah Piepenbreier.

With this a reduction of UPP-dephosphorylation activity was predicted to mainly reduce the concentration needed of the UPP binding antibiotic bacitracin to critically inhibit PG synthesis (Figure 2.13a). The concentration needed for inhibition of PG synthesis of lipid II binding antibiotics, such as nisin, ramoplanin and vancomycin, was reduced to a lower extent. Furthermore, a reduction of dephosphorylation activity by more than 60% was predicted to be lethal without addition of antibiotics.

In contrast to this a reduction of transglycosylation activity was predicted to have a great effect on the activity of lipid II-binding antibiotics but to hardly impact bacitracin action (Figure 2.13b).

To verify these results in vivo a similar reduction of enzymatic activity was required. However, as antibiotics targeting the enzymes of UPP-dephosphorylation and transglycosylation are not too common a finely tuned reduction of enzymatic activity is much more complicated in vivo. Both, the UPP-dephosphorylation and transglycosylation functions are performed by redundant enzymes, which means that in case of inhibition of one enzyme another can fulfill this function at least partly. However, as these redundant enzymes are not mainly evolved to maintain this function a reduction in enzymatic activity is plausible. Therefore, strains carrying deletions of non-essential UPP-dephosphorylation and transglycosylation enzymes were tested for susceptibility towards bacitracin, vancomycin, ramoplanin and nisin.

One of the non-essential enzymes is BcrC, which catalyzes the dephosphorylation of UPP [26, 27]. In its absence or during cell envelope stress UppP is expressed and replaces/supports BcrC-activity [28]. As BcrC is the main UPP-phosphatase a Δ*bcrC* deletion strain should have a reduced UPP-dephosphorylation activity compared to the wild-type.

The transglycosylation function of *B. subtilis* is heavily redundant with 2 SEDS glycosylation proteins (RodA, FtsW) and 4 bifunctional PBPs [22, 23]. While the two SEDS proteins, which are assumed to function in the elongasome and divisome, are essential, the bifunctional PBPs are not [167]. As these are thought to mainly act in cell envelope repair [24] their deletion does not necessarily reduce the transglycosylation function in any substantial manner.

Of the four class A PBPs only a deletion of *ponA* has a noticeable effect on growth, as growth rate is decreased slightly and the morphology of colonies is changed [167]. Its gene product PBP1a/1b (*ponA*) has been found to predominantly localize at the septum [168]. PBP4 and PBP2c (gene products of *pbpD* and *pbpF*, respectively) localize at the septum to a lower extent and at randomly positioned foci at the lateral cell wall [168]. PBP2d (*pbpG*) is only expressed during sporulation [169].

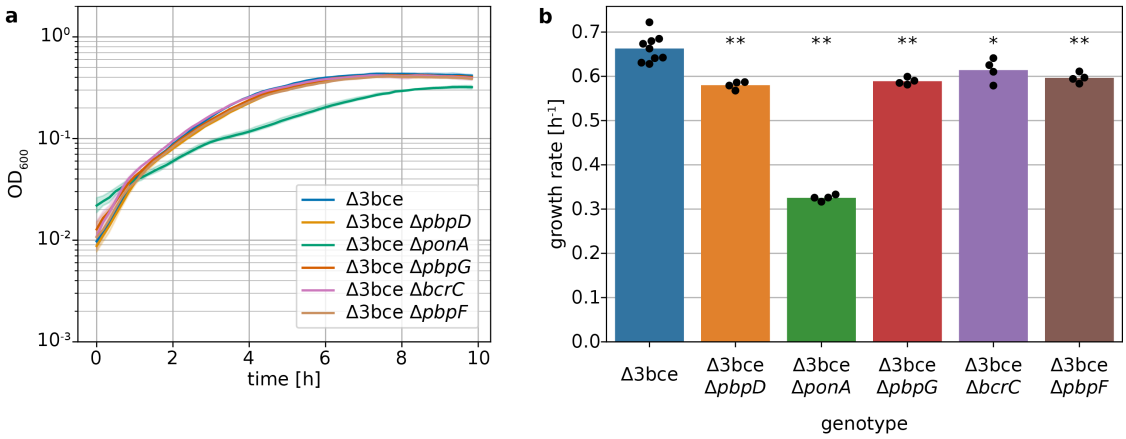

Figure 2.14.: Growth (a) and growth rates (b) of deletion mutants in cation-adjusted MHB media. Shaded areas depict 95% confidence intervals. Black dots show single replicates. Statistical significance was calculated in relation to the Δ3bce strain using two-sided unpaired t-tests (*: p<0.05, **: p<0.005). (n≥4)

To minimize the effect of stress response modules a *B. subtilis* strain that carried deletions of all bce-like modules was utilized. In this background (Δ3bce), *bcrC* or either of the four class A PBP genes was deleted. Deletion of most of these genes had little effect on growth (Figure 2.14a). Only a Δ*ponA* deletion resulted in a strong growth defect as has been described before in a wild type strain (Figure 2.14b) [167].

The susceptibility was determined via minimal inhibitory concentration (MIC) measurements in MHB. For this exponentially growing cultures were challenged with an antibiotic dilution series and growth (OD_{600}) was measured after 24 h. The antibiotic concentration leading to a growth reduction of ≥90% in comparison to no antibiotic was considered as the MIC similar to a traditional MIC measurement, where the absence of growth is determined by eye.

Laspartomycin C, which targets UP, was included in this assay as a control, since these deletions should have only a small effect on the UP pool size. First the MICs of all antibiotics used here were measured in the Δ3bce strain (Figure 2.15a). Subsequently, the MIC of other strains was compared to these values. The Δ*bcrC* deletion strain showed higher susceptibility towards bacitracin and nisin with a reduction of the MIC to 20% and 33% of the wild type level, respectively (Figure 2.15b). The MIC of vancomycin was also reduced to 75% although without being significant. The Δ*pbpD*, Δ*pbpF* and Δ*pbpG* strains did not show any significant changes in the MIC compared to the Δ3bce strain (Figure 2.15c-d). In contrast, the Δ*ponA* deletion strain behaved similarly as Δ*bcrC* with a decrease of the MICs of bacitracin and nisin to 32% and 25%, respectively (Figure 2.15f). Again, the MIC of vancomycin was also reduced to 75% without being statistically significant. In all strains the MIC of laspartomycin C was largely unchanged.

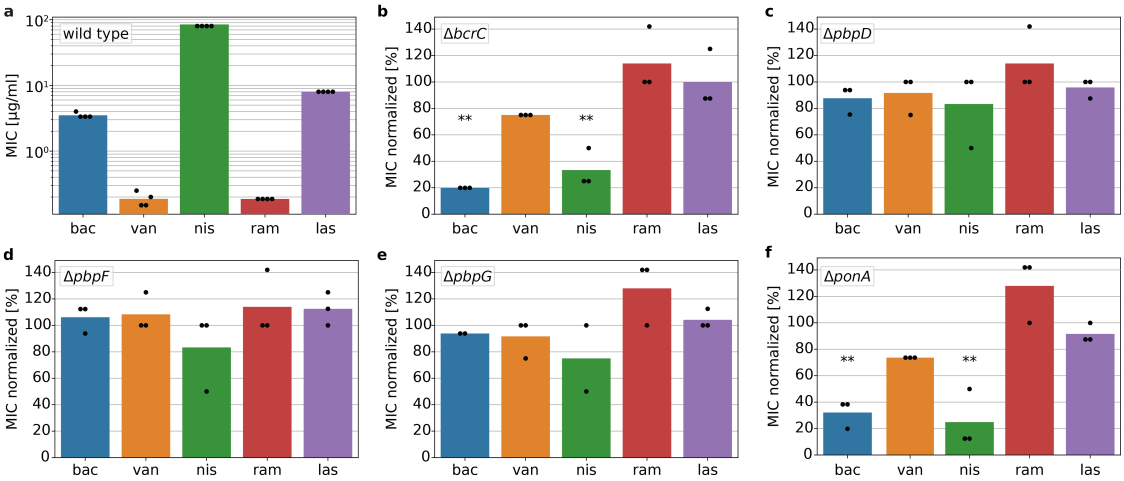

Figure 2.15.: MIC measurements of selected antibiotics in lipid II cycle pertubed *B. subtilis* deletion strains. (a) Measurements in the Δ3bce strain without lipid II cycle perturbation. Measurements of other strains are normalized to these values. (b) Δ*bcrC* strain. (c) Δ*pbpD* strain. (d) Δ*pbpF* strain. (e) Δ*pbpG* strain. (f) Δ*ponA* strain. Black dots show single replicates. Statistical significance was calculated in relation to the Δ3bce strain using two-sided unpaired t-tests (**: p<0.005). (n≥3)

As the MIC in the Δ*bcrC* strain is reduced to 20% of the MIC in the wild type, the reduction of UPP-dephosphorylation activity in the Δ*bcrC* strain can be estimated to around 50% with the help of the model (Figure 2.13a). With this, the model predicts a decrease in the MIC of nisin to around 40% and in the MICs of vancomycin and ramoplanin to around 65%. While our experimental data of nisin and vancomycin is in accordance with model prediction, ramoplanin does not seem to be affected. Overall, the mathematical model predicted the changes in susceptibility caused by a reduction of UPP-dephosphorylation activity quite well. The missing reduction in ramoplanin resistance could be due to precision errors of the relatively inaccurate MIC measurements due to long incubation times after antibiotic challenge.

The transglycosylation activity of the Δ*pbpD*, Δ*pbpF* and Δ*pbpG* strains seems not to be affected much, as no significant changes in the MICs are observed. This is not the case for Δ*ponA*. Judging by the 75% reduction of the nisin MIC compared to the wild type, the reduction of transglycosylation activity can be estimated with the model to around 35% in the Δ*ponA* deletion strain (Figure2.13b). With this a reduction in the MIC by 50% for vancomycin and ramoplanin and by 2% for bacitracin is predicted. However, this is not in accordance with the measured in vivo MICs. This might be a result of the specialized activity of *ponA*s gene product PBP1a/1b. While the model assumes a uniform reduction of transglycosylation activity, PBP1a/1b was described to fulfill a repairing function [24, 34] rather than cell growth. As such, a deletion of *ponA* would not necessarily lead to a reduction of transglycosylation activity at all.

2.3.5. Tunicamycin resistance

In 1986, Hashiguchi et al. found that overexpression of *tmrB* induces tunicamycin resistance in *B. subtilis* [170, 171]. Since then, TmrB has been identified as a hydrophilic protein with an amphiphilic α-helix and a Walker A ATP-binding pocket [48]. Later, tunicamycin was shown to directly bind TmrB and that tunicamycin resistance is also developed when *Bs-tmrB* in overexpressed in an otherwise tunicamycin-sensitive *E. coli* strain [172, 173]. More recently, the TmrB-homologue TmrD of *Deinococcus radiodurans* was crystallized revealing structural similarity to CPT of *Streptomyces venezuelae*, which confers resistance against the ribosome-targeting antibiotic chloramphenicol by phosphorylation [174]. As such, TmrB is the founding member of the tunicamycin-resistance protein family, which are thought to be kinases conferring resistance against tunicamycin [174].

So far, only overexpression of *tmrB* has been studied and it is unclear whether TmrB also protects *B. subtilis* from tunicamycin at wild type expression rates. To test this,

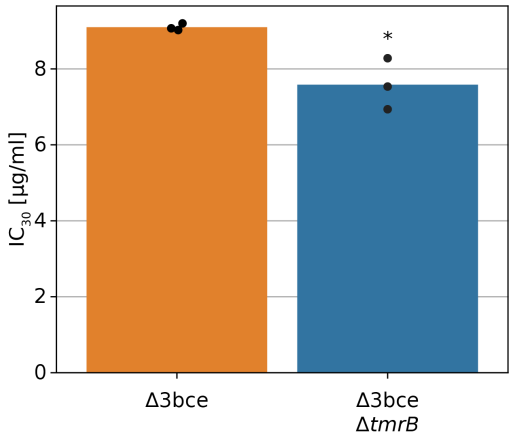

Figure 2.16.: TmrB confers only little resistance against tunicamycin. IC_{30} values were determined 5 h after antibiotic challenge in steady-state exponential growth. Black dots show single replicates. Statistical significance is depicted with * (Student's t-test: $p<0.05$, equal variance). (n=3)

tmrB was deleted in a *B. subtilis* background devoid of bce-like modules (Δ3bce) to prevent interactions of other resistance modules. Both strains (with and without *tmrB*) were challenged with tunicamycin at steady-state exponential growth and the IC_{30} was determined after 5 h (Figure 2.16).

Interestingly, the Δ*tmrB* strain is significantly less resistant than the wild type (Student's t-test: $p<0.05$, equal variance). However, the change of the IC_{30} was small with 7.6 to 9.1 µg/ml. Growth of both strains, also after tunicamycin challenge, was very similar (Figure S.4). As most other resistance modules confer a much higher resistance at wild type expression levels [57] it seems unlikely that protection against tunicamycin is the main function of *tmrB*. As tunicamycin resistance was only observed in *tmrB*-overexpressing strains [170, 171], the provided protection might rather be an off-target effect of TmrB.

3. Discussion

3.1. Active resistance determinants in *B. subtilis*

The development of active resistance mechanisms in clinical pathogens is one of the most pressing issues of our time. This section explores the resistance modules of the cell envelope stress response in *B. subtilis* and their potential evolutionary path. In this regard, the response of Bce-like modules to laspartomycin C are highlighted, as these modules are widespread in the Firmicutes phylum, which contains important clinical pathogens. Furthermore, the potential resistance determinant TmrB for tunicamycin is discussed.

3.1.1. Predisposed resistance against laspartomycin C

The calcium-dependent lipopeptide laspartomycin C is a novel antibiotic, that targets the lipid carrier UP. Here, we monitored the natural cell envelope stress response of *B. subtilis* after laspartomycin C challenge and compared it with the stress response induced by friulimicin B, which is also a calcium-dependent lipopeptide and targets the same lipid carrier. While friulimicin B was known to induce only the σ^M module [44], we found that laspartomycin C additionally activates the Lia and both of the Bce-like resistance modules tested here (BceRSAB and PsdRSAB).

As the activation of a resistance module in presence of an antibiotic is only the first step of functional resistance, we wondered whether these resistance modules also protect *B. subtilis* from damage caused by friulimicin B and laspartomycin C. For this, single and double deletion strains of either a target of the resistance module (*bcrC* and *liaIH* in case of σ^M and Lia, respectively) or the resistance determinants themselves (in case of Bce and Psd) were constructed. Interestingly, the susceptibility of all deletion strains towards both friulimicin B and laspartomycin C were identical to the wild type.

While the absence of protection conferred by the activated resistance modules is reassuring, we have to be mindful about a potential facilitated evolution of these modules to provide said protection. Bce-like resistance modules sense antibiotics with membrane-

bound targets such as the lipid carrier UPP (bacitracin) and SdpI (cannibalism toxins) [91, 111]. The antibiotic is recognized in complex with its target by specialized ABC-transporters (e.g. BceAB), which are able to sever this interaction [87, 109]. This separation is directly coupled with ATP hydrolysis, the energy of which is presumably used for antibiotic detachment [87, 109]. However, while ATP hydrolysis is needed for signal transduction, the effective removal of the antibiotic is not. This means, that while the signal transduction is flux-dependent, i.e. dependent on the activity of the transporter, a functional protection mechanism is not required. As such, a disparity between signaling, which only requires the binding of antibiotic-target complex by the transporter, and effective release of the target, which would lead to resistance and would require more specific kinetic properties of the transporter, is plausible.

The substrate-specificity of BceAB-like transporters is mainly determined by a large extracellular loop in the C-terminal region of the BceB-like protein [126]. As seen by the induction of both modules, these loops in BceB and PsdB are capable of recognizing laspartomycin C. While the detachment of laspartomycin C from its target is not functional so far, few amino acid substitutions in the large extracellular loop might change the kinetic properties of the BceAB-like transporters enough to allow effective laspartomycin C detachment. This suggests that the evolution of BceAB-like transporters to provided protection against laspartomycin C is facilitated if they are induced by it.

Bce-like modules are well researched in *B. subtilis* and are widespread in the Firmicutes phylum, which includes important pathogens such as *Staphylococcus aureus* and *Enterococcus faecalis* [106, 107]. Since the Bce-like modules in other Firmicutes species are similar to the ones in *B. subtilis*, they might also be able to recognize laspartomycin C and therefore facilitate the evolution of conferred resistance. Furthermore, other Bce-like modules might already be equipped to provide protection against laspartomycin C. As such, further development of this novel antibiotic as a medicinal drug candidate should explore modifications of the antibiotic to prevent the induction of Bce-like modules to avoid an increased risk of resistance. This is of particular interest as the phenomenon of induction without conferred resistance by Bce-like modules occurs also for other antibiotics like actagardine with PsdRSAB of *B. subtilis* [91]. As such, the risk of developing resistance against these antibiotics is similarly high.

Besides the Bce-like modules, the σ^M- and Lia-modules of *B. subtilis* were also induced by laspartomycin C. Since σ^M is essential in *B. subtilis*, we tested whether BcrC confers resistance against either of the two lipopeptide antibiotics as it is highly induced by friulimicin C [44] and catalyzes the dephosphorylation of UPP, which produces the

target of the two antibiotics - UP [63, 64]. While we found that BcrC does not provide protection against either laspartomycin C or friulimicin B, other members of the σ^M-regulon might do so.

In general, every induced resistance module could expand its regulon to entail proteins that provide protection against the antibiotic in question. In case of laspartomycin C, this might be an UP-flippase, that shuttles extracellular UP to the inner surface of the membrane. As this UP-flippase would reduce the accessible UP, laspartomycin C would need to be more highly concentrated to sequester enough lipid carrier to effectively slow down the lipid II cycle as illustrated for lipid II binding antibiotics [3]. However, this would require the existence of an UP-flippase, which has not been identified so far and the slow flipping rate of UP might rather indicate a passive flipping mechanism [3, 29].

While the cell envelope stress response of *B. subtilis* does not seem to be able to provide protection against the novel antibiotic laspartomycin C at this point its further evolution to acquire a working resistance mechanism seems to be on the horizon. An antibiotic that does not induce the cell envelope stress response modules despite targeting the lipid II cycle is tunicamycin. In the following section TmrB, a potential resistance determinant against tunicamycin, is discussed.

3.1.2. Tunicamycin resistance

TmrB is the founding member of a protein family termed tunicamycin-resistance, which are thought to be kinases conferring resistance against tunicamycin [174]. However, while TmrB overexpression has been shown to confer resistance against tunicamycin [170, 171] it has not been examined if TmrB also does so when expressed at natural levels.

Here, a *tmrB* deletion strain was shown to be significantly more susceptible ($p<0.05$) to tunicamycin than *tmrB* containing *B. subtilis* strain. Although the difference is significant, the IC_{30} in the deletion strain is with 16% only marginally lower than the IC_{30} of the strain containing *tmrB* (Figure 2.16). As most other resistance modules confer a much higher resistance (e.g. BceRSAB confers 50-fold resistance against bacitracin [57]) it seems implausible that the main function of *tmrB* is tunicamycin resistance under wild type conditions. As all previous experiments used overexpressed TmrB [170, 171] the observed tunicamycin resistance could be an off-target function of TmrB. As such, the main function of TmrB remains elusive. One possibility is that TmrB confers resistance against another antibiotic with structural similarities to tunicamycin. However, this remains to be tested.

3.2. Growth rate dependency of cell envelope targeting antibiotics

The location and stage (acute vs. chronic) of an infection can have great impact on the growth speed of a pathogen ranging from very rapid to very slow [146]. As such, knowledge about the effect of growth rate on susceptibility is vital for an optimal antibiotic treatment to ensure both a speedy recovery and minimal dosage to prevent further development of resistance. Recently a non-trivial dependency of susceptibility towards ribosome targeting antibiotics and growth rate has been uncovered [75]. However, although the growth rate dependent susceptibility towards β-lactam antibiotics has been examined a number of times [62, 145, 151, 152], all of these studies have (inadvertently or not) focused on tolerance rather than resistance [78].

In this work the growth rate dependent resistance of the gram-positive bacterium *B. subtilis* against a wide range of different cell envelope targeting antibiotics was examined. Measuring a dependency of growth rate provides the challenge that every technique to modify the growth rate of a culture can have secondary effects that might introduce artifacts. For instance, growth rate can be modulated via antibiotics, temperature, as well as quality (e.g. different carbon sources) and quantity (concentration) of nutrients. As the presence of one antibiotic can significantly change the susceptibility towards other antibiotics [175], their use as growth rate modulators is unsuitable for measuring antibiotic susceptibility. While the use of different growth temperatures is an easy-to-use method for growth-rate modulation, cell size has been reported to be almost independent of temperature [136]. As cell size and with it PG demand is assumed to be driving factors of a potential growth rate dependency of cell envelope targeting antibiotics, this technique was also unsuitable for our question at hand.

This leaves nutrient availability to control the growth rate of *B. subtilis*. To maximize growth rate in natural environments and to outcompete rivaling microorganisms, bacteria have evolved to utilize the most energy-rich nutrients first, independent of their concentration with e.g. the carbon catabolite repression system [176]. As such, when a medium provides a small amount of high-energy nutrient (e.g. glucose) and higher amounts of lower-energy nutrients (e.g. fructose), *B. subtilis* will not grow with an intermediate growth rate. Instead, *B. subtilis* will grow very quickly at first while utilizing glucose. Then growth will stop when glucose is depleted as the bacteria reorganize their metabolism to utilize fructose (diauxic shift) to subsequently resume growth with a reduced growth rate on fructose. In this process the culture looses its steady-state due to the diauxic shift and the remodeling of the metabolism. As such, in our assay all nutrients had to be supplied in excess to retain steady-state exponential growth throughout the measurement.

To further reduce artifacts through changing osmolarity, pH or nutrient quality as much as possible we decided to modulate growth rate in MOPS minimal media with changing concentrations of α-MG. As a glucose-analogue α-MG competes with the sugar for import and thereby decreases the intracellular glucose concentration and finally growth rate (Figure 2.1). To control for an influence of the α-MG concentration on susceptibility all experiments were repeated in the same media, but with fructose as the sole carbon source instead of glucose. Susceptibility was also measured in LB media, which differs widely in nutritional value and type, and is not controlled in osmolarity or pH, to see whether it follows the same trend as in heavily controlled media compositions.

Interestingly, only bacitracin showed a significant change in susceptibility in MOPS minimal media with changing growth rate (Figure 2.4). This same trend of decreasing susceptibility with faster growth continues in LB media (Figure 2.6). However, In contrast to ribosome targeting antibiotics this change seems rather small as Greulich et al. observed an increase by up to 500% in susceptibility [75], while the susceptibility towards bacitracin reduces by only 40% in slow growth compared to fast growth.

Both ampicillin and tunicamycin depicted a insignificant change in activity under changing growth rates (Figure 2.4c, d). Given the high standard deviation and similar trends in fructose supplemented MOPS media, in which α-MG has a smaller effect on growth rate, it appears to be an artifact created by α-MG addition. This might be caused by an increased osmolarity of the media with increased α-MG addition as both antibiotics induce cell lysis (Figure 2.2d) [62] and the increased osmotic pressure of the medium might have a stabilizing effect on ampicillin- and tunicamycin-damaged cells. Susceptibility of *B. subtilis* towards both antibiotics is very similar in MOPS and LB media (Figure 2.6a, f).

The susceptibility towards lipid II binding antibiotics (nisin, ramoplanin and vancomycin) as well as laspartomycin C remained unchanged over the entire range of growth rates tested in minimal MOPS media. However, *B. subtilis* displays a 1.8- to 3.3-fold increase in resistance against lipid II binding antibiotics and laspartomycin C from the fastest growth condition in MOPS media to LB (Figure 2.6c-e, g). This leads to the question whether the sudden increase of resistance in LB is caused by an increase in growth rate in combination with a non-continuous correlation of growth rate and susceptibility (e.g. opposing trends) or by growth rate independent changes in the media. While cell size is known to depend linearly on growth rate [177], the regulation of involved genes is too complex to easily deduce a type of correlation for susceptibility and growth rate. This can be facilitated with a mathematical model of the lipid II cycle that depicts changes in growth rate and will be discussed below.

Greulich et al. have studied the susceptibility of ribosome targeting antibiotics in dependency of growth rate using MOPS minimal media supplemented with either glucose or glycerol and amino acids to control growth rate [75]. A closer look reveals that while the growth rate dependency of each antibiotic is similar with both sugars, the trend curves of cultures grown in glucose-supplemented media display higher resistance than cultures grown in glycerol-supplemented media [75]. This indicates a dependence of susceptibility on the nutritional quality (e.g. type of supplemented sugar) in addition to growth rate. As the differences between MOPS media and LB are far greater than just the substitution of one sugar, the differences we see in the susceptibility might be entirely caused by the composition of the media and not the growth rate.

The sudden increase of resistance between MOPS media and LB might also be caused by an inconsistent dependence of susceptibility on growth rate. This inconsistency could be caused by opposing trends that might allow an unchanged resistance at slow growth rates (in MOPS media) but a higher capability of the PG synthesis machinery to withstand antibiotic attacks during fast growth (LB). If this was the case *B. subtilis* would be expected to also be more resistant to lipid II binding antibiotics and laspartomycin C in other media promoting a fast growth rate. To test this a range of faster growth rates should also be tested. For this, and to reduce further effects of media composition, the MOPS minimal media could be supplemented with a range of canonical amino acids to increase the overall growth rate. When glucose is used as the sole sugar in this modified media, a fine-tuning of growth rate should still be possible with addition of α-MG. Here, a continuous trend of susceptibility in MOPS media with and without amino acids would not necessarily be expected. However, both, a range of slower growth rates and a range of faster growth rates, would shed light on the dependency of susceptibility.

A strong dependency on growth rate such as seen for some ribosome targeting antibiotics could provide an advantage in the treatment of infections with extreme growth rates [75]. For example kanamycin, which is 6-fold more active in slow growth, could be very effective to clear slow-growing chronic infections. However, as e.g. other antibiotics display the opposite trend, medical personnel has to be mindful about which antibiotic to administer for each infection and stage of the infection as the pathogens growth rate might be subject to fluctuations. As medical personnel are overworked [178] the requirement of additional analysis of infections puts further strain on highly stressed workers.

The independence of cell envelope targeting antibiotics observed here suggests a similar independence in other gram-positive bacteria, including important pathogens such as *Staphylococcus aureus* and *Clostridium tetani*. This would facilitate the application

of cell envelope targeting antibiotics as a medicinal drug, since the growth rate of the pathogen does not have to considered for dosage. While susceptibility towards bacitracin is dependent on growth rate, its magnitude seems negligible.

3.2.1. Proposal of a growth rate dependent mathematical model of the lipid II cycle

The knowledge of growth rate dependencies is important for the optimal selection of antibiotics in clinical practice. A deeper understanding of the underlying principles could guide further development of clinical drugs to exploit arising bottlenecks in metabolic pathways. The processes involved in the adaptions to different growth rates are very complex as they encompass the required PG synthesis output, expression profiles of involved enzymes and the interaction between the antibiotic and its target. To aid our understanding of these processes and their interaction a mathematical model can be utilized. As a model of the lipid II cycle in *B. subtilis* already exists [3], this can be modified in the future to adjust for growth rate dependent changes.

Demand of cell wall material

To determine the demand of cell wall material in dependency of the growth rate three aspects have to be considered: (1) cell wall thickness, (2) cell surface, which is determined by cell size, and (3) growth rate itself as the entirety of one cell wall sacculus has to be produced within one doubling.

The membrane-wall ratio of *Bacillus megaterium* has been found to be fairly consistent over generation times of 23 to 86 min [179] indicating that the cell wall thickness is constant over different growth rates. As a close relative to *B. megaterium*, a change in cell wall thickness of *B. subtilis* in dependence of growth rate would not be expected.

Variations in the cell size of a bacterial cell as well as the cell's composition under different growth rates was extensively studied in diverse model organisms [136, 155, 179]. With this, a set of bacterial growth laws was developed, which describes the cell size expansion of faster growing cells compared to slower growing ones. These describe growth rate-dependent adaptations in the growth-related processes as DNA replication and protein biosynthesis [138, 147, 180, 181]. Consequently, the process of cell wall synthesis has to follow similar growth rate-dependent variations to adapt the production of the cell wall to the expanded cell size of faster growing cells. Since the cell wall surrounds the whole bacterial cell, the growth rate-dependent variations in cell surface area should determine the demand of peptidoglycan – the major component of the bacterial cell wall – under different growth rates.

In fact, it was shown for *E. coli* that variations in the cell surface area by a factor of ~2.3 within doubling times of 25 to 190 min implicate a 2.2-fold difference in the amount of PG per cell comparing the fastest and the slowest generation time [182]. To estimate the PG amount in *B. subtilis* in the growth conditions used here the cells dimensions should be measured under a microscope and used to calculate the surface area. As variations in the cell area implicate a similar variation in the PG amount per cell an average PG amount per cell can be estimated for every growth condition.

Finally, balanced growth requires the production of one equivalent of a cell envelope during one doubling time as each daughter cell needs to have a complete cell wall after division. With the PG amount per cell and the growth rate the required PG synthesis rate can be determined. This means, that in fast growth the required PG synthesis rate increases due to two processes: (1) Bigger cells have higher surface areas and therefore require more PG molecules per cell and (2) the doubling time shortens which leaves less time to synthesize the equivalent of one cell envelope.

Adaptions to expression profiles

While fast-growing bacteria are expected to require a high PG synthesis rate, slow-growing bacteria need to preserve energy. As such the rate of PG synthesis needs to be closely regulated to match the demand.

As the lipid II cycle is made up of individual enzymatic reactions each one needs to be regulated. The rate of an enzymatic reaction depends on the biochemical properties of the enzyme as well as the availability of substrates and the abundance of enzymes according to Michaelis-Menten kinetics. The biochemical properties of the involved enzymes are fixed as they are always transcribed from the same genes. The substrates are produced through enzymatic activity so that their availability scales directly with the enzyme abundance. This leaves the abundance of enzymes as a parameter for PG synthesis rate that can be modulated through differential gene expression.

As described in section 1.5.4 in more detail, the production of proteins changes in dependency of growth rate. While the concentration of constitutively expressed proteins decreases in faster growth, regulated expression of proteins can drastically change this behavior. As the expression of enzymes involved in the lipid II cycle is highly regulated [28, 93, 140, 183, 184], modeling this aspect would require detailed insights into these mechanisms. Instead transcriptomic and proteomic data from previous studies can be used to determine the abundances of relevant proteins. However, the proteomic data

available does not provide the abundances of all enzymes involved in the lipid II cycle [147, 185]. Fortunately, the mRNA-abundance of all relevant enzymes for PG synthesis has been measured [140]. As such, translation of these mRNAs could be modeled and compared with available proteomic data. With this approach an approximate enzyme abundance can be determined, which can be used in turn to establish lipid carrier abundances.

Taken together, a mathematical model of the lipid II cycle that incorporates growth rate dependent changes could illustrate how *B. subtilis* meets the increased demand of peptidoglycan. This could help to understand why susceptibility only to bacitracin and not to any other cell wall targeting antibiotics is growth rate dependent.

3.3. Effect of amino acids

During the course of this work selected amino acids were examined for their effect on *B. subtilis* growth. As bacteria can cease energy-intensive amino acid synthesis when they are supplied, faster growth was expected in their presence. Interestingly, while the combined addition of arginine, histidine, methionine, proline and threonine lead to an 1.8-fold increase of growth rate only arginine significantly increased growth rate when added separately and that even to a lower extent (Figure 2.8a). While most other amino acids did not generate a significant effect on growth, histidine even decreased growth rate 1.2-fold. Therefore, the growth rate increase of each amino acid separately cannot explain the effect generated by all of them combined. As such the fast growth is rather a collective effect. Since amino acids are mostly used in translation, which requires the availability of all amino acids, it is comprehensible that the presence of a single amino acid might have little impact.

The diverging effect on growth rates when different amino acids are supplied is quite enigmatic. They might arise from the energy needed to produce them in sufficient amounts for translation. However, in *B. subtilis* the average energy cost per amino acid correlates almost linearly with the frequency that this amino acid is used in proteins [186]. This means that relatively cheap amino acids are much more commonly used than energetically expensive amino acids. Therefore, the overall energy that can be saved by extracellularly available amino acids should be relatively similar for both energetically cheap and expensive amino acids.

Another possibility is that some of the amino acids used here can be catabolized while others cannot. However, to my knowledge the only amino acid used here that cannot be catabolized by *B. subtilis* is threonine [187–190], which generates similar responses as the other amino acids.

The differences we see might also arise from the cells ability to repress the respective biosynthesis machinery. When amino acids are supplied in the media *E. coli* has been shown to downregulate the respective biosynthesis pathways [158]. In *B. subtilis* the addition of canonical amino acids (CAA) induced a 30-fold reduction in the arginine biosynthesis genes, however other amino acid biosynthesis pathways (e.g. methionine, threonine and histidine) were less effected [191].

Additionally to the differences in growth a strong repression of the stationary phase stress response by the five amino acid mix and methionine alone was observed. This stress response has been found to be induced by cannibalism toxins that are produced by a subpopulation of *B. subtilis* in order to gain access to more nutrients and delay sporulation [90, 111, 164]. The non-producing subpopulation does not express specific resistance determinants and are damaged by the cannibalism toxins. As these target the cell envelope an induction of CESR modules can be observed [111].

Possible causes of the observed elimination of the stationary phase stress response in the presence of methionine are (1) a higher intrinsic resistance to cell wall stress and therefore antibiotics targeting the cell envelope, (2) inhibition of Lia induction or (3) inhibition of cannibalism toxins synthesis.

As the activity of other cell envelope targeting antibiotics is not affected significantly in the presence of different amino acids (Figure 2.9a), it is unlikely that *B. subtilis* possess a higher intrinsic passive resistance against these types of antibiotics. However, it is to note that the antibiotics tested here mainly target PG synthesis, while cannibalism toxins- like YydF - predominantly disturb membrane integrity [166]. As such, the induced changes might be more specific to the membrane and reduce YydF activity more prominently.

The same antibiotics were used to observe Lia induction. As with susceptibility, no significant changes of Lia induction were observed with different amino acids supplemented (Figure 2.9b). This negates a reduced capability of the Lia module to be activated in presence of the tested amino acids.

This leaves a potential inhibition of cannibalism toxin synthesis by methionine to be explored. While this was not tested here, a *yydF* reporter strain (P_{yydF}) growing in media supplemented with different amino acids could shed light on the activation of cannibalism toxin synthesis in these conditions.

Spo0A and with it sporulation and synthesis of cannibalism toxins has been found to be repressed by excess glucose in protein-rich media [164, 192]. As such a repression of Spo0A in protein-poor media containing glucose with the addition of amino acids makes sense. However, it remains elusive why methionine might have an effect while the other amino acids tested here do not. Given that Spo0A activity is repressed when

both glucose and amino acids are present, supplement of both sugars and amino acids might have a repressing effect on Spo0A. Since *B. subtilis* can use methionine as the sole sulfur source for growth [193] its addition might reduce Spo0A induction. However, as the stationary phase stress response is also induced in MCSE media, which contains 25.47 mM SO_4^{2-} [111] an addition of 3.35 mM methionine would not be expected to alleviate sulfur shortage in a MOPS minimal media background containing 2.86 mM SO_4^{2-} [194]. In any case, it would be interesting to see if methionine does indeed repress YydF synthesis and if it has a similar effect on sporulation.

3.4. Origin of regrowth-dominated inhibition pattern

Most of the antibiotics used in this work display a regrowth dominated inhibition pattern (Section 2.2.2). Here, not fully perturbed bacterial cultures first exhibit a concentration dependent lag period, before growing normally with the same growth rate as an unperturbed culture. This is the case for ampicillin and the lipid II binding antibiotics (section 2.2.2). Laspartomycin C and friulimicin B induce both a concentration dependent lag period and growth rate reduction.

All of these antibiotics (ampicillin excluded) target the lipid II cycle and are therefore expected to induce the same ultimate damage, which is the reduction of PG synthesis. As such the induced growth kinetics would be expected to be similar as well. The differences we see here might reflect general differences on how they affect PG synthesis or originate from moonlighting effects on other pathways. For instance, tunicamycin, which induces a rapid lysis event after ~5 doublings of unperturbed growth, has been shown to also bind TagO, a homolog of MraY involved in wall teichoic acid synthesis [8]. Furthermore, its inhibition of an enzyme rather than a lipid carrier as the other antibiotics used here might affect inhibition kinetics.

More general mechanistic origins should not be disregarded. If the antibiotics used here were quickly deteriorating, antibiotic concentrations would lose activity and cease to inhibit bacterial growth. As higher antibiotic concentrations would need longer until they fall below inhibitory concentrations the observed lag-phase would be concentration dependent. This would result in inhibitory patterns similar to the ones we observe. For this reason, the bacteria-independent degradation of some of the antibiotics used throughout this work was investigated.

Here, nisin and ramoplanin showed an interesting degradation pattern with a short half-life time of 0.27 h^{-1} and 1.0 h^{-1} in the first 40 min, respectively (Figure 2.11). Both antibiotics were much more stable in the following ~15 h with half-life times of 403.7 h^{-1} and 44.4 h^{-1}, respectively. This diphasic degradation hints towards an active degrada-

tion process when they first come in contact with MOPS minimal media. As no bacterial culture is present during the incubation step, an antibiotic degrading resistance module of the bacteria is improbable. While the initial pH of MOPS minimal media is neutral and nisin has been described to be more stable in acidic conditions [195] a pH induced degradation is unlikely, as the buffering capacity of the media would not allow such a drastic drop of the pH that degradation could cease. If the pH was driving antibiotic degradation it would not do so at two different rates. Another possibility is that a component of the MOPS minimal media reacts with the antibiotics. However, no component seems to have fitting chemical properties or is present in reasonable concentrations.

It is to note that bacitracin, which does not induce regrowth, has a more homogeneous degradation than ramoplanin and nisin, which display a regrowth dominated inhibition pattern. However, the degradation of all antibiotic was relatively low for the majority of the experiment with half-life times exceeding the the duration of the measurements. This cannot explain the regrowth after long lag phases as observed in Figure 2.2, S.1. While half-life times of nisin and ramoplanin are in the correct range within the first 40 min, they can only explain the regrowth within that same time frame.

Another possible origin of the regrowth-dominated inhibition pattern might lie in the experimental setup used in this work. In IC assays it is vital that all cultures are in a similar growth phase. However, unperturbed cultures reach stationary phase relatively quickly. As these were used as a control and normalized against, the IC measurements were taken during mid-exponential phase of the control to prevent a bias or artifact. If the IC measurement is taken too soon after antibiotic challenge little differentiation has occurred between antibiotic concentrations. To allow for an optimal timing between antibiotic challenge, IC measurement, and stationary phase, a long exponential growth is vital. To achieve this, bacterial densities close to the lower sensitivity of the plate reader devices were chosen.

While this was necessary to achieve precise and unbiased IC measurements it might have created a contorted view of the inhibition pattern generated by many of the antibiotics used here. Since the bacterial density is close to the lower sensitivity threshold of the plate reader a further reduction by e.g. lysis would not necessarily be visible (Figure 3.1). This means that a maintained low OD_{600} could be generated by both a lag phase as well as lysis.

Of the antibiotics used here ampicillin, nisin and vancomycin are described to have a bactericidal effect, which would lead to a decrease of bacterial density below the lower sensitivity threshold after antibiotic challenge [62, 196, 197]. As not the entire culture is killed the surviving bacteria are able to regrow. The duration until surviving bacteria have reached measurable densities would increase with antibiotic concentrations as

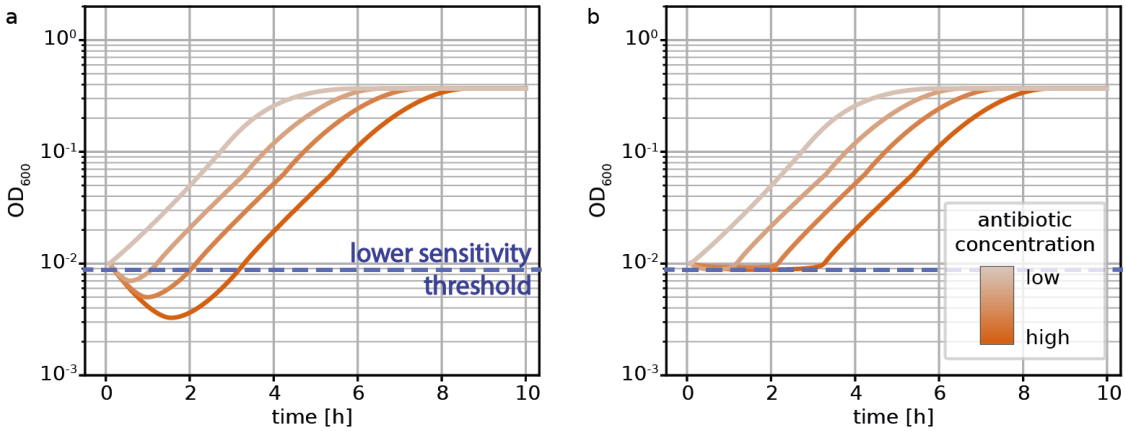

Figure 3.1.: Model of the potential impact of a loss of inital bacterial density close to the sensitivity threshold. (a) True growth curves of a bacterial culture challenged with a bactericidal antibiotic at a low density close to the lower sensitivity threshold (blue) of the used device. (b) Measured growth curve of the same culture shown in (a).

these would lead to fewer surviving cells.

The last antibiotic in this work displaying a purely regrowth-dominated inhibition pattern is ramoplanin, which is described to only show bactericidal effect at high concentrations. While its MIC has been measured at 2 µg/ml in *Staphylococcus aureus*, the minimal bactericidal concentration was determined at 4 µg/ml in the same study [50]. Ramoplanin concentrations used in the present work did not exceed 3 µg/ml and the MIC was measured here as 0.19 µg/ml in *B. subtilis*. As such it is difficult to discern to which extend ramoplanin exhibits bactericidal activity in our experiments.

To my knowledge laspartomycin C, which generates a mixed inhibition pattern with both a lag phase and growth rate reduction, has not been tested on its bactericidal activity so far.

The type of antibiotic activity of bacitracin is controversial as it has been described as entirely bacteriostatic [198] as well as bactericidal at high concentrations [199]. With this, the effect of bactericidal activity on inhibition patters is difficult to determine. However, as bacitracin generates a purely growth rate reducing inhibition pattern a strong bactericidal effect of bacitracin seems unlikely.

With the current information the origin of the regrowth dominated inhibition pattern cannot be fully elucidated. While degradation rates of nisin and ramoplanin seem to be sufficiently high to generate the observed inhibition pattern at the beginning of the measurements, it quickly slows down to half-life times that do not support the hypothesis.

While it is possible that cell lysis has been misidentified as a lag phase, the classification of antibiotics as bacteriostatic and bacteriocidal is often controversial or has

not been investigated so far. As of yet tangible evidence for this hypothesis is lacking. However, experiments could easily be performed by repeating the IC measurements but increasing the initial cell density at antibiotic challenge. The higher initial concentration would allow the measurement of a reducing optical density directly following the antibiotic challenge. If a lysis event occurs the regrowth-dominated inhibition pattern was indeed caused by a bacteriocidal effect of antibiotics.

3.5. Impact of antibiotic degradation on susceptibility as measured here

In most assays conducted in this work the susceptibility of cultures is compared at the same time after antibiotic challenge, which ultimately led to the same amount of degradation in all samples and did not cause a bias. Only in assays examining growth rate-dependent susceptibility the IC is measured after varying times (section 2.2). Here, a high degradation rate could lead to reduced active antibiotic concentrations during slow-growth. However, as the period with a high degradation rate is short (and might be overestimated with 40 min as there was no measurement between 10 and 40 min) its impact on the different growth conditions is relatively similar. Furthermore, as long half-life times apply for the majority of the experiment a degradation-dependent bias is not probable.

3.6. Lipid II deletion mutants and the effect on susceptibility

Based on the mathematical model of the lipid II cycle published in [3], Hannah Piepenbreier has predicted to which extent a reduction in enzymatic activity within the lipid II cycle would effect the susceptibility towards lipid carrier targeting antibiotics. This work focuses on the transglycosylation activity that inserts new PG building blocks into growing PG strands and the dephosphorylation of UPP, which is important for lipid carrier recycling.

Here, a reduction in UPP-dephosphorylation activity was predicted to have a stronger effect on bacitracin susceptibility than it has on vancomycin, ramoplanin or nisin activity (Figure 2.13a). This is mainly caused by the increased portion of lipid carrier molecules that are present as UPP. Therefore, UPP binding by bacitracin and further reduction of UPP-dephosphorylation is facilitated. However, as UPP entails over 75% of the total lipid carrier molecules in the cycle a further increase easily absorbs a large proportion of the other pools [3]. This can quickly slow down the whole lipid II cycle and therefore facilitate inhibition by lipid II-targeting antibiotics.

Experimentally, the UPP-dephosphorylation activity was reduced via a *bcrC* deletion strain, as BcrC is the main enzyme executing this activity [26–28]. While UppP and YodM can also dephosphorylate UPP, a lower reaction rate was expected. Susceptibility of this deletion strain was compared with a strain expressing *bcrC* (Figure 2.15b). The MIC of bacitracin was reduced by 80% in the deletion strain while the MIC of nisin and vancomycin were reduced by 67% and 25%, respectively. However, susceptibility towards ramoplanin was unchanged. This fits quite nicely with the mathematical model, as the greatest reduction in resistance was predicted to occur towards bacitracin followed by nisin and finally vancomycin and ramoplanin. The missing reduction in ramoplanin resistance in the *bcrC* deletion strain could be due to precision errors of the relatively inaccurate MIC measurements due to the long incubation times.

When considering the model prediction for a reduced transglycosylation activity, the resistance towards lipid II binding antibiotics is much more affected by a reduction of enzyme activity than bacitracin (Figure 2.13b). This is caused by an increase of the lipid II pool that facilitates binding of vancomycin, ramoplanin and nisin as transglycosylating enzymes utilize lipid II as a substrate. As the pool size of lipid II in unperturbed bacterial growth is very small, a several-fold increase has only little effect on the total distribution of lipid carrier. Therefore, the PG synthesis rate and with it antibiotics that do not target lipid II are less affected by a reduction of transglycosylation activity.

Even though nisin, vancomycin and ramoplanin have the same target, nisin is much more affected by a reduction in enzymatic activity (Figure 2.13). This is likely caused by the binding-mode of the antibiotics, since nisin binds lipid II as a monomer while ramoplanin and vancomycin do so in a cooperative manner [129, 200].

An in vivo reduction of the transglycosylation activity was more complicated than the reduction of UPP-dephosphorylation activity as there are six known proteins catalyzing this step. While the two SEDS proteins are essential for growth, the class A PBPs are not. Similar to *bcrC* above, the respective genes were deleted to investigate a reduction of transglycosylation function. The deletion of either PBP4 (*pbpD*), PBP2c (*pbpF*) or PBP2d (*pbpG*) had no significant influence on the susceptibility towards any of the antibiotics tested here (Figure 2.13c-e). However, a PBP1a/1b (*ponA*) deletion reduced the MIC towards nisin and vancomycin by 75% and 25%, respectively. Interestingly, the MIC of bacitracin also decreased by 68% while the measured ramoplanin MIC even increased by 30%. As a reduced transglycosylation activity was predicted to lower the resistance towards all lipid II binding antibiotics but hardly affect bacitracin susceptibility these results do not match the model.

The large discrepancy between the model predictions and the MIC measurements of the Δ*ponA* strain might be a result of the specialized activity of the gene product

PBP1a/1b. While the model assumes that the transglycosylation function is reduced to the same extent across the cell and for all enzymes, this is not necessarily the case in vivo. PBP1a/1b is believed to mainly execute repairs at thin patches of the cell envelope and to play only a minor role in the divisome [24, 34]. Therefore, in its absence the lipid carrier pool size distribution might not be changed significantly. However, a challenge with antibiotics used here is likely to produce thin patches in the cell envelope that would normally be repaired by PBP1a/1b resulting in higher susceptibility without altering lipid carrier pool size distributions.

The well predicted reduction of MICs in the *bcrC* deletion strain indicates that a reduction in UPP-dephosphorylation activity and the entailed redistribution of lipid carrier pools might have a significant effect on antibiotics targeting the lipid II cycle. However, none of the other strains tested here corroborate this, which is presumably caused by the selection of tested enzymes. When comparing the number of enzymes involved in UPP-dephosphorylation (3) and transglycosylation (6) it becomes apparent that the latter is much more redundant in *B. subtilis*. Furthermore, BcrC is considered the main acting enzyme for its catalysis while the PBPs tested here perform less systemic functions. As such, a deletion of *pbpD*, *pbpF* or *pbpG* is likely not having any substantial effect on the overall transglycosylation activity in the cell and cannot be used to answer the question at hand.

Slight adjustments to the assay could greatly improve the data quality and lead to less ambiguous results. These adjustments mainly include a more precise assay such as IC measurements and a more refined selection of transglycosylating enzymes. For the latter the SEDS enzymes RodA and FtsW seem a good choice. While they are essential, which prohibits a deletion approach as used here, an induced inhibition strategy (e.g. with CRISPRi) would be feasible.

In conclusion, the research presented here has given an insight into the complex interplay of enzymes and substrates within the lipid II cycle and antibiotics targeting them. As a reduction in enzyme activity can also be mediated by antibiotics these findings reinforce the idea that a combinatorial administration of antibiotics targeting the lipid II cycle can lower the overall antibiotic concentration needed for an effective inhibitory effect. Pursuing this project with the adaptions mentioned here to the experimental setup can further our knowledge in the inner workings of the lipid II cycle and inform research into the development of lipid II cycle targeting antibiotics as clinical drugs.

4. Conclusion

By analyzing the susceptibility of the gram-positive bacterium *B. subtilis* towards a vast range of cell envelope targeting antibiotics, this thesis has shown a remarkable independence of antibiotic activity on environmental conditions.

The first project focused on the cell envelope stress response triggered by the novel antibiotic laspartomycin C. Interestingly, while it induced all CESR modules of *B. subtilis*, none of them were able to provide any resistance. The absence of conferred resistance appears promising for laspartomycin C's further development as a clinical drug. However, the triggered stress response might indicate a facilitated evolution of the induced resistance modules to provide protection against this novel antibiotic.

The very similar antibiotic friulimicin B, which also targets the lipid carrier UP, only triggers the σ^M module. As such, a comparative biochemical analysis of the antibiotics in combination with the resistance modules in question might shed light on the specific interactions that allow the sensing of laspartomycin C, while friulimicin B goes undetected.

The required peptidoglycan synthesis rate is expected to fluctuate to a high degree between slow and fast growth conditions as the size of the cell and with it the cell envelope increases at high growth rates. As such, the peptidoglycan synthesis needs to be heavily regulated, which could lead to shifting bottlenecks in different conditions and might heavily affect the activity of cell envelope targeting antibiotics. In this work, the susceptibility of *B. subtilis* towards cell envelope targeting antibiotics was found to be remarkably independent of the growth rate.

This poses the question how the regulation of the cell wall synthesis is organized to create such a highly stable pathway. Extending the previously published mathematical model of the lipid II cycle of *B. subtilis* [3] to adjust for growth rate and the entailed changes to the cell wall could reveal the required changes to the synthesis apparatus. Understanding this regulation could uncover why the activity of most cell envelope targeting antibiotics are not subject to growth rate dependent changes while bacitracin activity increases to a small extend in slow growth. Furthermore, this research might reveal if small changes to bacitracins biochemical properties could intensify this dependency as a new tool to fight chronic bacterial infections.

5. Materials and methods

Strains and growth conditions

Bacillus subtilis was routinely grown at 37°C with agitation (220-250 rpm) in the same media as was later used for assays. Solid media additionally contained 1.5% (w/v) Difco™ agar. In selective media chloramphenicol (5 µg/mL), tetracycline (12.5 µg/mL) or kanamycin (5 µg/mL) were added.

Table 5.1.: Strains used in this work. All strains were based on *B. subtilis* W168. Δ3bce: Δ*bceRSAB** Δ(*yxdJKLM yxeA*)* Δ*psdRSAB**. * signifies a clean deletion.

strain	genotype	constructed by/reference
W168	trpC2	Laboratory stock
GFB0020	Δ3bce sacA::pBsC3lux (P_{liaI}-lux)	Annika Thorhauer
GFB0088	Δ3bce *tmrB*::spec	Annika Thorhauer
TMB1518	Δ3bce	[201]
TMB423	P_{bcrC}-lux	[27]
TMB1617	P_{liaI}-lux	[27]
TMB1619	P_{bceA}-lux	[27]
TMB2120	P_{psdA}-lux	[111]
TMB3410	*bcrC*::kan	[27]
TMB1151	Δ*liaIH**	[27]
TMB1461	Δ*bceRSAB**	[43]
TMB1466	Δ*psdRSAB**	Intermediate strain to produce TMB1518 [201]
TMB2127	Δ*liaIH bceAB*::kan	[27]
TMB2128	Δ*liaIH bcrC*::tet	[27]
TMB1629	*bceAB*::kan *bcrC*::tet P_{liaI}-lux	Carolin Höfler
BKK31490	*pbpD*::kan trpC2	[202]
BKK10110	*pbpF*::kan trpC2	[202]
BKK37510	*pbpG*::kan trpC2	[202]
BKK22320	*ponA*::kan trpC2	[202]
GFB0154	Δ3bce *bcrC*::kan sacA::pBsC3lux (P_{liaI}-lux)	Angelika Diehl
GFB0155	Δ3bce *pbpF*::kan sacA::pBsC3lux (P_{liaI}-lux)	Angelika Diehl
GFB0156	Δ3bce *pbpG*::kan sacA::pBsC3lux (P_{liaI}-lux)	Angelika Diehl
GFB0157	Δ3bce *ponA*::kan sacA::pBsC3lux (P_{liaI}-lux)	Angelika Diehl
GFB0158	Δ3bce *pbpD*::kan sacA::pBsC3lux (P_{liaI}-lux)	Angelika Diehl

Media

LB ((1% (w/v) tryptone, 0.5% (w/v) yeast extract, 1% (w/v) NaCl) and Mueller Hinton Broth (Sigma, 70192, prepared as instructed) were autoclaved before usage. MOPS buffered minimal media was prepared as described [194]. Tryptophan was added at 0.05% (w/v) due to auxotrophy of the strains. Either glucose (1.8-2.3% (w/v)) or fructose (2% (w/v)) were use as carbon sources. Growth rate-reduction was achieved by addition of Methyl α-D-glucopyranoside (Sigma, 60940). If amino acids were used they were concentrated at 0.05% (w/v) (histidine, methionine, proline, threonine) or 0.2% (w/v) (arginine).

IC measurements

To measure the susceptibility exponentially growing cells in steady-state were used. For this a single colony was picked from a plate and grown in the respective media overnight with selection. All cultures were inoculated very weakly as to prevent reaching stationary phase in the morning as to ensure true steady-state exponential growth. In the morning these cultures were then diluted 1:1000 in prewarmed rich media or 1:100/to OD_{600} 0.05 in prewarmed minimal media. When these cultures reached an OD_{600} of about 0.5 they were diluted in fresh, prewarmed media to OD_{600} 0.005 (or 0.05 in the victor^2 (plate reader) due to a high detection limit). These were then aliquoted in a 96-well plate with 200 µl per well and 10 µl antibiotic dilution was added per well to achieve the desired concentration. After antibiotic challenge the measurement was started without delay. Growth (OD_{600}) and luminescence were measured every 10 min for 10-48 h, dependent on the project. Cultures were agitated between measurements (table 5.2). If the plate reader allowed a lid it was used, if not the spaces in between the wells were filled with water.

Table 5.2.: Plate readers used in this work. Shaking times were set to the maximum possible.

device	manufacturer	shaking mode	speed
victor^2	Perkin Elmer, US	2 mm, linear	normal
SPECTROstar Nano	BMG Labtech, Germany	double orbital	700 rpm
FLUOstar Omega	BMG Labtech, Germany	corner well meandering	300 rpm
CLARIOstar	BMG Labtech, Germany	corner well meandering	300 rpm

Degradation measurements

Antibiotic degradation was measured in similar assays as ICs. A bacterial culture that was used at various times to fill the well plate was kept in steady-state exponential growth at 37°C and 220 rpm throughout the experiment. This culture was repeatedly used to inoculate MOPS media in the well plate that contained antibiotic.

First, the entire well plate was first filled with 100 µl MOPS media per well. Subsequently, antibiotic dilution was added to every well. For the first run, the bacterial solution (100 µl, OD_{600} 0.01) was only added in one set of wells per antibiotic. The measurement was started and left running as described above. After a certain incubation time had passed another set of wells per antibiotic was filled with bacterial solution (100 µl, OD_{600} 0.01) and the measurement was restarted. This way the antibiotic in not yet inoculated wells had time to degrade in the absence of bacteria.

The observed inhibitory concentration reducing growth to 30% of growth of an unperturbed culture (OIC_{30}), was measured 5 h after inoculation similar to the IC measurements.

MIC measurements

Overnight cultures in MHB were diluted 1:1000 and further incubated for growth at 37°C and 220 rpm for 3 h. Cultures were then diluted to OD_{600} 0.005, dispensed with 200 µl per well in a 96-well plate and challenged with antibiotic dilution series. The plate was covered with breathable membrane and incubate at 37°C and 1000 rpm in a well plate shaker-thermostat (PST-60HL-4, Biosan, Latvia). The OD_{600} was measured in a plate reader (victor^2) after 24 h. The lowest antibiotic concentration leading to less than 10% of unperturbed growth was determined as the MIC.

Data processing

All data was processed with python scripts (V3.8).

OD_{600} of cultures was background corrected by subtracting OD_{600} values of sterile media of the same type. Growth and luminescence data was smoothed with a median filter over a window size of 3. Luminescence data is normalized by its corresponding OD_{600} values. Growth rates are determined between the timepoints of first reaching OD_{600} 0.05 and 0.2. To detect susceptibility the inhibitory antibiotic concentrations leading to a reduction in growth to 50% (IC_{50}) were determined at a specific timepoint during mid-exponential phase. This timepoint should be late enough to allow easy differentiation of the strength of antibiotic inhibition but before the control culture reaches

stationary phase as this leads to artifacts. After extraction of OD_{600} values of a given replicate all were normalized by the growth of the unperturbed culture. The antibiotic concentrations inhibiting growth to just more and just less then 50% of the control were fit linearly to estimate the concentration inhibiting the culture to exactly 50%.

In some cases the IC_{30} was determined, which represents the antibiotic concentration reducing growth to 30%. IC_{30} and IC_{50} differ only marginally as the IC_{50} is slightly higher. However, ratios and trends remain the same between the two.

Isolation of chromosomal DNA from *B. subtilis* for transformation

The strain of which chromosomal DNA was to be prepared was used to inoculate 3 ml LB culture and incubated at 37°C with agitation (220-250 rpm) overnight. On the next day 2.5 ml of this culture was mixed 1:2 with SC buffer (0.15 M NaCl, 0.01 M Sodium citrate, pH 7.0). Subsequently, cells were harvested by centrifugation (5 min, 8000 rpm, RT). The pellet was resuspended in 1 ml SC buffer. 100 µl of 2 µg/ml lysozyme was added, mixed well and incubated for 15 min at 37°C. Afterwards, 1 ml 4 M NaCl was added. The entire solution was filtered with a 0.45 µm filter. 100 µl of this was used for *B. subtilis* transformation.

Transformation of *B. subtilis*

B. subtilis was grown overnight at 30°C on LB agar plate. In this work, all transformations were performed with the strain GFB0020 (table 5.1). In the morning 10 ml of medium 1 (prewarmed to 37°C) was inoculated with cells from the plate to OD_{600} 0.2 and incubated at 37°C, 250 rpm for 3 h. 10 ml medium 2 (prewarmed to 37°C) was added and further incubated for 2 h. 400 µl of this culture was transferred to a 2 ml tube and 100 µl isolated chromosomal DNA was added. 50 µl of the culture was plated under selective pressure after further incubation for 1 h at 37°C at 250 rpm.
All transformations were verified by colony PCR.

Medium 1

10 ml	basic salts
120 µl	40% (w/v) Glucose
400 µl	0.5% (w/v) Tryptophan
60 µl	1 M $MgSO_4 \cdot 7H_2O$
10 µl	20% (w/v) Casaminoacids
5 µl	2.2 mg/mL Ferric ammonium citrate (kept dark)

Medium 2

10 ml	basic salts
120 µl	40% (w/v) Glucose
60 µl	1 M $MgSO_4 \cdot 7H_2O$

Basic salts (can be prepared in advance and autoclaved)

2.0 g/l	$(NH_4)_2SO_4$
14.0 g/l	K_2HPO_4
6.0 g/l	KH_2HPO_4
1.0 g/l	Na_3-citrate·$2H_2O$
0.2 g/l	$MgSO_4 \cdot 7H_2O$

Colony PCR

Using the same tip a colony from a transformation plate was streaked onto a new plate and subsequently smeared into a PCR tube with 15 µl dH_2O. This was microwaved for 8 min. 1 µl was used as a template per 15 µl reaction mix.
Annealing temperature and elongation time were chosen appropriately for the given template.

Reaction mix

313 µl	dH_2O
7.5 µl	dNTPs
7.5 µl	10 µM Primer forward
7.5 µl	10 µM Primer reverse
37.5 µl	Taq polymerase buffer
1.88 µl	Taq polymerase

Program

1.	inital denaturation	95°C	5 min
2.	denaturation	95°C	45 s
3.	annealing	*	45 s
4.	elongation	72°C	*
5.	final elongation	72°C	5 min

Steps 2.-4. were repeated 34 times

Table 5.3.: Oligonucleotides used in this work.

ID	Nucleotide sequence (5' -> 3')	Description
GF0922	TTCTCGGCTACAATGTCAGC	DpdpD-up-fwd
GF0923	AGGCGTTTATCAAAGCCTTC	DpdpD-up-rev
GF0924	GAAGGCTTTGATAAACGCCT	DpdpD-do-fwd
GF0925	GCATAAATTGCAGACACCGT	DpdpD-do-rev
GF0926	CACCAGGTGACGGTAAAATA	DbcrC-up-fwd
GF0927	TGTATGCACTGTATGCGCAA	DbcrC-up-rev
GF0928	TTGCGCATACAGTGCATACA	DbcrC-do-fwd
GF0929	TATATGTGTTGGCGAAGCGA	DbcrC-do-rev
GF0930	GATGAGTTGGAAGAAACAGC	DponA-up-fdw
GF0931	AGATGGATCGACATCAGATT	DponA-up-rev
GF0932	TTGGCTACACACCGCAATAT	DponA-do-fdw
GF0933	TCCTGTTAAAACGGGAGGTT	DponA-do-rev
GF0934	CCTTTCGAGGCTGTATTCAT	DpdpG-up-fdw
GF0935	TGTATAGACGTTTAACCCGC	DpdpG-up-rev
GF0936	ATCAAAAAAGCCCGTTTGAC	DpdpG-do-fdw
GF0937	CGATTATGAAGGAACCATACGA	DpdpG-do-rev
GF0938	GCGAGTGCTTCGAACATAAT	DpdpF-up-fdw
GF0939	TTAATAAAGACCGCGCTTCC	DpdpF-up-rev
GF0940	GTCTGGACGCTGAATGAGAT	DpdpF-do-fdw
GF0941	TCGTTTACTCATCTGATTTCCAC	DpdpF-do-rev
GF0950	GGCATTGAAGCCGTGGAAGAGAC	Dyxd-check-fwd
GF0951	CAGCACTGCATGAGACCGGAGA	Dyxd-check_in-rev
GF0952	CAGGTGGATATCATCACCGACATGCTG	Dyxd-check_out-rev
GF0953	CGAGCCTTGTGATCATTGCCGT	Dbce-check-fwd
GF0954	CCTGGCCCACCTTTGTCTCG	Dbce-check_in-rev
GF0955	GGTTATCGGGCGCCAAAACGAT	Dbce-check_out-rev
GF0956	GAATTGACGTCATTGCCAGAAACAGCATG	Dpsd-check-fwd
GF0957	TGGCTAAGCGGTCGATGAGATAAGT	Dpsd-check_in-rev
GF0958	AACATGTGCAAACAGGCCGCC	Dpsd-check_out-rev

6. Bibliography

[1] C. Lee Ventola. The antibiotic resistance crisis: part 1: causes and threats. *Pharmacy and Therapeutics*, 40(4):277–283, 2015.

[2] Sina Jordan, Matthew I. Hutchings, and Thorsten Mascher. Cell envelope stress response in gram-positive bacteria. *FEMS microbiology reviews*, 32(1):107–146, 2008.

[3] Hannah Piepenbreier, Angelika Diehl, and Georg Fritz. Minimal exposure of lipid II cycle intermediates triggers cell wall antibiotic resistance. *Nature communications*, 10(1):1–13, 2019.

[4] L. Pasquina-Lemonche, J. Burns, R. D. Turner, S. Kumar, R. Tank, N. Mullin, J. S. Wilson, B. Chakrabarti, P. A. Bullough, S. J. Foster, and J. K. Hobbs. The architecture of the Gram-positive bacterial cell wall. *Nature*, 582(7811):294–297, 2020.

[5] Eefjan Breukink and Ben de Kruijff. Lipid II as a target for antibiotics. *Nature reviews. Drug discovery*, 5(4):321–332, 2006.

[6] Jonathan G. Swoboda, Jennifer Campbell, Timothy C. Meredith, and Suzanne Walker. Wall teichoic acid function, biosynthesis, and inhibition. *Chembiochem : a European journal of chemical biology*, 11(1):35–45, 2010.

[7] Obaidur Rahman, Lynn G. Dover, and Iain C. Sutcliffe. Lipoteichoic acid biosynthesis: two steps forwards, one step sideways? *Trends in Microbiology*, 17(6):219–225, 2009.

[8] Nathanael A. Caveney, Franco Kk Li, and Natalie Cj Strynadka. Enzyme structures of the bacterial peptidoglycan and wall teichoic acid biogenesis pathways. *Current opinion in structural biology*, 53:45–58, 2018.

[9] Terry J. Beveridge and Lori L. Graham. Surface layers of bacteria. *Microbiol. Mol. Biol. Rev.*, 66(4):684–705, 1991.

[10] Ahmed El Zoeiby, François Sanschagrin, and Roger C. Levesque. Structure and function of the Mur enzymes: development of novel inhibitors. *Molecular microbiology*, 47(1):1–12, 2003.

[11] Imène Kouidmi, Roger C. Levesque, and Catherine Paradis-Bleau. The biology of Mur ligases as an antibacterial target. *Molecular microbiology*, 94(2):242–253, 2014.

[12] D. Mengin-Lecreulx, B. Flouret, and J. van Heijenoort. Cytoplasmic steps of peptidoglycan synthesis in *Escherichia coli*. *Journal of bacteriology*, 151(3):1109–1117, 1982.

[13] D. Mengin-Lecreulx, B. Flouret, and J. van Heijenoort. Pool levels of udp n-acetylglucosamine and udp n-acetylglucosamine-enolpyruvate in *Escherichia coli* and correlation with peptidoglycan synthesis. *Journal of bacteriology*, 154(3):1284–1290, 1983.

[14] E. J. Lugtenberg, L. de Haas-Menger, and W. H. Ruyters. Murein synthesis and identification of cell wall precursors of temperature-sensitive lysis mutants of *Escherichia coli*. *Journal of bacteriology*, 109(1):326–335, 1972.

[15] Shehadeh Mizyed, Anna Oddone, Bartosz Byczynski, Donald W. Hughes, and Paul J. Berti. UDP-N-acetylmuramic acid (UDP-MurNAc) is a potent inhibitor of MurA (enolpyruvyl-UDP-GlcNAc synthase). *Biochemistry*, 44(10):4011–4017, 2005.

[16] E. E. Ishiguro and W. D. Ramey. Involvement of the relA gene product and feedback inhibition in the regulation of DUP-N-acetylmuramyl-peptide synthesis in *Escherichia coli*. *Journal of bacteriology*, 135(3):766–774, 1978.

[17] Angelika Diehl, Thomas M. Wood, Susanne Gebhard, Nathaniel I. Martin, and Georg Fritz. The cell envelope stress response of *Bacillus subtilis* towards laspartomycin C. *Antibiotics (Basel, Switzerland)*, 9(11):729, 2020.

[18] Heng Zhao, Vaidehi Patel, John D. Helmann, and Tobias Dörr. Don't let sleeping dogmas lie: new views of peptidoglycan synthesis and its regulation. *Molecular microbiology*, 106(6):847–860, 2017.

[19] Natividad Ruiz. Bioinformatics identification of MurJ (MviN) as the peptidoglycan lipid II flippase in *Escherichia coli*. *Proceedings of the National Academy of Sciences*, 105(40):15553–15557, 2008.

[20] Lok-To Sham, Emily K. Butler, Matthew D. Lebar, Daniel Kahne, Thomas G. Bernhardt, and Natividad Ruiz. Bacterial cell wall. MurJ is the flippase of lipid-linked precursors for peptidoglycan biogenesis. *Science*, 345(6193):220–222, 2014.

[21] Alexander J. Meeske, Lok-To Sham, Harvey Kimsey, Byoung-Mo Koo, Carol A. Gross, Thomas G. Bernhardt, and David Z. Rudner. MurJ and a novel lipid II flippase are required for cell wall biogenesis in *Bacillus subtilis*. *Proceedings of the National Academy of Sciences*, 112(20):6437–6442, 2015.

[22] Yuping Wei, Teresa Havasy, Derrell C. McPherson, and David L. Popham. Rod shape determination by the *Bacillus subtilis* class B penicillin-binding proteins encoded by *pbpA* and *pbpH*. *Journal of bacteriology*, 185(16):4717–4726, 2003.

[23] Alexander J. Meeske, Eammon P. Riley, William P. Robins, Tsuyoshi Uehara, John J. Mekalanos, Daniel Kahne, Suzanne Walker, Andrew C. Kruse, Thomas G. Bernhardt, and David Z. Rudner. SEDS proteins are a widespread family of bacterial cell wall polymerases. *Nature*, 537(7622):634–638, 2016.

[24] Antoine Vigouroux, Baptiste Cordier, Andrey Aristov, Laura Alvarez, Gizem Özbaykal, Thibault Chaze, Enno Rainer Oldewurtel, Mariette Matondo, Felipe Cava, David Bikard, and Sven van Teeffelen. Class-A penicillin binding proteins do not contribute to cell shape but repair cell-wall defects. *eLife*, 9, 2020.

[25] Tamimount Mohammadi, Vincent van Dam, Robert Sijbrandi, Thierry Vernet, André Zapun, Ahmed Bouhss, Marlies Diepeveen-de Bruin, Martine Nguyen-Distèche, Ben de Kruijff, and Eefjan Breukink. Identification of FtsW as a transporter of lipid-linked cell wall precursors across the membrane. *The EMBO journal*, 30(8):1425–1432, 2011.

[26] Heng Zhao, Yingjie Sun, Jason M. Peters, Carol A. Gross, Ethan C. Garner, and John D. Helmann. Depletion of undecaprenyl pyrophosphate phosphatases disrupts cell envelope biogenesis in *Bacillus subtilis*. *Journal of bacteriology*, 198(21):2925–2935, 2016.

[27] Jara Radeck, Susanne Gebhard, Peter Shevlin Orchard, Marion Kirchner, Stephanie Bauer, Thorsten Mascher, and Georg Fritz. Anatomy of the bacitracin resistance network in *Bacillus subtilis*. *Molecular microbiology*, 100(4):607–620, 2016.

[28] Jara Radeck, Nina Lautenschläger, and Thorsten Mascher. The essential UPP phosphatase pair BcrC and UppP connects cell wall homeostasis during growth and sporulation with cell envelope stress response in *Bacillus subtilis*. *Frontiers in microbiology*, 8:2403, 2017.

[29] Guillaume Manat, Sophie Roure, Rodolphe Auger, Ahmed Bouhss, Hélène Barreteau, Dominique Mengin-Lecreulx, and Thierry Touzé. Deciphering the metabolism of undecaprenyl-phosphate: the bacterial cell-wall unit carrier at the membrane frontier. *Microbial drug resistance (Larchmont, N.Y.)*, 20(3):199–214, 2014.

[30] C. M. Apfel, B. Takács, M. Fountoulakis, M. Stieger, and W. Keck. Use of genomics to identify bacterial undecaprenyl pyrophosphate synthetase: cloning, expression, and characterization of the essential uppS gene. *Journal of bacteriology*, 181(2):483–492, 1999.

[31] J. Kato, S. Fujisaki, K. Nakajima, Y. Nishimura, M. Sato, and A. Nakano. The *Escherichia coli* homologue of yeast RER2, a key enzyme of dolichol synthesis, is essential for carrier lipid formation in bacterial cell wall synthesis. *Journal of bacteriology*, 181(9):2733–2738, 1999.

[32] Julia Domínguez-Escobar, Arnaud Chastanet, Alvaro H. Crevenna, Vincent Fromion, Roland Wedlich-Söldner, and Rut Carballido-López. Processive movement of MreB-associated cell wall biosynthetic complexes in bacteria. *Science*, 333(6039):225–228, 2011.

[33] Ethan C. Garner, Remi Bernard, Wenqin Wang, Xiaowei Zhuang, David Z. Rudner, and Tim Mitchison. Coupled, circumferential motions of the cell wall synthesis machinery and mreb filaments in *B. subtilis*. *Science (New York, N.Y.)*, 333(6039):222–225, 2011.

[34] Tanneke den Blaauwen, Leendert W. Hamoen, and Petra Anne Levin. The divisome at 25: the road ahead. *Current Opinion in Microbiology*, 36:85–94, 2017.

[35] James Wagstaff and Jan Löwe. Prokaryotic cytoskeletons: protein filaments organizing small cells. *Nature Reviews Microbiology*, 16(4):187–201, 2018.

[36] James M. Wagstaff, Matthew Tsim, María A. Oliva, Alba García-Sanchez, Danguole Kureisaite-Ciziene, José Manuel Andreu, and Jan Löwe. A polymerization-associated structural switch in FtsZ that enables treadmilling of model filaments. *mBio*, 8(3), 2017.

[37] Alexandre W. Bisson-Filho, Yen-Pang Hsu, Georgia R. Squyres, Erkin Kuru, Fabai Wu, Calum Jukes, Yingjie Sun, Cees Dekker, Seamus Holden, Michael S. VanNieuwenhze, Yves V. Brun, and Ethan C. Garner. Treadmilling by FtsZ filaments drives peptidoglycan synthesis and bacterial cell division. *Science*, 355(6326):739–743, 2017.

[38] Xinxing Yang, Zhixin Lyu, Amanda Miguel, Ryan McQuillen, Kerwyn Casey Huang, and Jie Xiao. GTPase activity-coupled treadmilling of the bacterial tubulin FtsZ organizes septal cell wall synthesis. *Science*, 355(6326):744–747, 2017.

[39] Prahathees J. Eswara and Kumaran S. Ramamurthi. Bacterial cell division: Nonmodels poised to take the spotlight. *Annual review of microbiology*, 71:393–411, 2017.

[40] Helge Feddersen, Laeschkir Würthner, Erwin Frey, and Marc Bramkamp. Dynamics of the *Bacillus subtilis* Min system. *mBio*, 12(2), 2021.

[41] E. J. Harry, J. Rodwell, and R. G. Wake. Co-ordinating DNA replication with cell division in bacteria: a link between the early stages of a round of replication and mid-cell Z ring assembly. *Molecular microbiology*, 33(1):33–40, 1999.

[42] Pamela Gamba, Jan-Willem Veening, Nigel J. Saunders, Leendert W. Hamoen, and Richard A. Daniel. Two-step assembly dynamics of the *Bacillus subtilis* divisome. *Journal of bacteriology*, 191(13):4186–4194, 2009.

[43] Georg Fritz, Sebastian Dintner, Nicole Simone Treichel, Jara Radeck, Ulrich Gerland, Thorsten Mascher, and Susanne Gebhard. A new way of sensing: Need-based activation of antibiotic resistance by a flux-sensing mechanism. *mBio*, 6(4):e00975, 2015.

[44] Tina Wecke, Daniela Zühlke, Ulrike Mäder, Sina Jordan, Birgit Voigt, Stefan Pelzer, Harald Labischinski, Georg Homuth, Michael Hecker, and Thorsten Mascher. Daptomycin versus friulimicin B: in-depth profiling of *Bacillus subtilis* cell envelope stress responses. *Antimicrobial agents and chemotherapy*, 53(4):1619–1623, 2009.

[45] Laurens H. J. Kleijn, Hedwich C. Vlieg, Thomas M. Wood, Javier Sastre Toraño, Bert J. C. Janssen, and Nathaniel I. Martin. A high-resolution crystal structure that reveals molecular details of target recognition by the calcium-dependent lipopeptide antibiotic laspartomycin C. *Angewandte Chemie (International ed. in English)*, 56(52):16546–16549, 2017.

[46] Hongxia Liu, Houbao Pei, Zhinan Han, Guangli Feng, and Dapeng Li. The antimicrobial effects and synergistic antibacterial mechanism of the combination of ϵ-polylysine and nisin against *Bacillus subtilis*. *Food Control*, 47:444–450, 2015.

[47] Kittichoat Tiyanont, Thierry Doan, Michael B. Lazarus, Xiao Fang, David Z. Rudner, and Suzanne Walker. Imaging peptidoglycan biosynthesis in *Bacillus subtilis* with fluorescent antibiotics. *Proceedings of the National Academy of Sciences*, 103(29):11033–11038, 2006.

[48] Y. Noda, K. Yoda, A. Takatsuki, and M. Yamasaki. TmrB protein, responsible for tunicamycin resistance of *Bacillus subtilis*, is a novel ATP-binding membrane protein. *Journal of Bacteriology*, 174(13):4302–4307, 1992.

[49] M. Mota-Meira, G. LaPointe, C. Lacroix, and M. C. Lavoie. MICs of mutacin B-Ny266, nisin a, vancomycin, and oxacillin against bacterial pathogens. *Antimicrobial agents and chemotherapy*, 44(1):24–29, 2000.

[50] Mu Cheng, Johnny X. Huang, Soumya Ramu, Mark S. Butler, and Matthew A. Cooper. Ramoplanin at bactericidal concentrations induces bacterial membrane depolarization in *Staphylococcus aureus*. *Antimicrobial agents and chemotherapy*, 58(11):6819–6827, 2014.

[51] Shang-Te D. Hsu, Eefjan Breukink, Eugene Tischenko, Mandy A. G. Lutters, Ben de Kruijff, Robert Kaptein, Alexandre M. J. J. Bonvin, and Nico A. J. van Nuland. The nisin-lipid II complex reveals a pyrophosphate cage that provides a blueprint for novel antibiotics. *Nature structural & molecular biology*, 11(10):963–967, 2004.

[52] Hester Emilie Hasper, Ben de Kruijff, and Eefjan Breukink. Assembly and stability of nisin-lipid II pores. *Biochemistry*, 43(36):11567–11575, 2004.

[53] I. Wiedemann, E. Breukink, C. van Kraaij, O. P. Kuipers, G. Bierbaum, B. de Kruijff, and H. G. Sahl. Specific binding of nisin to the peptidoglycan precursor lipid II combines pore formation and inhibition of cell wall biosynthesis for potent antibiotic activity. *The Journal of biological chemistry*, 276(3):1772–1779, 2001.

[54] Ashutosh Prince, Anuj Tiwari, Pankaj Ror, Padmani Sandhu, Jyoti Roy, Suman Jha, Bibekanand Mallick, Yusuf Akhter, and Mohammed Saleem. Attenuation of neuroblastoma cell growth by nisin is mediated by modulation of phase behavior and enhanced cell membrane fluidity. *Physical chemistry chemical physics : PCCP*, 21(4):1980–1987, 2019.

[55] M. Ge, Z. Chen, H. R. Onishi, J. Kohler, L. L. Silver, R. Kerns, S. Fukuzawa, C. Thompson, and D. Kahne. Vancomycin derivatives that inhibit peptidoglycan biosynthesis without binding D-Ala-D-Ala. *Science (New York, N.Y.)*, 284(5413):507–511, 1999.

[56] Yuan Qiao, Veerasak Srisuknimit, Frederick Rubino, Kaitlin Schaefer, Natividad Ruiz, Suzanne Walker, and Daniel Kahne. Lipid II overproduction allows direct assay of transpeptidase inhibition by β-lactams. *Nature Chemical Biology*, 13(7):793–798, 2017.

[57] Thorsten Mascher, Neil G. Margulis, Tao Wang, Rick W. Ye, and John D. Helmann. Cell wall stress responses in *Bacillus subtilis*: the regulatory network of the bacitracin stimulon. *Molecular microbiology*, 50(5):1591–1604, 2003.

[58] K. J. Stone and J. L. Strominger. Mechanism of action of bacitracin: complexation with metal ion and C55 -isoprenyl pyrophosphate. *Proceedings of the National Academy of Sciences of the United States of America*, 68(12):3223–3227, 1971.

[59] Li-June Ming and Jon D. Epperson. Metal binding and structure–activity relationship of the metalloantibiotic peptide bacitracin. *Journal of Inorganic Biochemistry*, 91(1):46–58, 2002.

[60] U.S. Food and Drug Andiministration. FDA requests withdrawal of bacitracin for injection from market. *https://www.fda.gov/drugs/drug-safety-and-availability/fda-requests-withdrawal-bacitracin-injection-market*. Last checked: 04.01.2021 14:09.

[61] Christopher S. Ealand, Edith E. Machowski, and Bavesh D. Kana. β-lactam resistance: The role of low molecular weight penicillin binding proteins, β-lactamases and LD-transpeptidases in bacteria associated with respiratory tract infections. *IUBMB life*, 70(9):855–868, 2018.

[62] E. Tuomanen, R. Cozens, W. Tosch, O. Zak, and A. Tomasz. The rate of killing of *Escherichia coli* by β-lactam antibiotics is strictly proportional to the rate of bacterial growth. *Journal of general microbiology*, 132(5):1297–1304, 1986.

[63] Laurens H. J. Kleijn, Sabine F. Oppedijk, Peter 't Hart, Roel M. van Harten, Leah A. Martin-Visscher, Johan Kemmink, Eefjan Breukink, and Nathaniel I. Martin. Total synthesis of laspartomycin C and characterization of its antibacterial mechanism of action. *Journal of medicinal chemistry*, 59(7):3569–3574, 2016.

[64] T. Schneider, K. Gries, M. Josten, I. Wiedemann, S. Pelzer, H. Labischinski, and H-G Sahl. The lipopeptide antibiotic friulimicin B inhibits cell wall biosynthesis through complex formation with bactoprenol phosphate. *Antimicrobial agents and chemotherapy*, 53(4):1610–1618, 2009.

[65] Katrin Reder-Christ, Hildegard Falkenstein-Paul, Gabriela Klocek, Saad Al-Kaddah, Udo Bakowsky, and Gerd Bendas. Model membrane approaches to determine the role of calcium for the antimicrobial activity of friulimicin. *International journal of antimicrobial agents*, 37(3):256–260, 2011.

[66] Thomas M. Wood and Nathaniel I. Martin. The calcium-dependent lipopeptide antibiotics: structure, mechanism, & medicinal chemistry. *MedChemComm*, 10(5):634–646, 2019.

[67] Fabian Grein, Anna Müller, Katharina M. Scherer, Xinliang Liu, Kevin C. Ludwig, Anna Klöckner, Manuel Strach, Hans-Georg Sahl, Ulrich Kubitscheck, and Tanja Schneider. Ca^{2+}-daptomycin targets cell wall biosynthesis by forming a tripartite complex with undecaprenyl-coupled intermediates and membrane lipids. *Nature communications*, 11(1):1455, 2020.

[68] Andrea Mescola, Gregorio Ragazzini, and Andrea Alessandrini. Daptomycin strongly affects the phase behavior of model lipid bilayers. *The journal of physical chemistry. B*, 124(39):8562–8571, 2020.

[69] Anna Müller, Michaela Wenzel, Henrik Strahl, Fabian Grein, Terrens N. V. Saaki, Bastian Kohl, Tjalling Siersma, Julia E. Bandow, Hans-Georg Sahl, Tanja Schneider, and Leendert W. Hamoen. Daptomycin inhibits cell envelope synthesis by interfering with fluid membrane microdomains. *Proceedings of the National Academy of Sciences of the United States of America*, 113(45):E7077–E7086, 2016.

[70] Jenny Hering, Elin Dunevall, Margareta Ek, and Gisela Brändén. Structural basis for selective inhibition of antibacterial target MraY, a membrane-bound enzyme involved in peptidoglycan synthesis. *Drug discovery today*, 23(7):1426–1435, 2018.

[71] Jonna K. Hakulinen, Jenny Hering, Gisela Brändén, Hongming Chen, Arjan Snijder, Margareta Ek, and Patrik Johansson. Mray-antibiotic complex reveals details of tunicamycin mode of action. *Nature chemical biology*, 13(3):265–267, 2017.

[72] Jenny Hering, Elin Dunevall, Arjan Snijder, Per-Olof Eriksson, Michael A. Jackson, Trina M. Hartman, Ran Ting, Hongming Chen, Neil P. J. Price, Gisela Brändén, and Margareta Ek. Exploring the active site of the antibacterial target MraY by modified tunicamycins. *ACS chemical biology*, 15(11):2885–2895, 2020.

[73] Matthew E. Falagas, Evridiki K. Vouloumanou, George Samonis, and Konstantinos Z. Vardakas. Fosfomycin. *Clinical microbiology reviews*, 29(2):321–347, 2016.

[74] Nathalie Q. Balaban, Sophie Helaine, Kim Lewis, Martin Ackermann, Bree Aldridge, Dan I. Andersson, Mark P. Brynildsen, Dirk Bumann, Andrew Camilli, James J. Collins, Christoph Dehio, Sarah Fortune, Jean-Marc Ghigo, Wolf-Dietrich Hardt, Alexander Harms, Matthias Heinemann, Deborah T. Hung, Urs Jenal, Bruce R. Levin, Jan Michiels, Gisela Storz, Man-Wah Tan, Tanel Tenson, Laurence van Melderen, and Annelies Zinkernagel. Definitions and guidelines for research on antibiotic persistence. *Nature Reviews Microbiology*, 17(7):441–448, 2019.

[75] Philip Greulich, Matthew Scott, Martin R. Evans, and Rosalind J. Allen. Growth-dependent bacterial susceptibility to ribosome-targeting antibiotics. *Molecular systems biology*, 11(3):796, 2015.

[76] S. W. Lee, E. J. Foley, and Jeanne A. Epstein. Mode of action of penicillin: I. bacterial growth and penicillin activity - *Staphylococcus aureus* FDA. *Journal of bacteriology*, 48(4):393–399, 1944.

[77] Michael Ronald Millar and Jane Pike. Bactericidal activity of antimicrobial agents against slowly growing *Helicobacter pylori*. *Antimicrobial agents and chemotherapy*, 36(1):185–187, 1992.

[78] Tobias Dörr. Understanding tolerance to cell wall-active antibiotics. *Annals of the New York Academy of Sciences*, 2020.

[79] Kim Lewis. Persister cells, dormancy and infectious disease. *Nature Reviews Microbiology*, 5(1):48–56, 2007.

[80] Jurgen Wuyts, Patrick van Dijck, and Michelle Holtappels. Fungal persister cells: The basis for recalcitrant infections? *PLoS pathogens*, 14(10):e1007301, 2018.

[81] Kim Lewis. Persister cells. *Annual review of microbiology*, 64:357–372, 2010.

[82] Tobias Dörr, Kim Lewis, and Marin Vulić. Sos response induces persistence to fluoroquinolones in *Escherichia coli*. *PLoS genetics*, 5(12):e1000760, 2009.

[83] Iris Keren, Niilo Kaldalu, Amy Spoering, Yipeng Wang, and Kim Lewis. Persister cells and tolerance to antimicrobials. *FEMS Microbiology Letters*, 230(1):13–18, 2004.

[84] Ariane Müller, Diana Wolf, and Herwig O. Gutzeit. The black soldier fly, *Hermetia illucens* - a promising source for sustainable production of proteins, lipids and bioactive substances. *Zeitschrift fur Naturforschung. C, Journal of biosciences*, 72(9-10):351–363, 2017.

[85] Milla Pietiäinen, Marika Gardemeister, Maria Mecklin, Soile Leskelä, Matti Sarvas, and Vesa P. Kontinen. Cationic antimicrobial peptides elicit a complex stress response in *Bacillus subtilis* that involves ECF-type sigma factors and two-component signal transduction systems. *Microbiology (Reading, England)*, 151(Pt 5):1577–1592, 2005.

[86] Eva Rietkötter, Diana Hoyer, and Thorsten Mascher. Bacitracin sensing in *Bacillus subtilis*. *Molecular microbiology*, 68(3):768–785, 2008.

[87] Carolin M. Kobras, Hannah Piepenbreier, Jennifer Emenegger, Andre Sim, Georg Fritz, and Susanne Gebhard. BceAB-type antibiotic resistance transporters appear to act by target protection of cell wall synthesis. *Antimicrobial agents and chemotherapy*, 2020.

[88] Sina Jordan, Anja Junker, John D. Helmann, and Thorsten Mascher. Regulation of LiaRS-dependent gene expression in *Bacillus subtilis*: identification of inhibitor proteins, regulator binding sites, and target genes of a conserved cell envelope stress-sensing two-component system. *Journal of bacteriology*, 188(14):5153–5166, 2006.

[89] Diana Wolf, Falk Kalamorz, Tina Wecke, Anna Juszczak, Ulrike Mäder, Georg Homuth, Sina Jordan, Janine Kirstein, Michael Hoppert, Birgit Voigt, Michael Hecker, and Thorsten Mascher. In-depth profiling of the LiaR response of *Bacillus subtilis*. *Journal of bacteriology*, 192(18):4680–4693, 2010.

[90] Julia Domínguez-Escobar, Diana Wolf, Georg Fritz, Carolin Höfler, Roland Wedlich-Söldner, and Thorsten Mascher. Subcellular localization, interactions and dynamics of the phage-shock protein-like Lia response in *Bacillus subtilis*. *Molecular microbiology*, 92(4):716–732, 2014.

[91] Anna Staroń, Dora Elisabeth Finkeisen, and Thorsten Mascher. Peptide antibiotic sensing and detoxification modules of *Bacillus subtilis*. *Antimicrobial agents and chemotherapy*, 55(2):515–525, 2011.

[92] Kei Asai. Anti-sigma factor-mediated cell surface stress responses in *Bacillus subtilis*. *Genes & genetic systems*, 92(5):223–234, 2018.

[93] Min Cao and John D. Helmann. Regulation of the *Bacillus subtilis* bcrC bacitracin resistance gene by two extracytoplasmic function sigma factors. *Journal of bacteriology*, 184(22):6123–6129, 2002.

[94] Penny D. Thackray and Anne Moir. SigM, an extracytoplasmic function sigma factor of *Bacillus subtilis*, is activated in response to cell wall antibiotics, ethanol, heat, acid, and superoxide stress. *Journal of bacteriology*, 185(12):3491–3498, 2003.

[95] Theresa D. Ho, Jessica L. Hastie, Peter J. Intile, and Craig D. Ellermeier. The *Bacillus subtilis* extracytoplasmic function σ factor σ^V is induced by lysozyme and provides resistance to lysozyme. *Journal of bacteriology*, 193(22):6215–6222, 2011.

[96] Anthony W. Kingston, Xiaojie Liao, and John D. Helmann. Contributions of the σ^W, σ^M and σ^X regulons to the lantibiotic resistome of *Bacillus subtilis*. *Molecular microbiology*, 90(3):502–518, 2013.

[97] Christopher McDonald, Goran Jovanovic, Oscar Ces, and Martin Buck. Membrane stored curvature elastic stress modulates recruitment of maintenance proteins PspA and Vipp1. *mBio*, 6(5):e01188–15, 2015.

[98] John D. Helmann. *Bacillus subtilis* extracytoplasmic function (ECF) sigma factors and defense of the cell envelope. *Current Opinion in Microbiology*, 30:122–132, 2016.

[99] Thorsten Mascher, John D. Helmann, and Gottfried Unden. Stimulus perception in bacterial signal-transducing histidine kinases. *Microbiology and molecular biology reviews : MMBR*, 70(4):910–938, 2006.

[100] Emily J. Capra and Michael T. Laub. Evolution of two-component signal transduction systems. *Annual review of microbiology*, 66:325–347, 2012.

[101] Lara Rajeev, Megan E. Garber, and Aindrila Mukhopadhyay. Tools to map target genes of bacterial two-component system response regulators. *Environmental microbiology reports*, 12(3):267–276, 2020.

[102] Jara Radeck, Georg Fritz, and Thorsten Mascher. The cell envelope stress response of *Bacillus subtilis*: from static signaling devices to dynamic regulatory network. *Current genetics*, 63(1):79–90, 2017.

[103] Shailee Jani, Karen Sterzenbach, Vijaya Adatrao, Ghazal Tajbakhsh, Thorsten Mascher, and Dasantila Golemi-Kotra. Low phosphatase activity of LiaS and strong LiaR-DNA affinity explain the unusual LiaS to LiaR in vivo stoichiometry. *BMC microbiology*, 20(1):104, 2020.

[104] Tina Wecke, Tobias Bauer, Henning Harth, Ulrike Mäder, and Thorsten Mascher. The rhamnolipid stress response of *Bacillus subtilis*. *FEMS microbiology letters*, 323(2):113–123, 2011.

[105] Scott McAuley, Stephen Vadia, Charul Jani, Alan Huynh, Zhizhou Yang, Petra Anne Levin, and Justin R. Nodwell. A chemical inhibitor of cell growth reduces cell size in *Bacillus subtilis*. *ACS chemical biology*, 14(4):688–695, 2019.

[106] Sebastian Dintner, Anna Staron, Evi Berchtold, Tobias Petri, Thorsten Mascher, and Susanne Gebhard. Coevolution of ABC transporters and two-component regulatory systems as resistance modules against antimicrobial peptides in Firmicutes bacteria. *Journal of bacteriology*, 193(15):3851–3862, 2011.

[107] Pascale Joseph, Gwennaele Fichant, Yves Quentin, and François Denizot. Regulatory relationship of two-component and ABC transport systems and clustering of their genes in the Bacillus/Clostridium group, suggest a functional link between them. *J. Mol. Microbiol. Biotechnol.*, 4(5):503–513, 2002.

[108] Sebastian Dintner, Ralf Heermann, Chong Fang, Kirsten Jung, and Susanne Gebhard. A sensory complex consisting of an ATP-binding cassette transporter and a two-component regulatory system controls bacitracin resistance in *Bacillus subtilis*. *The Journal of biological chemistry*, 289(40):27899–27910, 2014.

[109] Daniel N. Wilson, Vasili Hauryliuk, Gemma C. Atkinson, and Alex J. O'Neill. Target protection as a key antibiotic resistance mechanism. *Nature Reviews Microbiology*, pages 1–12, 2020.

[110] Alan Koh, Marjorie J. Gibbon, Marc W. van der Kamp, Christopher R. Pudney, and Susanne Gebhard. Conformation control of the histidine kinase BceS of *Bacillus subtilis* by its cognate ABC-transporter facilitates need-based activation of antibiotic resistance. *Molecular microbiology*, 2020.

[111] Carolin Höfler, Judith Heckmann, Anne Fritsch, Philipp Popp, Susanne Gebhard, Georg Fritz, and Thorsten Mascher. Cannibalism stress response in *Bacillus subtilis*. *Microbiology (Reading, England)*, 162(1):164–176, 2016.

[112] Delia Casas-Pastor, Raphael R. Müller, Sebastian Jaenicke, Karina Brinkrolf, Anke Becker, Mark J. Buttner, Carol A. Gross, Thorsten Mascher, Alexander Goesmann, and Georg Fritz. Expansion and re-classification of the extracytoplasmic function (ECF) σ factor family. *Nucleic acids research*, 2021.

[113] Tanja M. Gruber and Carol A. Gross. Multiple sigma subunits and the partitioning of bacterial transcription space. *Annual review of microbiology*, 57:441–466, 2003.

[114] Mark S. Paget. Bacterial sigma factors and anti-sigma factors: Structure, function and distribution. *Biomolecules*, 5(3):1245–1265, 2015.

[115] Anna Staroń, Heidi J. Sofia, Sascha Dietrich, Luke E. Ulrich, Heiko Liesegang, and Thorsten Mascher. The third pillar of bacterial signal transduction: classification of the extracytoplasmic function (ECF) sigma factor protein family. *Molecular microbiology*, 74(3):557–581, 2009.

[116] Delia Casas-Pastor, Angelika Diehl, and Georg Fritz. Coevolutionary analysis reveals a conserved dual binding interface between extracytoplasmic function σ factors and class i anti-σ factors. *mSystems*, 5(4), 2020.

[117] M. Cao, B. A. Bernat, Z. Wang, R. N. Armstrong, and J. D. Helmann. FosB, a cysteine-dependent fosfomycin resistance protein under the control of σ^W, an extracytoplasmic-function σ factor in *Bacillus subtilis*. *Journal of bacteriology*, 183(7):2380–2383, 2001.

[118] Anthony W. Kingston, Chitra Subramanian, Charles O. Rock, and John D. Helmann. A σ^W-dependent stress response in *Bacillus subtilis* that reduces membrane fluidity. *Molecular microbiology*, 81(1):69–79, 2011.

[119] Warawan Eiamphungporn and John D. Helmann. The *Bacillus subtilis* σ^M regulon and its contribution to cell envelope stress responses. *Molecular microbiology*, 67(4):830–848, 2008.

[120] Min Cao and John D. Helmann. The *Bacillus subtilis* extracytoplasmic-function σ^X factor regulates modification of the cell envelope and resistance to cationic antimicrobial peptides. *Journal of bacteriology*, 186(4):1136–1146, 2004.

[121] Mitchell T. Butler, Qingfeng Wang, and Rasika M. Harshey. Cell density and mobility protect swarming bacteria against antibiotics. *Proceedings of the National Academy of Sciences of the United States of America*, 107(8):3776–3781, 2010.

[122] Hannah R. Meredith, Jaydeep K. Srimani, Anna J. Lee, Allison J. Lopatkin, and Lingchong You. Collective antibiotic tolerance: mechanisms, dynamics and intervention. *Nature Chemical Biology*, 11(3):182–188, 2015.

[123] X. Ding, R. R. Baca-DeLancey, and P. N. Rather. Role of SspA in the density-dependent expression of the transcriptional activator AarP in *Providencia stuartii*. *FEMS Microbiology Letters*, 196(1):25–29, 2001.

[124] Míriam R. García and Marta L. Cabo. Optimization of *E. coli* inactivation by benzalkonium chloride reveals the importance of quantifying the inoculum effect on chemical disinfection. *Frontiers in microbiology*, 9:1259, 2018.

[125] Yuuma Yoshida, Miki Matsuo, Yuichi Oogai, Fuminori Kato, Norifumi Nakamura, Motoyuki Sugai, and Hitoshi Komatsuzawa. Bacitracin sensing and resistance in *Staphylococcus aureus*. *FEMS microbiology letters*, 320(1):33–39, 2011.

[126] Aurélia Hiron, Mélanie Falord, Jaione Valle, Michel Débarbouillé, and Tarek Msadek. Bacitracin and nisin resistance in *Staphylococcus aureus*: a novel pathway involving the BraS/BraR two-component system (SA2417/SA2418) and both the BraD/BraE and VraD/VraE ABC transporters. *Molecular microbiology*, 81(3):602–622, 2011.

[127] Aishath Shaaly, Falk Kalamorz, Susanne Gebhard, and Gregory M. Cook. Undecaprenyl pyrophosphate phosphatase confers low-level resistance to bacitracin in *Enterococcus faecalis*. *The Journal of antimicrobial chemotherapy*, 68(7):1583–1593, 2013.

[128] D. A. Beauregard, A. J. Maguire, D. H. Williams, and P. E. Reynolds. Semiquantitation of cooperativity in binding of vancomycin-group antibiotics to vancomycin-susceptible and -resistant organisms. *Antimicrobial agents and chemotherapy*, 41(11):2418–2423, 1997.

[129] Yanan Hu, Jeremiah S. Helm, Lan Chen, Xiang-Yang Ye, and Suzanne Walker. Ramoplanin inhibits bacterial transglycosylases by binding as a dimer to lipid II. *Journal of the American Chemical Society*, 125(29):8736–8737, 2003.

[130] Helen C. Leggett, Charlie K. Cornwallis, Angus Buckling, and Stuart A. West. Growth rate, transmission mode and virulence in human pathogens. *Philosophical transactions of the Royal Society of London. Series B, Biological sciences*, 372(1719), 2017.

[131] Patrick Kaiser, Roland R. Regoes, Tamas Dolowschiak, Sandra Y. Wotzka, Jette Lengefeld, Emma Slack, Andrew J. Grant, Martin Ackermann, and Wolf-Dietrich Hardt. Cecum lymph node dendritic cells harbor slow-growing bacteria phenotypically tolerant to antibiotic treatment. *PLoS biology*, 12(2):e1001793, 2014.

[132] R. H. Eng, F. T. Padberg, S. M. Smith, E. N. Tan, and C. E. Cherubin. Bactericidal effects of antibiotics on slowly growing and nongrowing bacteria. *Antimicrobial agents and chemotherapy*, 35(9):1824–1828, 1991.

[133] Mauricio H. Pontes and Eduardo A. Groisman. Slow growth determines nonheritable antibiotic resistance in *Salmonella enterica*. *Science signaling*, 12(592), 2019.

[134] Hans Bremer and Patrick P. Dennis. Modulation of chemical composition and other parameters of the cell at different exponential growth rates. *EcoSal Plus*, 3(1), 2008.

[135] Eduardo P. C. Rocha. The organization of the bacterial genome. *Annual review of genetics*, 42:211–233, 2008.

[136] M. Schaechter, O. Maaloe, and N. O. Kjeldgaard. Dependency on medium and temperature of cell size and chemical composition during balanced grown of *Salmonella typhimurium*. *Journal of general microbiology*, 19(3):592–606, 1958.

[137] Robert Schleif. Control of production of ribosomal protein. *Journal of molecular biology*, 27(1):41–55, 1967.

[138] Matthew Scott, Carl W. Gunderson, Eduard M. Mateescu, Zhongge Zhang, and Terence Hwa. Interdependence of cell growth and gene expression: origins and consequences. *Science (New York, N.Y.)*, 330(6007):1099–1102, 2010.

[139] Stefan Klumpp, Zhongge Zhang, and Terence Hwa. Growth rate-dependent global effects on gene expression in bacteria. *Cell*, 139(7):1366–1375, 2009.

[140] Olivier Borkowski, Anne Goelzer, Marc Schaffer, Magali Calabre, Ulrike Mäder, Stéphane Aymerich, Matthieu Jules, and Vincent Fromion. Translation elicits a growth rate-dependent, genome-wide, differential protein production in *Bacillus subtilis*. *Molecular systems biology*, 12(5):870, 2016.

[141] Katherine Luby-Phelps. Cytoarchitecture and physical properties of cytoplasm: Volume, viscosity, diffusion, intracellular surface area. *International review of cytology*, 192:189–221, 1999.

[142] M. E. Sharpe, P. M. Hauser, R. G. Sharpe, and J. Errington. *Bacillus subtilis* cell cycle as studied by fluorescence microscopy: constancy of cell length at initiation of DNA replication and evidence for active nucleoid partitioning. *Journal of bacteriology*, 180(3):547–555, 1998.

[143] An-Chun Chien, Norbert S. Hill, and Petra Anne Levin. Cell size control in bacteria. *Current biology : CB*, 22(9):R340–9, 2012.

[144] Stephen Vadia, Jessica L. Tse, Rafael Lucena, Zhizhou Yang, Douglas R. Kellogg, Jue D. Wang, and Petra Anne Levin. Fatty acid availability sets cell envelope capacity and dictates microbial cell size. *Current biology : CB*, 27(12):1757–1767.e5, 2017.

[145] Allison J. Lopatkin, Jonathan M. Stokes, Erica J. Zheng, Jason H. Yang, Melissa K. Takahashi, Lingchong You, and James J. Collins. Bacterial metabolic state more accurately predicts antibiotic lethality than growth rate. *Nature Microbiology*, 4(12):2109–2117, 2019.

[146] Harry Smith. What happens to bacterial pathogens *in vivo*? *Trends in Microbiology*, 6(6):239–243, 1998.

[147] Anne Goelzer, Jan Muntel, Victor Chubukov, Matthieu Jules, Eric Prestel, Rolf Nölker, Mahendra Mariadassou, Stéphane Aymerich, Michael Hecker, Philippe Noirot, Dörte Becher, and Vincent Fromion. Quantitative prediction of genome-wide resource allocation in bacteria. *Metabolic engineering*, 32:232–243, 2015.

[148] Enno R. Oldewurtel, Yuki Kitahara, Baptiste Cordier, Gizem Özbaykal, and Sven van Teeffelen. *Bacteria control cell volume by coupling cell-surface expansion to dry-mass growth*. 2019.

[149] Jeff N. Anderl, Jeff Zahller, Frank Roe, and Philip S. Stewart. Role of nutrient limitation and stationary-phase existence in *Klebsiella pneumoniae* biofilm resistance to ampicillin and ciprofloxacin. *Antimicrobial agents and chemotherapy*, 47(4):1251–1256, 2003.

[150] D. Herbert, C. N. Paramasivan, P. Venkatesan, G. Kubendiran, R. Prabhakar, and D. A. Mitchison. Bactericidal action of ofloxacin, sulbactam-ampicillin, rifampin, and isoniazid on logarithmic- and stationary-phase cultures of *Mycobacterium tuberculosis*. *Antimicrobial agents and chemotherapy*, 40(10):2296–2299, 1996.

[151] R. Cozens, W. Tosch, O. Zak, Suter J., and A. Tomasz. Evaluation of the bactericidal activity of 1-lactam antibiotics on slowly growing bacteria cultured in the chemostat. *Antimicrobial Agents and Chemotherapy*, 29(5):797–802, 1986.

[152] Anna J. Lee, Shangying Wang, Hannah R. Meredith, Bihan Zhuang, Zhuojun Dai, and Lingchong You. Robust, linear correlations between growth rates and β-lactam-mediated

lysis rates. *Proceedings of the National Academy of Sciences of the United States of America*, 115(16):4069–4074, 2018.

[153] Milan Čižman. The use and resistance to antibiotics in the community. *International journal of antimicrobial agents*, 21(4):297–307, 2003.

[154] Jason A. Roberts, Peter Kruger, David L. Paterson, and Jeffrey Lipman. Antibiotic resistance–what's dosing got to do with it? *Critical care medicine*, 36(8):2433–2440, 2008.

[155] Fangwei Si, Dongyang Li, Sarah E. Cox, John T. Sauls, Omid Azizi, Cindy Sou, Amy B. Schwartz, Michael J. Erickstad, Yonggun Jun, Xintian Li, and Suckjoon Jun. Invariance of initiation mass and predictability of cell size in *Escherichia coli*. *Current biology : CB*, 27(9):1278–1287, 2017.

[156] Richard B. Weart and Petra Anne Levin. Growth rate-dependent regulation of medial FtsZ ring formation. *Journal of bacteriology*, 185(9):2826–2834, 2003.

[157] A. L. Koch and G. H. Gross. Growth conditions and rifampin susceptibility. *Antimicrobial agents and chemotherapy*, 15(2):220–228, 1979.

[158] Alon Zaslaver, Avi E. Mayo, Revital Rosenberg, Pnina Bashkin, Hila Sberro, Miri Tsalyuk, Michael G. Surette, and Uri Alon. Just-in-time transcription program in metabolic pathways. *Nature Genetics*, 36(5):486–491, 2004.

[159] Andre Delobbe, Rosine Haguenauer, and Georges Rapoport. Studies on the transport of -methyl-D-glucoside in *Bacillus subtilis* 168. *Biochimie*, 53(9):1015–1021, 1971.

[160] G. Gonzy-Tréboul, J. H. de Waard, M. Zagorec, and P. W. Postma. The glucose permease of the phosphotransferase system of *Bacillus subtilis*: evidence for II^{Glc} and III^{Glc} domains. *Molecular microbiology*, 5(5):1241–1249, 1991.

[161] S. Bachem, N. Faires, and J. Stülke. Characterization of the presumptive phosphorylation sites of the *Bacillus subtilis* glucose permease by site-directed mutagenesis: implication in glucose transport and catabolite repression. *FEMS microbiology letters*, 156(2):233–238, 1997.

[162] M. T. Hansen, M. L. Pato, S. Molin, N. P. Fill, and K. von Meyenburg. Simple downshift and resulting lack of correlation between ppGpp pool size and ribonucleic acid accumulation. *Journal of bacteriology*, 122(2):585–591, 1975.

[163] I. Fishov, A. Zaritsky, and N. B. Grover. On microbial states of growth. *Molecular microbiology*, 15(5):789–794, 1995.

[164] Sina Jordan, Eva Rietkötter, Mark A. Strauch, Falk Kalamorz, Bronwyn G. Butcher, John D. Helmann, and Thorsten Mascher. LiaRS-dependent gene expression is embedded in transition state regulation in *Bacillus subtilis*. *Microbiology (Reading, England)*, 153(Pt 8):2530–2540, 2007.

[165] José Eduardo González-Pastor. Cannibalism: a social behavior in sporulating *Bacillus subtilis*. *FEMS microbiology reviews*, 35(3):415–424, 2011.

[166] Philipp F. Popp, Alhosna Benjdia, Henrik Strahl, Olivier Berteau, and Thorsten Mascher. The epipeptide YydF intrinsically triggers the cell envelope stress response of *Bacillus subtilis* and causes severe membrane perturbations. *Frontiers in microbiology*, 11:151, 2020.

[167] D. L. Popham and P. Setlow. Cloning, nucleotide sequence, and mutagenesis of the *Bacillus subtilis ponA* operon, which codes for penicillin-binding protein (PBP) 1 and a PBP-related factor. *Journal of bacteriology*, 177(2):326–335, 1995.

[168] Dirk-Jan Scheffers, Laura J. F. Jones, and Jeffery Errington. Several distinct localization patterns for penicillin-binding proteins in *Bacillus subtilis*. *Molecular microbiology*, 51(3):749–764, 2004.

[169] D. C. McPherson, A. Driks, and D. L. Popham. Two class A high-molecular-weight penicillin-binding proteins of *Bacillus subtilis* play redundant roles in sporulation. *Journal of bacteriology*, 183(20):6046–6053, 2001.

[170] K. Hashiguchi, A. Tanimoto, S. Nomura, K. Yamane, K. Yoda, S. Harada, M. Mori, T. Furusato, A. Takatsuki, and M. Yamasaki. Amplification of the amyE-tmrB region on the chromosome in tunicamycin-resistant cells of *Bacillus subtilis*. *Molecular & general genetics : MGG*, 204(1):36–43, 1986.

[171] Akihiko Tanimoto, Shigeyoshi Harada, Masaki Mori, Noboru Yamaji, Kunio Yamane, Kiyotaka Otozai, Koji Yoda, Makari Yamasaki, and Gakuzo Tamura. Mutational site in tunicamycin-resistant mutation tmrB8 of *Bacillus subtilis* as revealed at the nucleotide sequence level. *Agricultural and Biological Chemistry*, 52(3):863–864, 1988.

[172] Y. Noda, A. Takatsuki, K. Yoda, and M. Yamasaki. TmrB protein, which confers resistance to tunicamycin on *Bacillus subtilis*, binds tunicamycin. *Bioscience, biotechnology, and biochemistry*, 59(2):321–322, 1995.

[173] Y. Noda, Itaru Urakawa, K. Yoda, and M. Yamasaki. *Bacillus subtilis* TmrB protein confers resistance to tunicamycin on *Escherichia coli*. *Journal of General and Applied Microbiology*, 42(4):343–347, 1996.

[174] Ulrike Kapp, Sofia Macedo, David Richard Hall, Ingar Leiros, Sean M. McSweeney, and Edward Mitchell. Structure of *Deinococcus radiodurans* tunicamycin-resistance protein (TmrD), a phosphotransferase. *Acta Crystallographica Section F: Structural Biology and Crystallization Communications*, 64(Pt 6):479–486, 2008.

[175] Ana Rita Brochado, Anja Telzerow, Jacob Bobonis, Manuel Banzhaf, André Mateus, Joel Selkrig, Emily Huth, Stefan Bassler, Jordi Zamarreño Beas, Matylda Zietek, Natalie Ng, Sunniva Foerster, Benjamin Ezraty, Béatrice Py, Frédéric Barras, Mikhail M. Savitski, Peer

Bork, Stephan Göttig, and Athanasios Typas. Species-specific activity of antibacterial drug combinations. *Nature*, 559(7713):259–263, 2018.

[176] Kalpana D. Singh, Matthias H. Schmalisch, Jörg Stülke, and Boris Görke. Carbon catabolite repression in bacillus subtilis: quantitative analysis of repression exerted by different carbon sources. *Journal of bacteriology*, 190(21):7275–7284, 2008.

[177] Stephen Vadia and Petra Anne Levin. Growth rate and cell size: a re-examination of the growth law. *Current Opinion in Microbiology*, 24:96–103, 2015.

[178] Pete Goodare. Literature review: Why do we continue to lose our nurses? *The Australian Journal of Advanced Nursing*, 34(4):50–56, 2017.

[179] I. J. Sud and M. Schaechter. Dependence of the content of cell envelopes on the growth rate of *Bacillus megaterium*. *Journal of bacteriology*, 88(6):1612–1617, 1964.

[180] Matthew Scott, Stefan Klumpp, Eduard M. Mateescu, and Terence Hwa. Emergence of robust growth laws from optimal regulation of ribosome synthesis. *Molecular systems biology*, 10:747, 2014.

[181] Hamid Nouri, Anne-Françoise Monnier, Solveig Fossum-Raunehaug, Monika Maciag-Dorszynska, Armelle Cabin-Flaman, François Képès, Grzegorz Wegrzyn, Agnieszka Szalewska-Palasz, Vic Norris, Kirsten Skarstad, and Laurent Janniere. Multiple links connect central carbon metabolism to DNA replication initiation and elongation in *Bacillus subtilis*. *DNA research : an international journal for rapid publication of reports on genes and genomes*, 25(6):641–653, 2018.

[182] D. Mengin-Lecreulx and J. van Heijenoort. Effect of growth conditions on peptidoglycan content and cytoplasmic steps of its biosynthesis in *Escherichia coli*. *Journal of bacteriology*, 163(1):208–212, 1985.

[183] Adrian J. Jervis, Penny D. Thackray, Chris W. Houston, Malcolm J. Horsburgh, and Anne Moir. SigM-responsive genes of *Bacillus subtilis* and their promoters. *Journal of bacteriology*, 189(12):4534–4538, 2007.

[184] Yun Luo, Kei Asai, Yoshito Sadaie, and John D. Helmann. Transcriptomic and phenotypic characterization of a *Bacillus subtilis* strain without extracytoplasmic function σ factors. *Journal of bacteriology*, 192(21):5736–5745, 2010.

[185] Jan Muntel, Vincent Fromion, Anne Goelzer, Sandra Maaß, Ulrike Mäder, Knut Büttner, Michael Hecker, and Dörte Becher. Comprehensive absolute quantification of the cytosolic proteome of *Bacillus subtilis* by data independent, parallel fragmentation in liquid chromatography/mass spectrometry (LC/MS(E)). *Molecular & cellular proteomics : MCP*, 13(4):1008–1019, 2014.

[186] Hiroshi Akashi and Takashi Gojobori. Metabolic efficiency and amino acid composition in the proteomes of *Escherichia coli* and *Bacillus subtilis*. *Proceedings of the National Academy of Sciences of the United States of America*, 99(6):3695–3700, 2002.

[187] S. Calogero, R. Gardan, P. Glaser, J. Schweizer, G. Rapoport, and M. Debarbouille. RocR, a novel regulatory protein controlling arginine utilization in *Bacillus subtilis*, belongs to the NtrC/NifA family of transcriptional activators. *Journal of bacteriology*, 176(5):1234–1241, 1994.

[188] Susanne Moses, Tatjana Sinner, Adrienne Zaprasis, Nadine Stöveken, Tamara Hoffmann, Boris R. Belitsky, Abraham L. Sonenshein, and Erhard Bremer. Proline utilization by *Bacillus subtilis*: uptake and catabolism. *Journal of bacteriology*, 194(4):745–758, 2012.

[189] L. A. Chasin and B. Magasanik. Induction and repression of the histidine-degrading enzymes of *Bacillus subtilis*. *The Journal of biological chemistry*, 243(19):5165–5178, 1968.

[190] Agnieszka Sekowska and Antoine Danchin. The methionine salvage pathway in *Bacillus subtilis*. *BMC Microbiology*, 2(1):8, 2002.

[191] Ulrike Mäder, Georg Homuth, Christian Scharf, Knut Büttner, Rüdiger Bode, and Michael Hecker. Transcriptome and proteome analysis of *Bacillus subtilis* gene expression modulated by amino acid availability. *Journal of bacteriology*, 184(15):4288–4295, 2002.

[192] Sasha H. Shafikhani, Amir Ali Partovi, and Terrance Leighton. Catabolite-induced repression of sporulation in *Bacillus subtilis*. *Current Microbiology*, 47(4):300–308, 2003.

[193] Marie-Françoise Hullo, Sandrine Auger, Olga Soutourina, Octavian Barzu, Mireille Yvon, Antoine Danchin, and Isabelle Martin-Verstraete. Conversion of methionine to cysteine in *Bacillus subtilis* and its regulation. *Journal of bacteriology*, 189(1):187–197, 2007.

[194] Frederick C. Neidhardt, Philip L. Bloch, and David F. Smith. Culture medium for enterobacteria. *Journal of bacteriology*, 119(3):736–747, 1974.

[195] E. A. Davies, H. E. Bevis, R. Potter, J. Harris, G. C. Williams, and J. Delves-Broughton. Research note: The effect of pH on the stability of nisin solution during autoclaving. *Letters in Applied Microbiology*, 27:186–187, 1998.

[196] J. R. Aeschlimann, E. Hershberger, and M. J. Rybak. Analysis of vancomycin population susceptibility profiles, killing activity, and postantibiotic effect against vancomycin-intermediate *Staphylococcus aureus*. *Antimicrobial agents and chemotherapy*, 43(8):1914–1918, 1999.

[197] Barbara Masschalck, Rob van Houdt, and Chris W. Michiels. High pressure increases bactericidal activity and spectrum of lactoferrin, lactoferricin and nisin. *International Journal of Food Microbiology*, 64(3):325–332, 2001.

[198] Sean I. Savitz, Martin H. Savitz, Howard B. Goldstein, Corinne T. Mouracade, and Sylvester Malangone. Topical irrigation with polymyxin and bacitracin for spinal surgery. *Surgical Neurology*, 50(3):208–212, 1998.

[199] R Nguyen, NR Khanna, AO Safadi, and Y Sun. Bacitracin topical. *Europe PMC*, 2019.

[200] ZhiGuang Jia, Megan L. O'Mara, Johannes Zuegg, Matthew A. Cooper, and Alan E. Mark. Vancomycin: ligand recognition, dimerization and super-complex formation. *The FEBS journal*, 280(5):1294–1307, 2013.

[201] Susanne Gebhard, Chong Fang, Aishath Shaaly, David J. Leslie, Marion R. Weimar, Falk Kalamorz, Alan Carne, and Gregory M. Cook. Identification and characterization of a bacitracin resistance network in *Enterococcus faecalis*. *Antimicrobial agents and chemotherapy*, 58(3):1425–1433, 2014.

[202] Byoung-Mo Koo, George Kritikos, Jeremiah D. Farelli, Horia Todor, Kenneth Tong, Harvey Kimsey, Ilan Wapinski, Marco Galardini, Angelo Cabal, Jason M. Peters, Anna-Barbara Hachmann, David Z. Rudner, Karen N. Allen, Athanasios Typas, and Carol A. Gross. Construction and analysis of two genome-scale deletion libraries for *Bacillus subtilis*. *Cell systems*, 4(3):291–305.e7, 2017.

S. Supplement

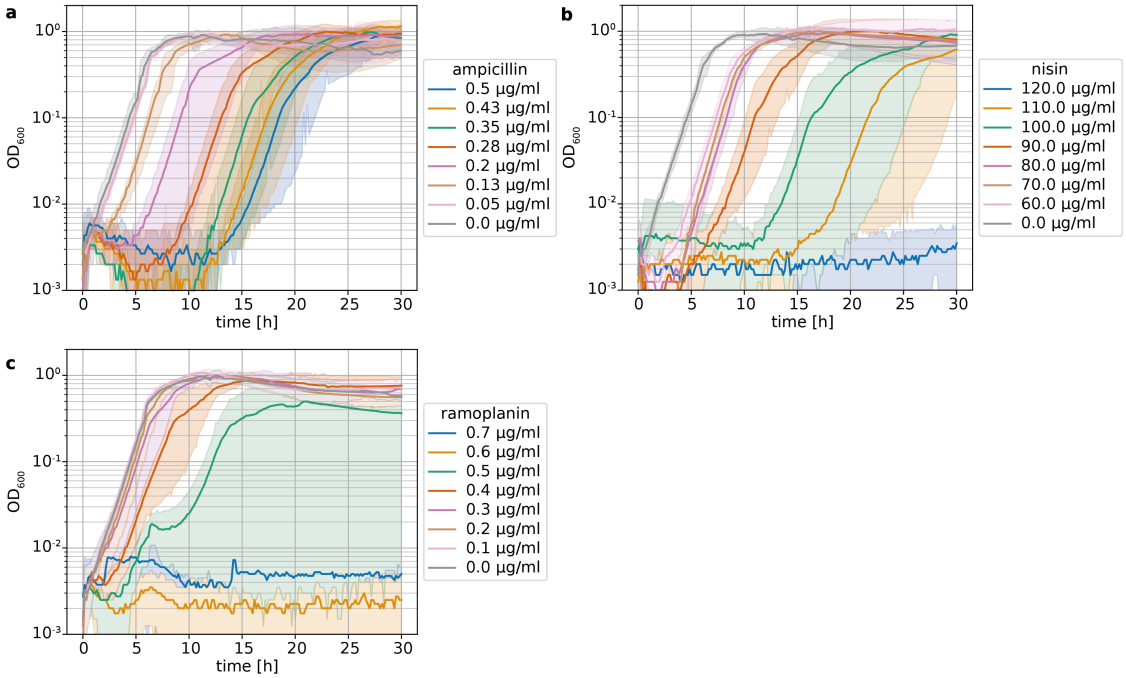

Figure S.1.: Mode of inhibition by cell wall targeting antibiotics. Growth curves of the fastest growth condition challenged with ampicillin (a), nisin (b) and ramoplanin (c) at t=0. Shaded areas depict 95% confidence intervals. (n≥3)

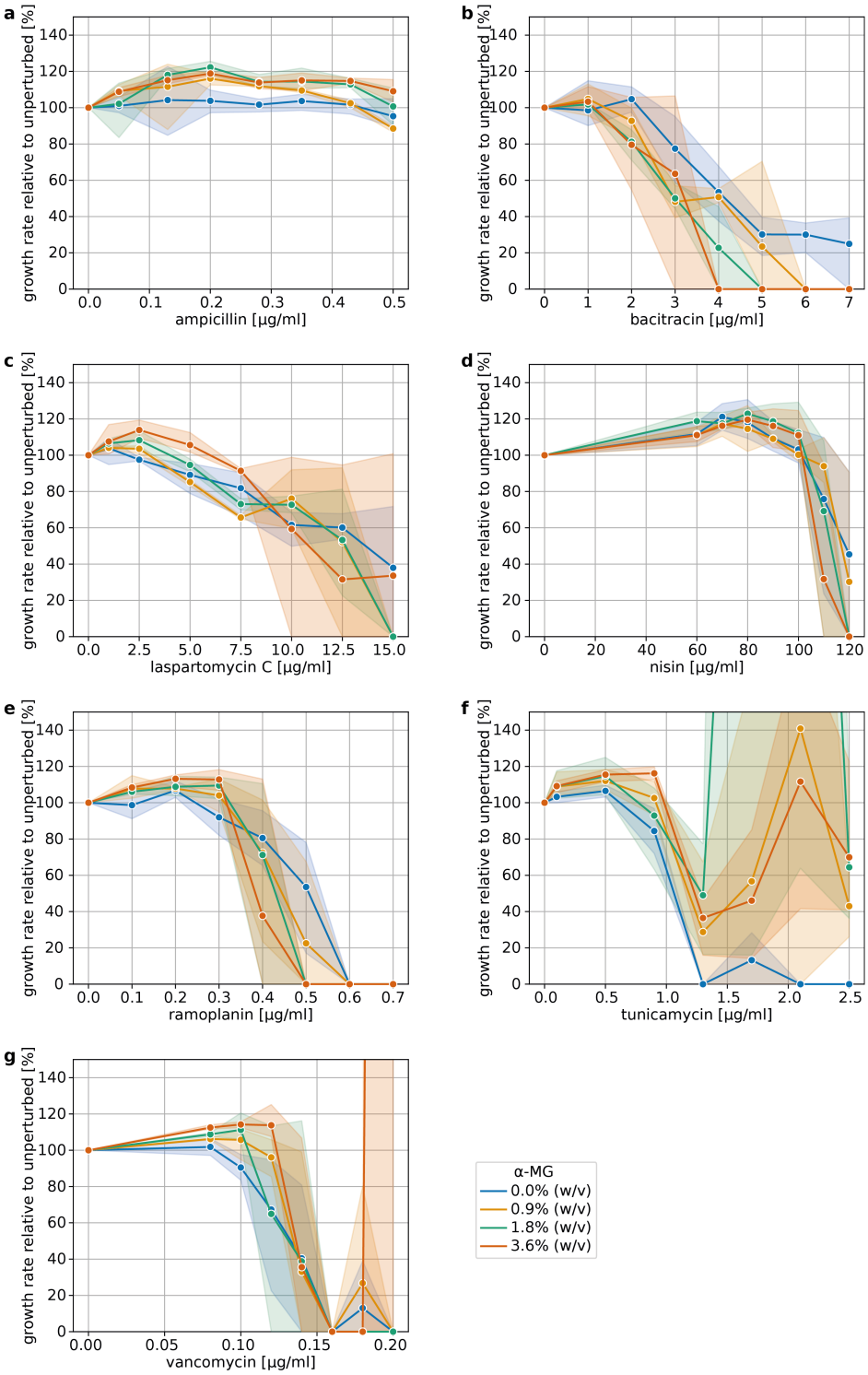

Figure S.2.: Modulation of growth rate by antibiotics is independent of α-MG addition. Dose-response curves of modulated growth rate by antibiotics at different α-MG concentrations. Ampicillin (a), bacitracin (b), laspartomycin C (c), nisin (d), ramoplanin (e), tunicamycin (f) and vancomycin (g). Shaded areas depict 95% confidence intervals. (n≥3)

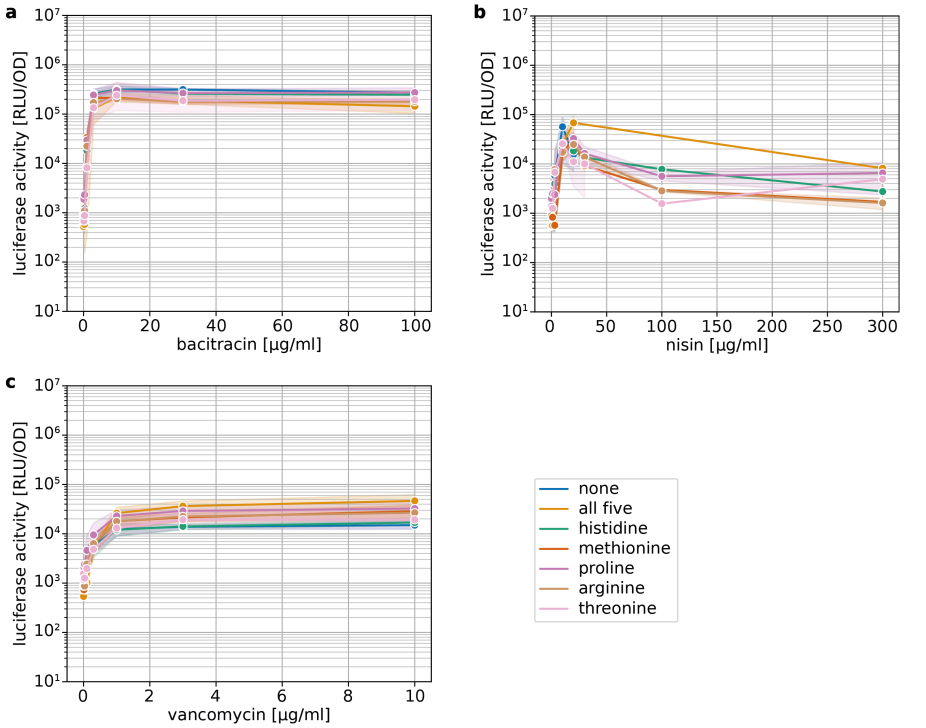

Figure S.3.: Presence of amino acids does not affect the antibiotic-induced Lia response. Lia response measured 30 min after challenge with either (a) bacitracin, (b) nisin or (c) vancomycin. (n≥2)

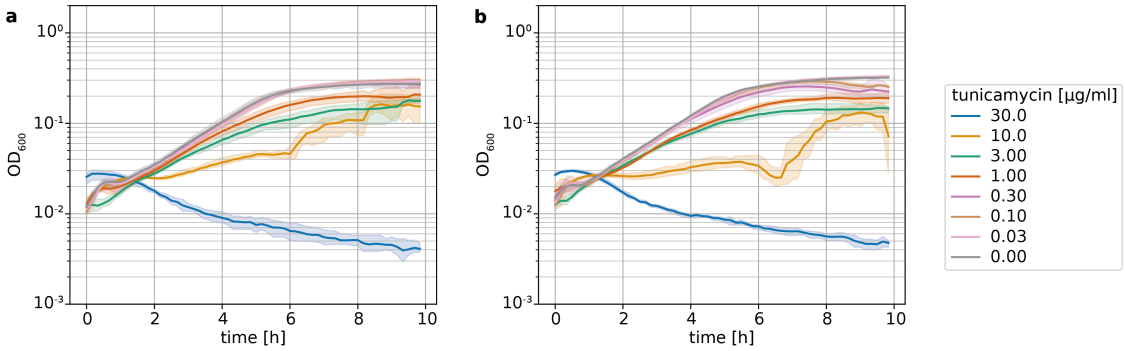

Figure S.4.: A *tmrB* deletion has only a small effect on growth after tunicamycin challenge in *B. subtilis*. Shaded areas depict 95% confidence intervals. (n=3)

Table S.1.: Unperturbed growth rate and susceptibility (IC_{50}) towards cell envelope targeting antibiotics in dependency of α-MG in MOPS media supplemented with fructose. Growth rate is given in h^{-1} and IC_{50} in µg/ml. IC_{50} was measured 6 doublings after antibiotic challenge, except for tunicamycin, which was measured 10 doublings after antibiotic challenge. Average values and standard deviation are given. (n≥3)

	MOPS + fructose			
α-MG	3.6% (w/v)	1.8% (w/v)	0.9% (w/v)	0% (w/v)
growth rate	0.69±0.05	0.56±0.02	0.55±0.02	0.54±0.04
ampicillin	0.11±0.02	0.15±0.01	0.12±0.02	0.14±0.02
bacitracin	2.84±0.02	2.86±0.08	2.85±0.12	3.02±0.2
laspartomycin C	7.21±0.38	8.77±0.93	9.24±1.16	9.43±1.09
nisin	32.67±1.13	32.00±0.81	32.89±1.28	32.69±0.93
ramoplanin	0.30±0.04	0.32±0.04	0.28±0.06	0.28±0.09
tunicamycin	1.10±0.07	1.32±0.12	1.48±0.02	2.23±0.25
vancomycin	0.07±0.01	0.08±0.01	0.09±0.02	0.08±0.02

Acknowledgments

First, I would like to thank my supervisor Dr. Georg Fritz for giving me the opportunity to work on this project and for supplying the necessary means. I am very grateful for all the good scientific discussions that we had during the last years, as well as for his constant support.

I would also like to thank the members of my thesis committee, Prof. Dr. Martin Thanbichler, Prof. Dr. Peter Graumann and Prof. Dr. Lennart Randau, who kindly accepted reviewing this thesis.

I would like to acknowledge the MArburg University Research Academy (MARA) for the financial support during the last 6 months with a completion scholarships.

My gratitude goes to everyone from my lab, past and present, who provided insightful discussions, scientific help and welcome distractions. Special thanks to Dr. Hannah Piepenbreier, who provided the theoretical framework for many of my projects, and Dr. Jamie Tedeschi, who performed the experiments concerning antibiotic degradation.

I am grateful to Dr. Mathias Diehl, Mira Diekmann, Erik Winterling, Rebecca Wolters and Dr. Jamie Tedeschi for corrections and critical reading of my thesis manuscript.

I would like to thank Clare Whyte for being the awesome roommate she is. You have made my stay in Perth so much more enjoyable. I will not forget your and your families warm welcome, the great travel advice, the botanical excursions and other sight seeing tours and of course your cats: Patch, Noora and Finn.

Mira Diekmann, thank you for always being there for me and for making my life outside of uni so much more fun.

I would like to thank Erik Winterling for his constant support, understanding and encouragement. Thank you for always having my back.

Finally, I am grateful to my family for their everlasting support.

Curriculum vitae

Auf dieser Seite befindet sich in der Druckversion dieser Arbeit der Lebenslauf, welcher aus Datenschutzgründen in der Online-Version entfernt wurde.

Erklärung

Ich versichere, dass ich meine Dissertation mit dem Titel

Active and passive resistance mechanisms of *Bacillus subtilis* against cell envelope targeting antibiotics

selbstständig ohne unerlaubte Hilfe angefertigt und mich dabei keiner anderen als der von mir ausdrücklich bezeichneten Quellen und Hilfsmittel bedient habe.

Diese Dissertation wurde in der jetzigen oder einer ähnlichen Form noch bei keiner anderen Hochschule eingereicht und hat noch keinen sonstigen Prüfungszwecken gedient.

Marburg, den 27. Juli 2021

Angelika Diehl